Dissertation

Drug-Induced Liver Injury in Psychiatric Disorders

submitted by

Anna Maria BIRKL-TÖGLHOFER, BSc MSc

for the Academic Degree of

Doctor of Philosophy

(PhD)

at the

Medical University of Graz

Diagnostic and Research Institute of Pathology

under the Supervision of

Assoz. Prof. Priv.-Doz. Dr.med.univ. Dr.sc.nat. Johannes Haybäck

2020

Statutory declaration

I hereby declare that this thesis is my own original work and that I have fully acknowledged by name all of those individuals and organizations that have contributed to the research for this thesis. Due acknowledgement has been made in the text to all other material used. Throughout this thesis and in all related publications I followed the “Standards of Good Scientific Practice and Ombuds Committee at the Medical University of Graz“.

Graz, August 2020 Anna Maria Birkl-Töglhofer

Disclosures

Parts of this thesis have been published in the following original article:

Translational Psychiatry, 2019 Dec 09; 9:331, doi: 10.1038/s41398-019-0666-4

Hepatic gene expression explains primary drug toxicity in bipolar disorder

Anna Maria Birkl-Toeglhofer[1,2], Christoph Birkl[3], Ida Cirila Llenos[4], Serge Weis[4,5,6], Johannes Haybaeck[1,2,7,8]

[1] Institute of Pathology, Medical University of Graz, Austria

[2] Department of Pathology, Neuropathology and Molecular Pathology, Medical University of Innsbruck, Innsbruck, Austria

[3] Department of Neurology, Medical University of Graz, Austria

[4] The Stanley Medical Research Institute, Chevy Chase, MD, USA

[5] Division of Neuropathology, Department of Pathology and Neuropathology, Neuromed Campus, Kepler University Hospital, Medical School, Johannes Kepler University, Linz, Austria

[6] Departments of Psychiatry and Pathology, Uniformed Services University of the Health Sciences, Bethesda, MD, USA

[7] Center for Biomarker Research in Medicine, Graz, Austria

[8] Department of Pathology, Medical Faculty, Otto von Guericke University Magdeburg, Germany

All co-authors gave their consent for the re-use of the published data in this thesis.

‘Life need not be easy, provided only that it is not empty.’

(Lise Meitner)

Acknowledgement

I would like to express my deep gratitude to my supervisor, Prof. Johannes Haybaeck. Thank you for giving me the opportunity to conduct my PhD under your guidance and for the enthusiastic encouragement and consistent support.

I would like to express my gratitude to my thesis committee members, Prof. Eva Reininghaus and Prof. Peter Fickert. Their valuable advice and comments during my thesis have been an enormous help to me. Furthermore, I wish to thank Susanne Bengesser for her steady support and the inspiring discussions.

I want to thank the Medical University of Graz, in particular the PhD program Molecular Medicine and the people involved in the program organization.

I appreciate the great help and insightful suggestions from all collaborators whose assistance was an invaluable support in the completion of this thesis. I wish to thank all the people of the Diagnostic and Research Institute of Pathology for the supportive advice and help. In particular, I would like to thank all the colleagues from the lab for the valuable support. Thank you for being a source of inspiration and motivation, and for all the countless legendary moments.

Finally, I wish to acknowledge the continuous support and encouragement of my dear family. Christoph, thank you for your relentless support and patients during good and bad times, I am glad to have you in my live. Special thanks go to my parents for their unlimited encouragement and motivation and to my sister and my brothers with their families for their unconditional help. I would like to thank all my friends for the good times we spent together, even when time was limited.

Table of contents

Abbreviations and definitions

AADAC	arylacetamide deacetylase
ACBD5	acyl-CoA binding domain containing 5
ACOT13	acyl-CoA thioesterase 13
ADAM10	ADAM metallopeptidase domain 10
AGL	amylo-alpha-1, 6-glucosidase, 4-alpha-glucanotransferase
AGTR1	angiotensin II receptor type 1
ALDH2	aldehyde dehydrogenase 2 family member
ANAPC13	anaphase promoting complex subunit 13
APOB	apolipoprotein B
A-SAA	acute-phase serum amyloid A
ATP	adenosine triphosphate
ATP5O	ATP synthase peripheral stalk subunit OSCP
ATP5PB	ATP synthase peripheral stalk-membrane subunit b
BMI	body mass index
BPD	bipolar disorder
C3	complement C3
CAT	catalase
CD	cluster of differentiation
CDH1	cadherin 1
cDNA	complementary desoxyribonucleic acid
CEP57	centrosomal protein 57
CMBL	carboxymethylenebutenolidase homolog
Ct	cycle treshold
CTRL	control
CYP	cytochrome P450
CYP3A5	cytochrome P450 family 3 subfamily A member 5
DECR1	2,4-dienoyl-CoA reductase 1

DEGs	differentially expressed genes
DHTKD1	dehydrogenase E1 and transketolase domain containing 1
DNA	desoxyribonucleic acid
DSM	Diagnostic and Statistical Manual of Mental Disorders
ERK	extracellular signal-regulated kinase
FDR	false discovery rate
FMO3	flavin containing dimethylaniline monooxygenase 3
FN1	fibronectin 1
GAPDH	glyceraldehyde-3-phosphate dehydrogenase
GATM	glycine amidinotransferase
GO	Gene ontology
HAO1	hydroxyacid oxidase 1
HCC	hepatocellular carcinoma
HGNC	Human Genome Organization (HUGO) Gene Nomenclature Committee
HIBADH	3-hydroxyisobutyrate dehydrogenase
HMGB1	high mobility group box 1
IDH1	isocitrate dehydrogenase (NADP(+)) 1
IL1RN	interleukin-1 receptor antagonist
IL-1Rα	interleukin-1 receptor antagonist protein
IPO8	importin 8
LRPPRC	leucine rich pentatricopeptide repeat containing
LSM5	LSM5 homolog, U6 small nuclear RNA and mRNA degradation associated
MAOI	Monoamine oxidase inhibitor
MAPK	mitogen-activated protein kinase
MCODE	Molecular Complex Detection
mRNA	messenger ribonucleic acid
NAFL	non-alcoholic fatty liver
NAFLD	non-alcoholic fatty liver disease
NASH	non-alcoholic steatohepatitis

NDUFA9	NADH:ubiquinone oxidoreductase subunit A9
PCA	principal component analysis
PGM1	phosphoglucomutase 1
PMI	*post mortem* intervall
PON1	paraoxonase 1
PPP2CA	protein phosphatase 2 catalytic subunit alpha
PRKAB2	protein kinase AMP-activated non-catalytic subunit beta 2
PSMA2	proteasome subunit alpha 2
PTEN	phosphatase and tensin homolog
RAP1	Ras-related protein
RAP1A	RAP1A, member of RAS oncogene family
RETC	respiratory electron transport chain
RIN	RNA integrity number
RMA	Robust Mulit-array Average algorithm
RNA	ribonucleic acid
RPL41	ribosomal protein L41
S100A12	S100 calcium binding protein A12
S100A8	S100 calcium binding protein A8
S100A9	S100 calcium binding protein A9
SAA2	serum amyloid A2
SDHB	succinate dehydrogenase complex iron sulfur subunit B
SLC38A4	solute carrier family 38 member 4
SNAP23	synaptosome associated protein 23
SNRI	Serotonin norepinephrine reuptake inhibitors
SOD1	superoxide dismutase 1
SSRI	selective serotonin reuptake inhibitors
STRING	Search Tool for the Retrieval of Interacting Genes/Proteins
SULT1E1	sulfotransferase family 1E member 1
TARDBP	TAR DNA binding protein pseudogene 1

TCA	tricyclic antidepressants
TCGA LIHC	The Cancer Genome Atlas Liver Hepatocellular Carcinoma
TDO2	tryptophan 2,3-dioxygenase
TNF	tumor necrosis factor
TNFRSF1B	TNF receptor superfamily member 1B
TNFSF10	TNF superfamily member 10
TRAIL	tumor necrosis factor related apoptosis inducing ligand
TUBE1	tubulin epsilon 1
UBQLN2	ubiquilin 2
UDP	uridine diphosphate
UGT	UDP-glucuronosyltransferase
UGT2B15	UDP glucuronosyltransferase family 2 member B15
VAMP8	vesicle associated membrane protein 8
WebGestalt	WEB-based GEne SeT AnaLysis Toolkit

Zusammenfassung

Bei schweren psychischen Erkrankungen, wie der bipolaren Störung, ist häufig eine akute aber auch langfristige medikamentöse Behandlung mit Psychopharmaka notwendig um auftretende Symptome zu lindern beziehungsweise zu verhindern. Neben deren positiven Effekten, sind einige Nebenwirkungen bekannt zu denen Störungen des Stoffwechsels zählen. Da die Leber die Funktion als zentrales Stoffwechselorgans für Nährstoffe aber auch pharmakologische Substanzen erfüllt, sind psychopharmakologische Nebenwirkungen durch eine eingeschränkte Entgiftung in Bezug auf die hepatische Funktion anzunehmen. Obwohl die nicht-alkoholische Fettlebererkrankung (NAFLD) häufig in der westlichen Bevölkerung auftritt, zeigen Patienten mit einer bipolaren Störung ein erhöhtes Risiko NAFLD zu entwickeln. Diese reicht von einer einfachen Steatosis bis hin zu einer nicht-alkoholischen Stetaohepatitis. Inwiefern Psychopharmaka die Entstehung von Leberschäden beeinflussen, insbesondere der zugrundeliegende molekulare Mechanismus, ist bisher noch unbekannt. Um die möglichen Psychopharmaka-induzierten Störungen auf molekularer Ebene zu erfassen, nimmt die Anwendung von ‚-omics' Technologien und der Einsatz von bioinformatischen Tools in Kombination mit histopathologischen Erkenntnissen eine zentrale Rolle ein. Die Erforschung von psychopharmakologischen Nebenwirkungen auf molekularer Ebene in der Leber trägt somit zur Erhöhung der Medikamentensicherheit und im weiteren Sinne zur Verbesserung des therapeutischen Effekts von Psychopharmaka für Patienten mit bipolarer Störung bei.

Der Fokus dieser Dissertation lag auf der Bestimmung der globalen Genexpression in postmortalem Lebergewebe von bipolaren Patienten mit psychopharmakologischer Behandlung. Die globale Genexpression wurde mit einer Kontrollgruppe, die eine ähnliche hepatische Histopathologie aufwies, verglichen. Der Großteil der differenziell exprimierten Gene war in der bipolaren Gruppe vorwiegend schwächer exprimiert als in den Kontrollen. Daraus wurde geschlossen, dass Psychopharmaka allgemein die Genexpression eher reduzieren, als antreiben. Für die biologische Funktionszuordnung der differenziell exprimierten Gene wurden umfassende bioinformatische Analysen durchgeführt. Besonders Gene, die in der Atmungskette involviert sind, waren von einer reduzierten Genexpression betroffen. Es wird angenommen, dass dies eine erniedrigte zelluläre Energieversorgung nach sich zieht. Dies ist wahrscheinlich mit einem seneszenten Phänotypen assoziiert und könnte auch histopathologisch erkennbar sein. Des Weiteren wurde eine verminderte Genexpression

für Gene, die im Lipid-, Aminosäuremetabolismus, und im Metabolismus von Xenobiotika beteiligt sind, festgestellt. Es wurde angenommen, dass als Konsequenz der zelluläre oxidative Stress ansteigt und somit schwere Schädigungen in der Zelle entstehen. Zusätzlich wurde *in silico* die Funktion der codierenden Gene auf Proteinebene untersucht. Hiermit wurden Einblicke in Protein-Protein-Interaktionen gewonnen und die Funktion des jeweiligen Proteins in diesen Netzwerken bestimmt. Um Muster der Genexpression aufzudecken, die eine Psychopharmaka-induzierte histopathologische Schädigung aufweisen, wurden mögliche Assoziationen zwischen der Genexpression und histopathologischen Veränderung der Leber ermittelt. Vor allem konnte eine Assoziation von degenerativen Veränderungen der Leber mit der Genexpression gezeigt werden.

Zusammenfassend zeigte diese Studie, dass Patienten mit bipolarer Störung und der Behandlung von Psychopharmaka eine veränderte Genexpression in der Leber aufweisen. Vor allem ist die zelluläre Energieversorgung beeinträchtigt und erhöhter zellulärer Stress vorliegend. All dies lässt auf einen gesonderten pathophysiologischen Mechanismus schließen, der einer Leberschädigung durch Psychopharmaka in bipolarer Störung zugrunde liegt.

Abstract

Acute and long-term psychotropic drug treatment is often necessary to improve symptoms and prevent relapses in severe mental disorders, such as bipolar disorder. Beside the beneficial effects of the pharmacological treatment, several adverse effects are known like the induction of metabolic disturbances. As the liver is the main site for metabolism of nutrients and pharmacological agents, an affected hepatic function by improper drug detoxification can be assumed. Although non-alcoholic fatty liver disease (NAFLD), ranging from simple steatosis to non-alcoholic steatohepatitis, is common in the Western population, patients with severe mental disorders have an increased risk for the development of NAFLD. To which extent psychotropic drug influence the underlying molecular mechanism leading to hepatic injury remains unknown. Therefore, to reveal the central physiology behind the emerging biological disturbances due to psychotropic drug treatment, the application of '-omics' technologies and the integration of advanced bioinformatical analyses in combination with basic histopathology is crucial. The assessment of possible interferences of psychotropic drugs on the molecular level of hepatic function are needed to subsequently improve the safety and therapeutic effect of pharmacological treatment in bipolar disorder.

This exploratory study addressed the global gene expression in hepatic *post mortem* tissue of patients with bipolar disorder and psychotropic drug treatment compared to control samples with similar hepatic histopathology. Differentially expressed genes were predominantly downregulated assuming that psychotropic drugs rather reduce gene expression than shifting to an increased state of gene expression. To allocate the differentially expressed genes to their biological function, comprehensive bioinformatical analyses were conducted including pathway and enrichment analyses. Particularly, a decreased expression was observed in the biological pathway of the respiratory energy transport chain. The anticipated resulting diminished cellular energy supply is probably associated with a senescent phenotype which might be also evident in hepatic histopathology. Moreover, gene expression was reduced for genes involved in the metabolism of lipids, amino acids and xenobiotics, where a consequent increase in oxidative stress might entail serious cell damage. Furthermore, protein-protein interactions of the encoding respective differentially expressed genes were assessed *in silico* to provide insights in terms of their function in an intricate network of proteins. For the examination of gene expression patterns defining or triggering a harmed histopathological

phenotype due to psychotropic drugs, gene expression data and histopathological features were integrated. Particularly, histopathological degenerative changes in the liver were associated with the enriched pathways indicating adverse effects on molecular level for psychotropic drugs.

In summary, this study highlights an altered hepatic gene expression in patients with bipolar disorder and psychotropic drug treatment. The presence of a diminished cellular energy supply and an increased cellular stress level are defining the molecular pattern in the liver evoked by psychotropic drugs. All of which indicates a differential underlying mechanism initiating or triggering hepatic injury in bipolar disorder with psychotropic drug treatment.

1 Introduction

1.1 Severe mental disorders

Severe mental disorders are characterized by problems in thinking, behavior, cognition, perception, mood, emotion and moving functions, all of which lead to an impaired functioning in live activities [1]. According to the World Mental Health surveys on behalf of the World Health Organization, the global prevalence of mental disorders amounted to 15.4% in all assessed countries, whereby higher income countries showed increased prevalence compared to lower income countries [2]. In Europe, a lifetime prevalence of 25% has been demonstrated for mental disorders in adults, whereas the experience of any mental disorder in the past 12-month was reported to be 10% [3]. The diagnostic subgroup of mood disorders revealed a lifetime and 12-month prevalence of 14% and 4.2%, respectively, whereas higher odds exists for females and young adults. In addition to the high prevalence, disturbing reduced life-expectancy have been observed for individuals with severe mental illnesses, such as bipolar disorder, major depression or schizophrenia [4–7]. Compared to the general population the life expectancy difference accounts for more than 10 years for all three mentioned mental disorders in the United Kingdom [4], yet lower life expectancy was observed for men in Denmark, Finland and Sweden [5]. Interestingly, death due to physical illnesses was the most frequent cause for the decreased life expectancy, whereas suicide rates were decreasing from adolescence to adulthood and older age in bipolar disorder [7]. The underlying reason for the observed premature deaths as consequence of physical health conditions in these severe mental disorders remains unknown. A possible interaction between mental and physical health and disease may exist.

1.2 Causes of severe mental disorders

Decades of extensive research chased the answer behind the underlying causes of mental disorders and the possibility of an effective therapeutic treatment. So far, it has been proposed that severe mental disorders are complex traits with environmental and multiple genetic contributing factors which may be shared between mental disorders.

One of these supposed environmental factors is nutrition, where an unhealthy diet is linked to mental problems even during the prenatal phase [8]. An association between nutrition and gene

expression due to epigenetic modifications probably exists. Concerning the genetic factors, high heritability estimates were revealed for schizophrenia [9] and bipolar disorder [10,11], whereas on the contrary major depressive disorder exposed lower heritability [12]. Several genome-wide studies revealed genetic loci of interest considered to contribute to those mental disorders and indicating for a highly polygenic disorder [13–15]. A possible shared genetic background among mental disorders and mood disorders was evaluated [16,17]. A strong correlation of single nucleotide polymorphisms was observed for bipolar disorder and schizophrenia, whereas a moderate correlation was present for bipolar disorder and major depressive disorder as well as schizophrenia and major depressive disorder [16]. So, an underlying genetic contribution to the susceptibility of mental disorder can be assumed. Beside genetic predispositions affecting mental health, their influence on pharmacological treatment by gene-drug interactions is getting more and more attention. Recently, a minimum pharmacogenetics testing panel of 16 genetic variants has been proposed to be integrated in the standard protocol of the therapeutic pharmacological treatment [18]. These variants are associated with the drug effectiveness by modifying the available drug dose in the body and the drug tolerability. In general, pharmacological treatment in severe mental disorders is often accompanied with various side effects. However, probable altered underlying molecular effects due to pharmacotherapy such as an altered gene expression are not well understood. Therefore, the main focus of this thesis lies on bipolar disorder and the effect of psychotropic drug treatment on hepatic gene expression.

1.3 Bipolar disorder, a mood disorder

Bipolar disorder, former known as manic depressive illness, manifests as chronic relapsing severe mental disorder typically characterized by unpredictable dramatic mood swings resulting in an impaired daily life functioning [11,19]. According to the World Health Organization report, the prevalence of bipolar disorder in the general population is 0.8%, whereas high income countries showed higher rates with 1.1% compared to low income countries with 0.4% [2]. These findings are consistent with data of the Global Burden of Disease Study 2017 for countries in Western Europe [20]. The age-standardized prevalence accounted for 1.0% for both sexes, whereas females have a slightly higher prevalence of 1.1% compared to males with a prevalence of 0.9%. With regard to the age at diagnosis, the highest prevalence of bipolar disorder is present in late adolescence and early adulthood for both sexes. Data sets of the

Global Burden of Disease Study 2017 has been used to outline the prevalence according to age and sex (***Figure 1***).

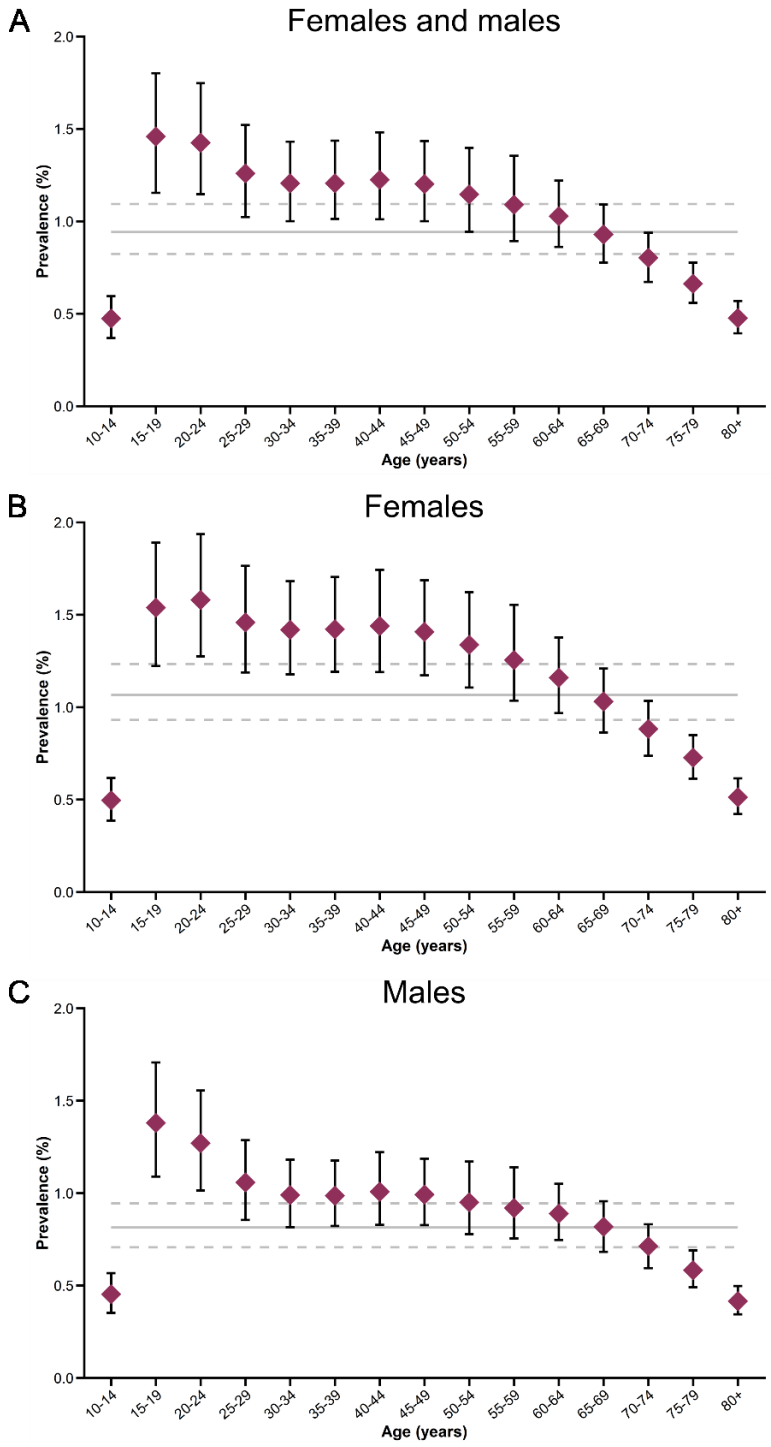

Figure 1. **Prevalence of bipolar disorder in Western Europe.** The prevalence according to the age categories are plotted for both sexes (A), and exclusively for females (B) and for males (C). The used data are provided by the Global Burden of Disease Study 2017 licensed under CC BY-NC 4.0 [20].

1.4 Subtypes of bipolar disorder

The classification and definition of severe mental disorders follows the widely used diagnostic criteria system of the Diagnostic and Statistical Manual of Mental Disorders (DSM), currently described in the fifth edition [21]. In general, bipolar disorder is characterized by the occurrence of interspersed mood swings comprising manic or hypomanic episodes, as well as depressive episodes alternating with phases of euthymia [19,22]. Based on the presence of those mood symptoms and their longitudinal appearance, different types of bipolar disorders are distinguishable (***Figure 2***).

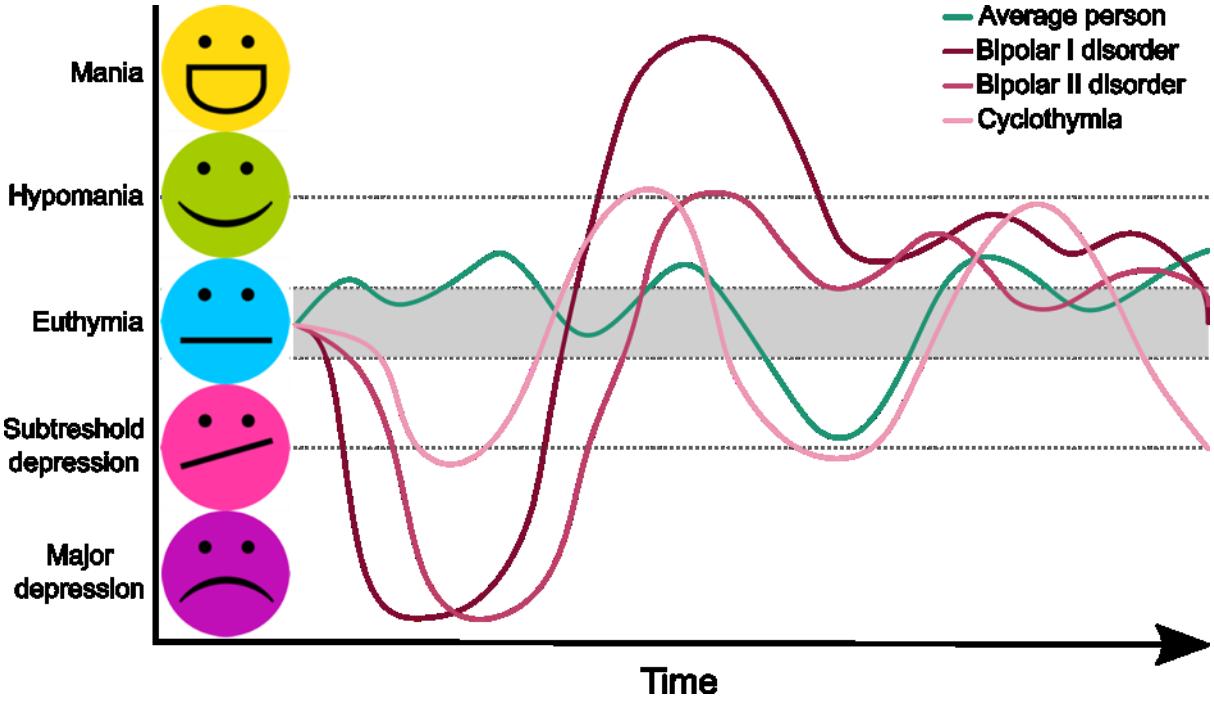

Figure 2. **Main subtypes of bipolar disorder.** The different mood states over time for typical courses of bipolar disorder subtypes are illustrated in a simplified form.

In bipolar I disorder, the occurrence of at least one manic episode characterizes this subtype, whereas the presence of major depressive episodes is not necessarily needed for the diagnosis. In contrast, patients with bipolar II disorder have at least one milder hypomanic episode often followed by a major depressive episode. A special feature of bipolar I and II disorder is the occurrence of mixed states, where manic or hypomanic symptoms occur simultaneously with features of depression [22]. Cyclothymic disorder is characterized by episodes of hypomanic and depression over a duration of two years, where the diagnostic criteria for mania or major

depression are not met [11,19]. A special subtype represents the bipolar disorder with the feature of rapid cycling, where at least four mood episodes per year appear [11,22].

1.4.1 Mood symptoms of bipolar disorder

According to the DSM criteria, mania describes states of marked elevated mood and increased motor drive [19]. Severe manic symptoms might cause severe social or occupational impairment or psychotic symptom manifestation that frequently results in the requirement of hospital admission to prevent self-harm or harm to others [19,22]. The minimum duration of a manic episode is defined as one week [22], but may last for months with an observed average of 3.25 months [23]. Numerous symptoms occur, such as increased activity, less need for sleep, excessive talkativeness, heightened self-esteem, grandiosity, megalomania and increased risk-taking [19,22]. In contrast, hypomania defines mood elevations milder than during manic episodes and with absent triggering of social or occupational impairment and the necessity for hospitalization [11,19,22]. The symptoms usually remain present for at least four consecutive days to be defined as hypomanic episode [19] and may last for months with an observed average of 3.63 months [23]. For major depressive episodes in bipolar disorder, the same DSM-V criteria are valid as for major depressive disorder and last for at least two weeks [22]. Depressive episodes are commonly longer lasting than manic or hypomanic episodes with a duration of 5.18 months averaged for all bipolar disorder types [23]. Common depressive symptoms are reflected by reduced motivation and loss of interest or pleasure, as well as weight loss or gain, changes in sleeping behavior including insomnia and hypersomnia, agitation, fatigue, difficulties with concentrating, feeling of worthlessness and guilt, as well as thoughts of death [22]. Severe depressive states might entail suicidal ideation or suicide attempt.

Although most of the patients with bipolar disorder recover from the first episode, a high recurrence probability exists [24–26]. A recurrence probability of more than 80% within seven years is shown [25]. The highest relapse risk persists during the first year after recovery, where 37% [26] to 50% [25] of patients relapse during this period. Despite a continuing prophylactic pharmacotherapy, a recurrence probability of more than 70% is present in patients within 5 years [25].

1.5 Therapeutic approaches in bipolar disorder

Those alternating and recurrent episodes of mania and depression considerably influence the functional and cognitive performance, as well as social and economic life of patients with bipolar disorder [25,27]. Due to fundamental differences of the therapeutic approaches in different mood states, a specified diagnosis is pivotal. Besides psychotherapy and psychoeducation with a wide range of therapy options including individual and interpersonal therapy settings, an effective drug treatment aiming to reduce symptoms and preventing mood episode recurrence by stabilizing the mood is essential [11,27–29]. In addition, electroconvulsive therapy might be applied to improve symptoms [29–31]. Therefore, to effectively manage and increase quality of live in patients with bipolar disorder, acute and long-term therapy and treatment is crucial.

1.6 Psychotropic drugs in the pharmacotherapy of bipolar disorder

Pharmacotherapy of bipolar disorder encompasses the usage of mood stabilizers, antipsychotics and antidepressants [19,27–29,32,33]. The use of specific pharmacological compounds in bipolar disorder relies predominately on observations of therapeutic effects in randomized control trials and the arising response to mood symptoms. The definite mode of action on molecular or biochemical levels remains mainly unknown. In general, these psychotropic drugs are supposed to target the regulation of neurotransmitters and neuronal hormones, the intracellular signaling affecting neuroprotection, neuronal growth and ion channels, as well as sleep and circadian rhythm [27,34]. The pharmacotherapy with psychotropic drugs may vary, a combined or adjunctive usage or the usage as monotherapy are applied.

1.6.1 Mood stabilizers

Pharmacological agents defined as mood stabilizers are drugs alleviating mood and psychotic symptoms predominantly during acute mania, and preventing recurrent mood episodes and prolong the inter-episode interval during prophylactic long-term treatment [35]. In addition, a sustained mood stabilizer treatment decreases the suicide rate in patients with bipolar disorder [36]. Despite their frequent clinical use, their underlying molecular mechanism of action remain unclear. Further, distinct drug characteristics, such as compound structure, aggravates the determination of overlapping molecular effects or targets [37]. Assumed downstream targets are supposed to be involved in neuronal and synaptic plasticity and

intracellular signaling [38]. Potentially affected intracellular signaling cascades are G-protein coupled signaling, protein kinase C signaling, glycogen synthase kinase-3 and Wnt signaling, and extracellular signal-regulated kinase (ERK) signaling cascade [37]. Moreover, possible epigenetic modifications based on mood stabilizers regulating gene expression are assumed [39].

1.6.2 Antipsychotics

Atypical antipsychotics are used during acute episodes and for long-term treatment as monotherapy or concomitant therapy [40]. A potential mechanism of antipsychotic treatment includes the reduction of manic behavior during an acute mania episode [41]. In addition, antipsychotics improve depressive mood symptoms during bipolar depression [42,43]. Antipsychotics potentially contribute to depressive symptom relief via their mediated effects for neurotransmitters including serotonin, dopamine and noradrenalin and the corresponding receptors in the brain [44].

1.6.3 Antidepressants

Since decades, acute depressive episodes are treated with antidepressants, though, a possible mood switch to a manic state, psychosis or aggressive behavior exist [33]. Despite their effectiveness for symptom relief, it is advised to use antidepressants in combination with mood stabilizers or antipsychotics, especially for bipolar I disorder, rather than as monotherapy [45,46]. Particularly the occurrence of mixed states represents a challenging setting to appropriate drug treatment [33,47]. Here, pharmacological treatment with antidepressants is discouraged due to their proposed potential to trigger a destabilized mood by provoking repeated induction of mixed states. Furthermore, long-term treatment with antidepressants is discouraged by most guidelines [29,48,49]. Sustained antidepressant monotherapy is associated with an increased risk of manic episode occurrence compared to mood stabilizer monotherapy or in combination with mood stabilizers [50]. In context of molecular effects, antidepressants are supposed to affect neuroplasticity probably by inducing gene expression and adaption of neurotransmitter function [51,52].

An overview of frequently used psychotropic drugs, the recommended scope of use and the targeted pharmacological profiles are listed (***Table 1***).

Table 1. **Recommended psychotropic drugs for bipolar disorder treatment.** Frequently used psychotropic drugs with their recommended application for the respective mood episode and during long-term treatment is indicated based on [19,29,47,48]. The pharmacological domains are listed for each drug and are based on the Neuroscience based Nomenclature devised by international psychopharmacological organizations [34,53].

Psychotropic drug	Acute mania	Acute bipolar depression	Acute mixed state	Long-term treatment	Modified neurotransmitter/ molecule/system
Mood stabilizers					
Carbamazepine	+	+	-	+	glutamate
Lamotrigine	--	+	+	++	glutamate
Lithium	++	+	-	++	glutamate
Valproate	+	+	+	+	glutamate
Antipsychotics					
Clozapine	+	+	-	+	dopamine, serotonin, norepinephrine
Olanzapine	++	++	++	+	dopamine, serotonin
Quetiapine	++	++	-	++	dopamine, serotonin, norepinephrine
Risperidone	+	-	-	+	dopamine, serotonin, norepinephrine
Ziprasidone	+	-	+	+	dopamine, serotonin
Antidepressants					
Monoamine oxidase inhibitor (MAOI)	--	+	-	-	serotonin, norepinephrine, dopamine
Serotonin norepinephrine reuptake inhibitors (SNRI)	--	+	-	-	serotonin, norepinephrine
Selective serotonin reuptake inhibitors (SSRI)	--	+	-	-	serotonin
Tricyclic antidepressants (TCA)	--	+	-	-	serotonin, norepinephrine, dopamine

++ = highly recommended; + = recommended; - = non-recommended; -- = definitely non-recommended

1.7 Biotransformation of psychotropic drugs

The kinetic of psychotropic drugs relies on drug absorption, distribution, metabolism and elimination [54]. The majority of psychotropic drugs are highly fat-soluble compounds and require biotransformation for the generation of a metabolic compound or prior to drug elimination, whereby the liver is the primary site for drug metabolism [55]. The biotransformation of xenobiotics such as psychotropic drugs consist of phase I and II. For a parent drug compound, biotransformation in phase I results in less lipophilic and more polar compound by oxidation, reduction or hydrolysis. Enzymes common in phase I biotransformation of psychotropic drugs are cytochrome P450 (CYP) enzymes [56–60]. In phase II, the conjugation of hydrophilic groups increase the water solubility of these compounds and, hence, their elimination from the body [55,56]. Enzymes mainly involved in the phase II biotransformation of psychotropic drugs are transferases for glucuronic acid, sulfate, acetate, glutathione, and methyl group [56,61]. Phase I and/or II biotransformation of the parent compound into metabolic compounds is sometimes necessary to achieve the therapeutic psychotropic drug effect [62]. The majority of drugs reveal reduced pharmacological activity after biotransformation, but some antipsychotics and antidepressants are metabolized into active metabolites [55]. However, biotransformation of the parent compound could also result in toxic metabolites, which are rather derived from phase I than phase II [57]. Due to the toxic potential of psychotropic drugs, it is hardly surprising that adverse drug effects are common during pharmacological treatment in bipolar disorder and, in general, in severe mental disorders.

1.8 Adverse side effects of psychotropic drugs

The first line treatment in bipolar disorder is pharmacotherapy, yet frequent and infrequent adverse side effects are known in association with acute and long-term psychotropic drug treatment. The side effects range from adverse cognitive and neurological events [58,63,64] to adverse hormonal [58,64,65], gastrointestinal [58,64], and immunological events [64]. In addition, teratogenic effects [64] and adverse effects on the renal function [64,65] are observed, as well as weight gain [58,63,65,66] and the development of the metabolic syndrome [63,64], and hepatotoxicity [67,68].

1.9 Hepatotoxicity and drug-induced liver injury

The liver, as the main site of systemic glucose and lipid biosynthesis [69], is frequently affected in severe mental disorder including bipolar disorder. Especially, patients with long-term psychotropic drug treatment are at risk of non-alcoholic liver disease (NAFLD) [70]. According to a recent meta-analysis, the general NAFLD prevalence in the population of Europe and North America is estimated to be 23.71% and 24.13%, respectively, which is slightly lower than the estimated global average prevalence of 25.24% [71]. The highest rates were observed in South America and Middle East with a prevalence more than 30%. In addition, increased NAFLD prevalence is associated with factors such as the presence of type 2 diabetes or an increased body mass index (BMI) [72]. Both, diabetes [73] and an increased BMI [74], have a higher prevalence in bipolar disorder compared to a reference population. Patients with NAFLD are faced with an elevated risk for the overall mortality, the development of liver cirrhosis and hepatocellular carcinoma (HCC) [75]. The determined hazard ratios were, 1.29, 3.20 and 6.55, respectively. With regard to patients with bipolar disorder, a 2.28 higher likelihood was determined for any chronic liver disease [76] and a 2.57 higher likelihood for the presence of NAFLD compared to controls without bipolar disorder [77]. Consequently, patients with bipolar disorder treated with psychotropic drugs represent a highly vulnerable group for the development NAFLD and its progression.

1.10 Spectrum of NAFLD

NAFLD covers a wide spectrum of liver diseases ranging from simple hepatic steatosis to non-alcoholic steatohepatitis (NASH), progressive fibrosis and cirrhosis, and a possibly increased risk for the development of HCC, but with the absence of significant alcohol consumption [78]. The underlying mechanism for the development of lipid accumulation, hepatocyte injury and inflammation in NAFLD is complex with multiple supposed intrinsic and extrinsic factors. Factors such as genetic predisposition and epigenetic modifications, environmental factors and to a great extent dietary habits influence hepatocellular fat and inflammatory conditions. NAFLD has been linked to insulin resistance, obesity and type 2 diabetes, all of which are signs of the metabolic syndrome [79–81]. Today, the assumed origin of NAFLD development underlies a multiple hit hypothesis [78,82]. Lipotoxicity and glucotoxicity seem to play a central role [81]. Accumulation of lipids is a key event of NAFLD, whereas the presence of excessive fatty acids relies on dietary intake, lipolysis of adipose tissue and substantially on *de novo*

lipogenesis [80]. The grading and staging of NAFLD comprises the evaluation of histopathological features for steatosis, inflammation and cellular injury [79,80].

1.11 Histopathological features of NAFLD

The lipid accumulation present during simple hepatic steatosis is reversible and defined as non-alcoholic fatty liver (NAFL) if at least 5% of hepatocytes present steatosis [79,83,84]. On the histological view, the intracellular lipid accumulation pushes the nucleus to the margins of the hepatocyte visually resembling an adipocyte [79]. The stored lipids visually manifest as lipid-containing vacuoles usually in macrovesicular or medio-macrovesicular form. However, the cellular excess of lipids due to a constant uptake, *de novo* synthesis and an insufficient lipid metabolism results in toxicity due to cellular injury by endoplasmic reticulum stress, mitochondrial damage and oxidative stress [80,85]. These intracellular stress signals based on the inability to resolve excessive lipids can induce apoptosis.

Advanced hepatocellular injury can be present as degenerative ballooned hepatocytes, a key feature for NASH [84]. These are hepatocytes without steatotic vacuoles but with a clear to flocculent cytoplasm and possible intracytoplasmic inclusion bodies primarily composed of misfolded cytokeratin 8 and 18 filaments, chaperone and heatshock proteins, which are defined as Mallory-Denk bodies [84,86]. Along with the occurrence of hepatocellular ballooning, an inflammatory response characterizes NASH [79,86]. Often mild chronic lobular inflammation is present at small foci with infiltrated lymphocytes, macrophages and neutrophils [79]. Usually, portal fibrosis is present in NASH [79,84,86], however, the degree of fibrosis highly varies and may already be present in NAFL [79]. During fibrosis, the architecture of the parenchymal liver tissue is being rearranged. Hepatocytes are separated and replaced by strands of collagen deposits along with extracellular matrix proteins [79,84]. Bridging fibrosis is present in advanced disease stages. With the progression of liver injury, functional liver tissue is largely replaced by scar tissue which severely interferes with the physiological liver function [84]. Cirrhosis is defined as end stage liver disease for chronic liver diseases, whereas the cirrhosis incidence based on NASH is higher than in NAFL [87]. In addition, NAFLD progressing to cirrhosis is assumed as primary indication for liver transplantation in future.

1.12 Complex underlying mechanisms of NAFLD

The molecular mechanisms contributing to the development and progression of NAFLD are not fully elucidated, however, assumed affected pathway candidates are the metabolism of lipids and glucose and inflammatory pathways. These affected pathways are probably based on dysregulated genes arising from the loss of regular gene expression maintenance and of precise transcriptional control. A gene expression study investigating the possible associations between simple steatosis and hepatic gene expression revealed various involved genes of diverse molecular pathways [88]. Particularly pathways, such as the metabolism of glucose, lipids and amino acids, insulin signaling, inflammatory response and cell adhesion, are supposed to be implicated in NAFLD. In addition, a gene expression signature comprising 218 genes has been identified in a meta-analysis of publicly available datasets investigating their association with histopathological NAFLD features [89]. This emphasizes the possible application of biomarkers based on gene expression level for the identification and stratification of NAFLD and its disease progression which in turn could be beneficial for disease monitoring and therapeutic interventions. Even though patients with bipolar disorder and psychotropic drug treatment are at higher risk to develop NAFLD, the possible effect of pharmacological treatment altering the gene expression and adversely influencing hepatic function remains unclear.

1.13 Rationale of this thesis

Up to now, less is known about the molecular effect of psychotropic drugs on hepatic gene expression and in the presence of NAFLD. Analysis of transcriptomics and their integration into comprehensive bioinformatical analyses, such as pathway, enrichment and interaction analyses, provides the basis for understanding complex disorders like NAFLD and in the special setting during psychotropic drug treatment. Therefore, the determination of deregulated genes in a disease and their respective protein function in an intricate network of protein interactions could provide insights into altered molecular processes and reactions associated with specific biochemical pathways. Further, the integration of gene expression data and histopathological features of NAFLD could be used to define molecular settings triggering an altered or a harmed phenotype.

This thesis addresses the fundamental effects of psychotropic drug treatment on gene expression level in the liver of patients with bipolar disorder compared to a histopathological

comparable control sample. Therefore, comprehensive bioinformatical analyses were established and the validation of the transcriptomics data was performed. Additionally, thorough association studies between gene expression and hepatic histopathological features were assessed.

2 Materials and Methods

The Materials and Methods section is in part identical to the information that was published in Birkl-Toeglhofer et al. [90].

2.1 Human liver tissue samples

Liver tissue of deceased patients with bipolar disorder and controls were collected as part of the Stanley Neuropathology Consortium Collection of the Stanley Medical Research Institute (Chevy Chase, MD, USA). Information regarding the patient's medical and psychiatric history was ascertained by the patient's medical records and by an interview with the next of kin. The clinical diagnosis was made according to the DSM-IV criteria. Liver tissue from patients was collected during autopsy after the donation permission was obtained from the patient's next of kin. For the sample collection, a technically standardized procedure was applied by trained medical examiners. Due to the presence of de-identifiable specimens of deceased human subjects the Institutional Review Board of the Uniformed Services University of the Health Sciences, Bethesda, decided that the Institutional Review Board ethical approval was not required for the collected samples of the Stanley Neuropathology Consortium Collection. A public statement of the Stanley Medical Research Institute is available at http://www.stanleyresearch.org. The study was approved by the local ethics committee of the Medical University of Graz (31-41 ex 18/19). Differences of demographic and clinical characteristics between the groups were tested for significance using the unpaired t-test for normally distributed data. The Fisher's exact test was used for binary data. All statistical analyses were performed using IBM SPSS Statistics, v23 (IBM Corp., Armonk, NY, USA).

2.2 Global gene expression analysis

2.2.1 Microarray processing

Post mortem liver tissue of patients with bipolar disorder and control samples from the Stanley Medical Research Institute (Chevy Chase, MD, USA) were included in the global gene expression analysis. All sample preparation, including RNA extraction, RNA quality and quantity assessment and array processing steps of the microarray analysis, were performed at the Microarray Core Facility of the Johns Hopkins University (Baltimore, MD, USA). In brief, frozen liver tissue was used for the RNA extraction. The liver tissue was extracted using TRIzol

(Invitrogen, Carlsbad, CA, USA) and chloroform method. Total RNA was precipitated with isopropyl alcohol and washed with 70% ethanol. The precipitated and washed RNA was dissolved in diethyl dicarbonate water. An additional RNA purification step was added using the RNeasy column purification (Qiagen, Valencia, CA, USA). The RNA quantity and quality was assessed using the Agilent Bioanalyzer (Agilent Technologies, Palo Alto, CA, USA). The quality was represented by the RNA integrity number (RIN). For the investigation of global gene expression, the oligonucleotide array GeneChip Human Genome U133 Plus 2.0 array (Affymetrix, Santa Clara, CA, USA) was used. The CEL files were kindly provided by Prof. Serge Weis (Division of Neuropathology, Department of Pathology and Neuropathology, Neuromed Campus, Kepler University Hospital, Medical School, Johannes Kepler University, Linz, Austria) for further processing.

2.2.2 Data pre-processing and assessment of quality metrics

Several steps were implemented prior to the assessment of differentially expressed genes (DEGs), including quality control steps, background adjustment, normalization and summarization. All of the bioinformatical analysis steps for the pre-processing and the quality assessment were performed using the open source software R 3.4.1 [91]. The Bioconductor package ‘affy’ [92] was used to read the generated CEL file of each chip.

Quality metrics were assessed for the raw data including average background and percentage of present calls. Visual exploration was performed on the probe intensity distribution. The relationship between probe intensity and difference to the median probe intensity was assessed. Quality control on the normalized data included a non-specific filtering step and the assessment of the overall sample variability. The average background and the percentage of genes called present were obtained using the Bioconductor package ‘simpleaffy’ [93]. To examine potential issues on RNA quality, the averaged probe intensity of all probes was plotted against the position of the probe. The focus was set on the appearance of the slope and the shape of the plotted curves from the 5’ to the 3’ end of the probesets. The Bioconductor package ‘affy’ [92] was used. To identify possible outliers deviating from the average intensity distribution, boxplots were generated prior and after normalization. Slight deviations were equalized by ensuing normalization, whereas extreme deviations would let to the exclusion of the sample. For the examination of the probe intensity and the difference to the median probe intensities, MA-plots were generated for each sample prior and after normalization. The M represents the

probe intensity ratio of one array and the median intensity of this probe over the entire arrays. The A denotes the average probe intensity of a single array and the median intensity of this probe over the entire arrays. The Bioconductor package 'affy' [92] was applied for the plotting.

An example R code is as follows:

```
# Load necessary packages
library('affy')
library('simpleaffy')
library('graphics')

# Read in .CEL files
data <- ReadAffy(celfiles)

# Perform quality control on the raw data
data.qc <- qc(data)

# Assess the average background for each sample
avbg <- avbg(data.qc)

# Obtain the percentage of present calls
pp <- percent.present(data.qc)

# Obtain RNA degradation
deg_data <- AffyRNAdeg(data)

# Plot the slope from the 5' to the 3' end
plotAffyRNAdeg(deg_data)

# Plot boxplot for perfect match probes for raw intensity data
boxplot(data,
        transfo = log2,
        which = 'pm')

# Plot boxplot for perfect match probes for normalized intensity data
boxplot(norm_data,
        transfo = identity,
        which = 'pm')

# Plot MA plot for raw intensity data
MAplot(object=data,
       which = 1)
```

```
# Plot MA plot for RMA normalized intensity data
MAplot(object=norm_data,
       which = 1)
```

2.2.3 Array-to-array normalization

To normalize the samples and, hence, control for array-to-array variation, the Robust Multi-array Average (RMA) algorithm [94] was applied. The RMA algorithm includes background correction, quantile normalization and the expression calculation. To generate RMA normalized expression values of the oligonucleotide arrays, the Bioconductor package 'affy' [92] was applied using the open source software R 3.4.1 [91].

Next, non-specific filtering was applied to the normalized expression data. Probes were removed when the low overall intensity was less than the $\log_2(100)$ in a minimum of 10% of the samples and when the low overall variability of the $\log_2$ intensities interquartile range was below 0.5. The Bioconductor package 'genefilter' [95] was applied to filter for low overall intensity values. To filter for low overall variability of expression values, an anonymous function was implemented.

An example R code for the non-specific filtering is as follows:

```
# Normalization of the raw expression data with RMA
norm_data = rma(data)

# Filtering of probes with low overall intensity values
filter1 <- pOverA(0.10,
                  log2(100))

# Filtering of probes with low overall variability across samples
filter2 <- function(x)(IQR(x)>0.5)

# Combining filter functions into one function
filter <- filterfun(f1, f2)

# Implementation of non-specific filtering to normalized data
data_filtered <- genefilter(norm_data,
                            filter)
```

2.2.4 Substructure analysis based on gene expression data

For the assessment of the overall sample variability, a principal component analysis (PCA) was performed with the normalized and filtered expression data using the open source software R 3.4.1 [91]. The PCA was used to acquire information on possible sample cluster formation and similarities between samples in an unsupervised manner.

An example R code for the substructure analysis is as follows:

```
# Computation of principal components of gene expression data
pca <- prcomp(t(exprs(norm_data)),
              center = TRUE,
              scale. = TRUE)

# Ploting of a screeplot of first ten principal components
fviz_screeplot(pca,
               ncp = 10)

# Ploting first principal component against second principal component
autoplot(pca)
```

2.2.5 Assessment of differential gene expression

To assess DEGs between bipolar disorder and the controls, a linear model with a moderate t-statistic was fitted to each probe. Several factors were used to adjust for probable confounding effects in the model. The factors included age, sex, BMI and *post mortem* interval (PMI). All probes were corrected for multiple testing by Benjamini and Hochberg adjustment. To define DEGs, the expression and the significance threshold of probes was set to a fold change of 1.5 and a false discovery rate (FDR) of less than 5%. All steps for the differential gene expression assessment were performed using R 3.4.1 [91]. The used Bioconductor package was ‘limma’ [96].

All probesets were annotated to the corresponding Human Genome Organization (HUGO) Gene Nomenclature Committee (HGNC) gene symbol, name and unique identifier using the Bioconductor package ‘biomaRt’ [97].

An example R code for the annotation is as follows:

```
# Create an appropriate design matrix
design <- model.matrix(~ 0 + factor)

# Fit the linear model
fit <- lmFit(data_filtered ~ design)

# Create the contrast matrix and compare groups
cont_matrix <- makeContrast(BPD-CTRL,
                            levels = design)
cont_fit <- eBayes(contrasts.fit(fit,
                                 cont_matrix))

# Extract a list of differentially expressed genes in bipolar disorder
topTable(cont_fit,
         coef = 1,
         adjust.method = 'BH')

# Query databases for entries of the Affymetrix probeset IDs
getBM(attributes = affy_ensembl,
      mart = ensembl,
      values = "*",
      uniqueRows = TRUE)
```

2.3 Protein-protein interaction network analysis

Gene names of the DEGs were used as input for the stringApp, version 1.5.0 [98], a built-in app of Cytoscape, version 3.7.2 [99], an open source software for visualizing complex networks. The stringApp extracts data from the Search Tool for the Retrieval of Interacting Genes/Proteins (STRING) database [100,101]. The STRING protein query was used to find reliable protein-protein interactions with a minimum confidence score of 0.7. Using Cytoscape, the protein-protein interaction network was generated, whereas the $\log_2$ fold change was used for the node color.

2.3.1 Analysis of key regulators of the protein-protein interaction network

A screening for topologically highly connected nodes, so called hubs, in the protein-protein interactome was performed using the Cytoscape built-in app cytoHubba, version 0.1 [102]. Global central nodes were measured based on the betweenness centralities providing normalized values which are independent to the network size.

2.3.2 Module analysis of the protein-protein interaction network

The modules of closely-connected subnetworks of the generated protein-protein interactome were investigated using the Cytoscape built-in app ClusterViz, version 1.0.3 [103]. The Molecular Complex Detection (MCODE) clustering algorithm [104] based on density weighted nodes was used for module identification. The following cluster identification criteria were chosen: a minimum number of 2 edges per node (degree threshold), less than 20 % node score deviation from the seed node for new cluster members (node score threshold), at least 2 or more connections per node (k-core threshold), and an virtually unlimited distance from seed node to cluster members of 100 (maximum depth). A module cut-off with a score of >4 was applied.

2.4 Analysis of functional pathways

For the identification of over-represented functional pathways in bipolar disorder compared to controls, the open-source tool WEB-based GEne SeT AnaLysis Toolkit (WebGestalt) [105,106] was used. The DEGs were examined for enriched functional pathways included in the Reactome Pathway Database. Pathways categories involving 5 to 1000 genes and a FDR of less than 0.05 for the multiple testing correction were set as analysis parameters. In addition, Gene Ontology (GO) terms were queried for cellular components, biological processes and molecular function using WebGestalt.

2.5 Validation of microarray data using quantitative real-time PCR

2.5.1 RNA isolation

For total RNA isolation, frozen post-mortem liver tissue from 16 bipolar disorder samples and 14 controls was used. Tissue homogenization was performed in 1 ml TRIzol Reagent (Thermo Fisher Scientific, Waltham, MA, USA) using a MagNA Lyser Instrument (Roche Diagnostics, Risch-Rotkreuz, Switzerland). The homogenization was performed in two rounds of 6500 rpm for 40 sec. After an incubation of 10 min on ice, the tissue homogenate was centrifuged at 10,000 x g for 10 min at 4 °C. For phase separation, 200 µl chloroform was added and vigorously mixed, followed by an incubation of 10 min at room temperature and a centrifugation at full speed for 15 min at 4 C. The upper aqueous phase containing RNA was precipitated with isopropyl alcohol and a high salt solution with 1.2 M sodium chloride and 0.8 M sodium citrate for 10 min at room temperature. After a centrifugation step at full speed

for 20 min at 4 °C and the removal of the supernatant, the pellet was washed twice with 80 % ethanol and dried for 5 min at 37 °C. The isolated RNA was dissolved in RNase-free water. RNA quantity and quality were measured using the NanoDROP 1000 (Thermo Fisher Scientific Inc., Waltham, MA, USA). The samples were stored at -20 °C until further processing.

2.5.2 Reverse transcription and quantitative real-time PCR

In total, 2 µg RNA was reverse transcribed using the High Capacity cDNA Reverse Transcription Kit (Applied Biosystems, Foster City, CA, USA) containing an RNase inhibitor (Applied Biosystems, Foster City, CA, USA). A reaction volume of 20 µl was cycled according to the manufacturers instruction in the GeneAmp 9700 Thermocycler (Applied Biosystems, Foster City, CA, USA). The gene expression validation analysis was performed for 14 genes and 3 endogenous control genes. Gene specific primers were designed using Primer-BLAST [107] (***Table 2***). For quantitative real-time PCR, the Luna Universal qPCR Master Mix (New England Biolabs, Ipswich, MA, USA) was used according to the manufactures protocol. The reaction volume of 10 µl contained a final concentration of 10 ng cDNA, 0.2 µM of the gene specific forward and reverse primer and 5 µl of the Luna Universal qPCR Master Mix. To exclude cDNA cross contamination and contaminating DNA, a no template control with absent cDNA and a no amplification control with lacking reverse transcription reaction was included for each tested gene. Gene expression values were assessed as triplicates for each sample in 384-well plates using the QuantStudio 7 Flex Real-Time PCR System (Applied Biosystems, Foster City, CA, USA). The cycling conditions were as follows: 50 °C for 2 min and 95 °C for 10 min for the initial denaturation, followed by 45 cycles of denaturation at 95 °C for 15 sec and extension at 60 °C for 60 sec, and a melting curve stage at the end at 95 °C for 15 sec, 60 °C for 60 sec and 95 °C for 15 sec. A run quality control was performed using the QuantStudio Real-Time PCR Software, version 1.3 (Applied Biosystems, Foster City, CA, USA) including melting curve examination. A random mixture of amplified samples were used to validate the amplicon size for each gene. The amplicon sizes were examined by loading 10 µl of amplification product in each slot on a 2 % agarose gel stained with HDGreen Plus DNA Stain (Intas Science Imaging, Goettingen, Germany). Gel electrophoresis was performed for 30 min at 100 V. The amplicons were visualized using the Gel iX20 Imager (Intas Science Imaging, Goettingen, Germany). Only samples with a proper melting curve indicating a specific amplicon were included for further analysis.

Table 2. **Primers used for gene expression validation by quantitative real-time PCR.** The RefSeq accession numbers of targeted transcripts, the forward (F) and reverse (R) primer sequences and the expected amplicon size of each gene and the endogenous controls are listed. [Published in [90]]

Gene	RefSeq accession number	Primer sequence (5'-3')	Amplicon size (bp)
LRPPRC	NM_133259	F: 5‘-GCCGGAGGACTACTGAGC-3‘ R: 5‘-AGCAAGGCATGACTACCACC-3‘	230
ATP5PB	NM_001688	F: 5‘-TGCTACCTGGACTTTCGTTGA-3‘ R: 5‘-CTGCAATACCCCTGGACCTA-3‘	110
SDHB	NM_003000	F: 5‘-CACTCTAGCTTGCACCCGAA-3‘ R: 5‘-CCGTCCAGTTTCTCACGCTCT-3‘	219
PON1	NM_000446	F: 5‘-ATCGAAACTGGCTCTGAAGAC-3‘ R: 5‘-ACGACCACGCTAAACCCAAA-3‘	469
ACOT13	NM_018473	F: 5‘-GGACTTTCCAGCTCTTCCGA-3‘ R: 5‘-GAGTAATCTTTCCCAAAACTCTCT-3‘	152
AADAC	NM_001086	F: 5‘-GCGTGGGAAGTGCTGCTCTAA-3‘ R: 5‘-CTGGGTCATCAAGGAGCTGTT-3‘	273
CMBL	NM_138809	F: 5‘-GTTCAAGTCGAGCACATCAAGG-3‘ R: 5‘-ACAATGCCATAGACGGACACC-3‘	401
HIBADH	NM_152740	F: 5‘-TGCAGGTGAACAGGTAGTATCTT-3‘ R: 5‘-CCAGAAACAGGGGCATCCAT-3‘	243
TDO2	NM_005651	F: 5‘-TATCTCCAGCATCAGGCTTCC-3‘ R: 5‘-GCCATGCCTCCACTAATTCC-3‘	186
HAO1	NM_017545	F: 5‘-ACAAGGACCGAGAAGTCACC-3‘ R: 5‘-CCTGGCATCATCACCTCTCAA-3‘	335
CAT	NM_001752	F: 5‘-CCTGTGAACTGTCCCTACCG-3‘ R: 5‘-ATAGAATGCCCGCACCTGAG-3‘	222
PSMA2	NM_002787	F: 5‘-CTACATTCAGCCCGTCTGGT-3‘ R: 5‘-GGTCGTCCCTCATTCCAAC-3‘	400
S100A9	NM_002965	F: 5‘-CAAGAAGGAGAATAAGAATGAAAAG-3‘ R: 5‘-AGCATGATGAACTCCTCGAA-3‘	144
S100A12	NM_005621	F: 5‘-TGCAAACACCATCAAGAATATCAAA-3‘ R: 5‘-GTGTGGTAATGGGCAGCCTT-3‘	99
GAPDH	NM_002046, NM_001256799, NM_001289745, NM_001289746, NM_001357943	F: 5‘-AAATCAAGTGGGGCGATGCT-3‘ R: 5‘-CAAATGAGCCCCAGCCTTCT-3‘	86
RPL41	NM_021104, NM_001035267	F: 5‘-AAGATGAGGCAGAGGTCCAA-3‘ R: 5‘-TCCAGAATGTCACAGGTCCA-3‘	248
IPO8	NM_001190995, NM_006390	Hs_IPO8_1_SG (QuantiTect Primer Assay; Qiagen, Hilden, Germany)	124

LRPPRC - leucine rich pentatricopeptide repeat containing; *ATP5PB* - ATP synthase peripheral stalk-membrane subunit b; *SDHB* - succinate dehydrogenase complex iron sulfur subunit; *PON1* - paraoxonase 1; *ACOT13* - acyl-CoA thioesterase 13; *AADAC* - arylacetamide deacetylase; *CMBL* - carboxymethylenebutenolidase homolog; *HIBADH* - 3-hydroxyisobutyrate dehydrogenase; *TDO2* - tryptophan 2,3-dioxygenase; *HAO1* - hydroxyacid oxidase 1; *CAT* - catalase; *PSMA2* - proteasome subunit alpha 2; *S100A9* - S100 calcium binding protein A9; *S100A12* - S100 calcium binding protein A12; *GAPDH* - glyceraldehyde-3-phosphate dehydrogenase; *RPL41* - ribosomal protein L41; *IPO8* - importin 8;

Obtained raw expression values were used to evaluate the relative gene expression by the $2^{-\Delta\Delta Ct}$ method [108]. The mean of the endogenous control genes was used for normalization. Differences in gene expression between the groups were assessed using the unpaired t-test or the Mann Whitney U test depending on data distribution. The differences were expressed as x-fold changes. The statistical analyses were performed using GraphPad Prism 6 (GraphPad Software, San Diego, CA, USA). The plots were generated using R 3.4.1 [91].

2.6 Histopathological assessment of liver tissue

For the histological assessment, 5 µm sections of formalin-fixed and paraffin-embedded liver tissue of patients with bipolar disorder and controls were stained with various histological and immunohistochemical staining methods for the features of interest. The histological parameters were assessed and scored by two experienced pathologists, both blinded to the diagnosis. The histological assessment and the scoring of the histopathological features were performed prior to this thesis and were provided for this study. The histopathological parameters were statistically analyzed using the chi-square test for binary data and the Mann Whitney U test for categorical data. The frequency distribution of the histopathological features were plotted as stacked bar plots. The statistical analyses and the graphical visualization were performed using R 3.4.1 [91].

2.7 Association analyses between gene expression and histopathological features

The association of histologically assessed characteristics (*feature*) and the $\log_2$ intensity values as measure of gene expression (*expression*) were visualized as feature-expression heatmaps based on a previously described approach [109]. All features were categorized into six groups: (1) degenerative changes, (2) hepatic activity, (3) endogenous hepatic activity, (4) steatosis, (5) fibrosis and (6) inflammation. Applying ordinal logistic regression and binary logistic regression with regard to the histological data type, association analyses with the $\log_2$ intensity values were performed for the bipolar disorder samples. The analyzed genes for the association analyses included the ten most altered DEGs discovered by the over-represented functional pathways analysis. The feature-expression heatmaps display the effect size, the standard error, the *p*-value and the FDR adjusted *p*-value from the Benjamini and Hochberg correction. An FDR adjusted *p*-value of <0.2 was considered as statistically significant. Statistical analyses

and plotting were performed using R 3.4.1 [91] and MATLAB 2012b (The MathWorks, Inc., Natick, Massachusetts, USA).

3 Results

3.1 Subject characteristics

The subject characteristics were examined (***Table 3***). The mean age of the bipolar disorder group and the control group was comparable. For the control group, a lower number of females was included in the analysis. The BMI was comparable, the mean BMI for the bipolar disorder group was classified as obesity class I (BMI range: 30.0-34.9) and for the controls as pre-obesity (BMI range: 25.0-29.9), according to the World Health Organization BMI classification [110]. A statistically significant difference was observed for PMI between the groups. The bipolar disorder group revealed longer PMI values than the controls.

Table 3. **Characteristics of subjects with bipolar disorder and controls.** [Published in [90]]

	Bipolar disorder (n=29)		**Controls (n=20)**		***p*-value**
Age, years, mean (±SD)	41.8	(±14.93)	45.9	(±11.13)	0.276
Gender, n (%)					
Female	15	(51.7)	4	(20.0)	0.037
Male	14	(48.3)	16	(80.0)	
BMI[1], kg/m², mean (±SD)	30.8	(±6.82)	27.8	(±6.34)	0.123
PMI[2], hours, mean (±SD)	39.1	(±20.36)	23.1	(±10.48)	0.002
Medication, n (%)					
antidepressants	15	(51.7)			
antipsychotics	16	(55.2)			
mood stabilizers	21	(72.4)			
anticholinergic	1	(3.5)			

[1]BMI, body mass index; [2]PMI, *post mortem* interval;

3.2 Pre-processing and normalization of microarray data

The microarray data were pre-processed and normalized in order to remove noise. In total, each array included 54675 probes in the analyses.

3.2.1 Assessment of average background and percent present calls

The individual average background values and percentage of genes called present were listed (***Table 4***). The average background and standard deviation of bipolar disorder and control samples was 38.5 ±8.28 and 43.8 ±8.36, respectively, whereas the mean average background and the standard deviation of both groups was 40.9 ±8.63. All of the samples fell into an average background range of 2.5 standard deviations. The mean and standard deviation of percent present calls in the groups was 29.1% ±3.06% and 19.7% ±6.53%, respectively. The overall mean and standard deviation of both groups was 23.5 ±7.08, of which all but one bipolar disorder sample fall into a range of 2.5 standard deviations.

Table 4. **Assessed averaged background and present calls.** Individual average background and percentage present calls (% PP) of bipolar disorder (BPD) and control (CTRL) samples are listed.

Sample	Average background	% PP	Sample	Average background	% PP
CTRL01	54.3	28.0	BPD01	30.9	18.3
CTRL02	41.6	26.7	BPD02	32.9	25.3
CTRL03	47.5	28.7	BPD03	30.5	17.2
CTRL04	43.5	27.7	BPD04	32.0	23.2
CTRL05	35.4	33.7	BPD05	33.1	14.3
CTRL06	33.2	34.0	BPD06	38.8	28.5
CTRL07	35.3	27.8	BPD07	42.6	24.7
CTRL08	34.1	30.5	BPD08	52.9	23.1
CTRL09	37.7	32.4	BPD09	46.3	18.0
CTRL10	29.3	28.4	BPD10	34.0	16.3
CTRL11	42.1	29.2	BPD11	30.6	28.6
CTRL12	45.5	31.3	BPD12	37.4	13.3
CTRL13	59.4	27.1	BPD13	46.8	9.9
CTRL14	57.3	29.8	BPD14	42.2	8.9
CTRL15	45.4	30.6	BPD15	47.5	20.5
CTRL16	44.6	34.3	BPD16	36.0	5.5
CTRL17	55.4	27.8	BPD17	39.2	19.0
CTRL18	52.9	25.1	BPD18	46.0	23.3
CTRL19	42.5	27.0	BPD19	31.0	18.1
CTRL20	39.8	21.5	BPD20	29.8	27.6
			BPD21	56.0	22.6
			BPD22	28.5	25.9
			BPD23	40.1	21.8
			BPD24	29.7	32.6
			BPD25	34.8	19.0
			BPD26	29.2	7.0
			BPD27	59.1	24.6
			BPD28	35.6	16.8
			BPD29	42.5	18.4

3.2.2 Assessment of RNA degradation

The RNA quality was compared between all samples and plotted as RNA degradation plot (***Figure 3***). An overall comparable RNA quality degradation was indicating similar RNA quality in all samples. The consistent ascending slopes of all samples represented an absence of intense RNA degradation differences between the samples.

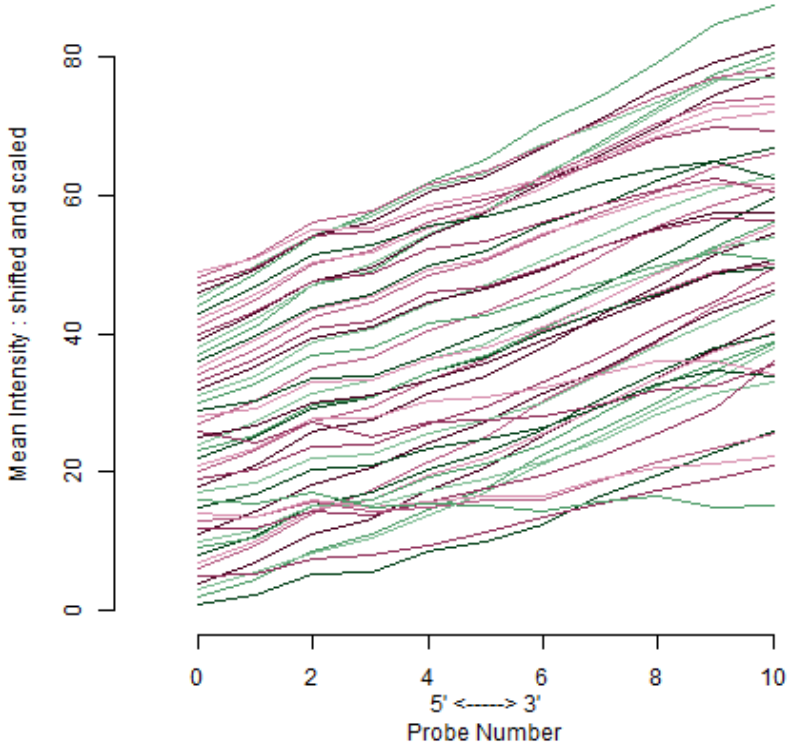

Figure 3. **RNA degradation analysis of bipolar disorder and control samples.** The mean intensity of each probe (y-axis) is given across all probe sets from the 5' to the 3' end (x-axis). Each line corresponds to one sample.

3.2.3 Assessment of inter-sample intensity distributions

The between-array intensity boxplots of the samples were plotted to evaluate the inter-sample distribution of the gene expression data. A noise removal was observed after RMA normalization represented by the comparable distribution of $\log_2$ intensity values across samples after normalization compared to the strong deviating distribution of the raw data (***Figure 4***).

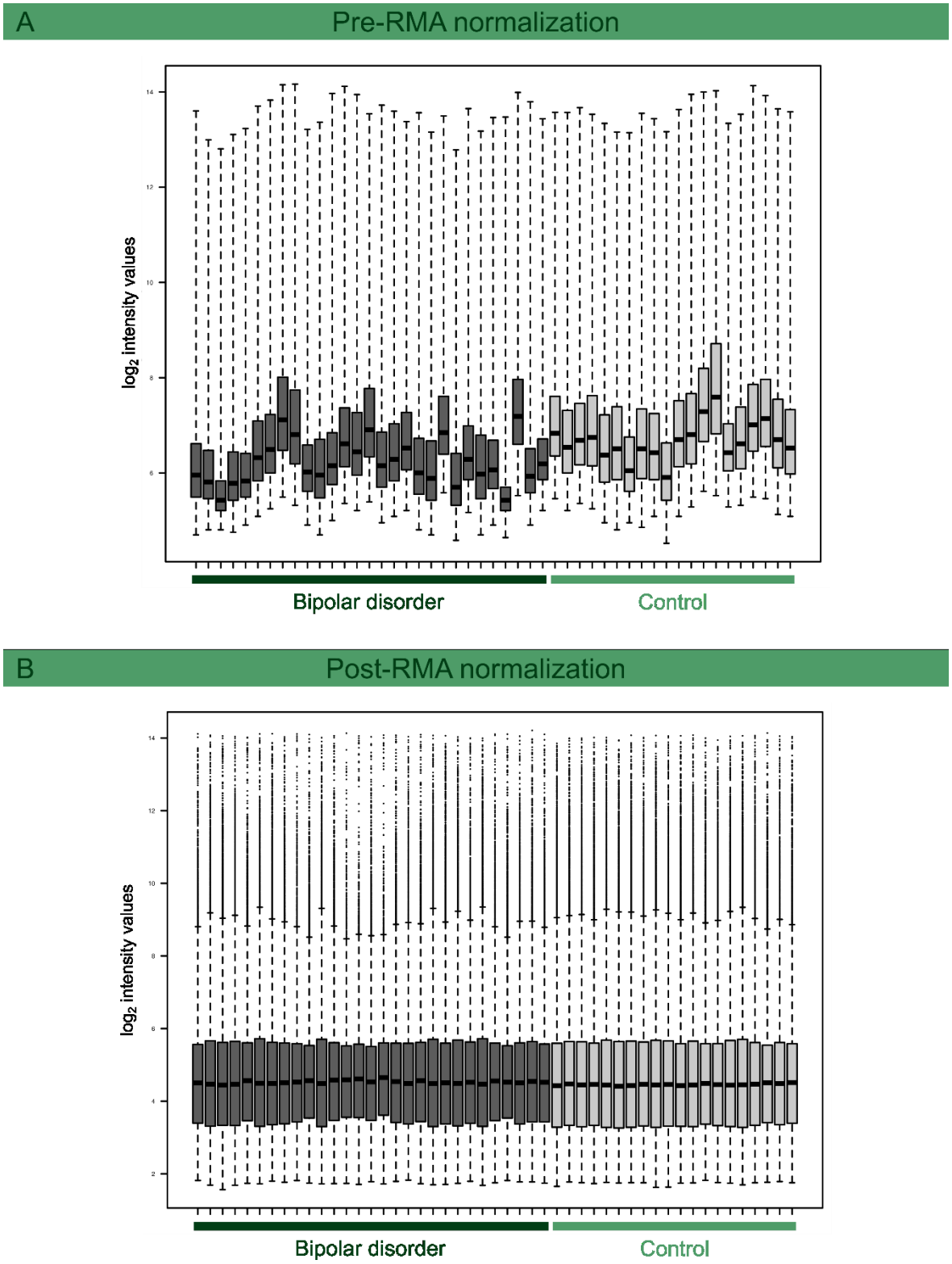

Figure 4. **Expression intensity distribution prior and after RMA normalization.** Each boxplot represents the chip-wise $\log_2$ intensity of bipolar disorder (dark gray) and control samples (light gray). Bars represent interquartile range. (A) The samples prior to normalization deviate strongly from each other. (B) After RMA normalization, all intensity distributions appear similar.

3.2.4 Assessment of the averaged spread of gene expression

The MA-plots of the controls and bipolar disorder samples were generated to investigated the averaged spread of the gene expression data. By comparing the MA-plots prior and after normalization, the spread of the $\log_2$ probe intensities and thus the variability is reduced in both groups by normalization (***Figure 5***). The centered distribution around M = 0 in the normalized data refers to a higher number of genes that were non-differentially expressed than differentially expressed.

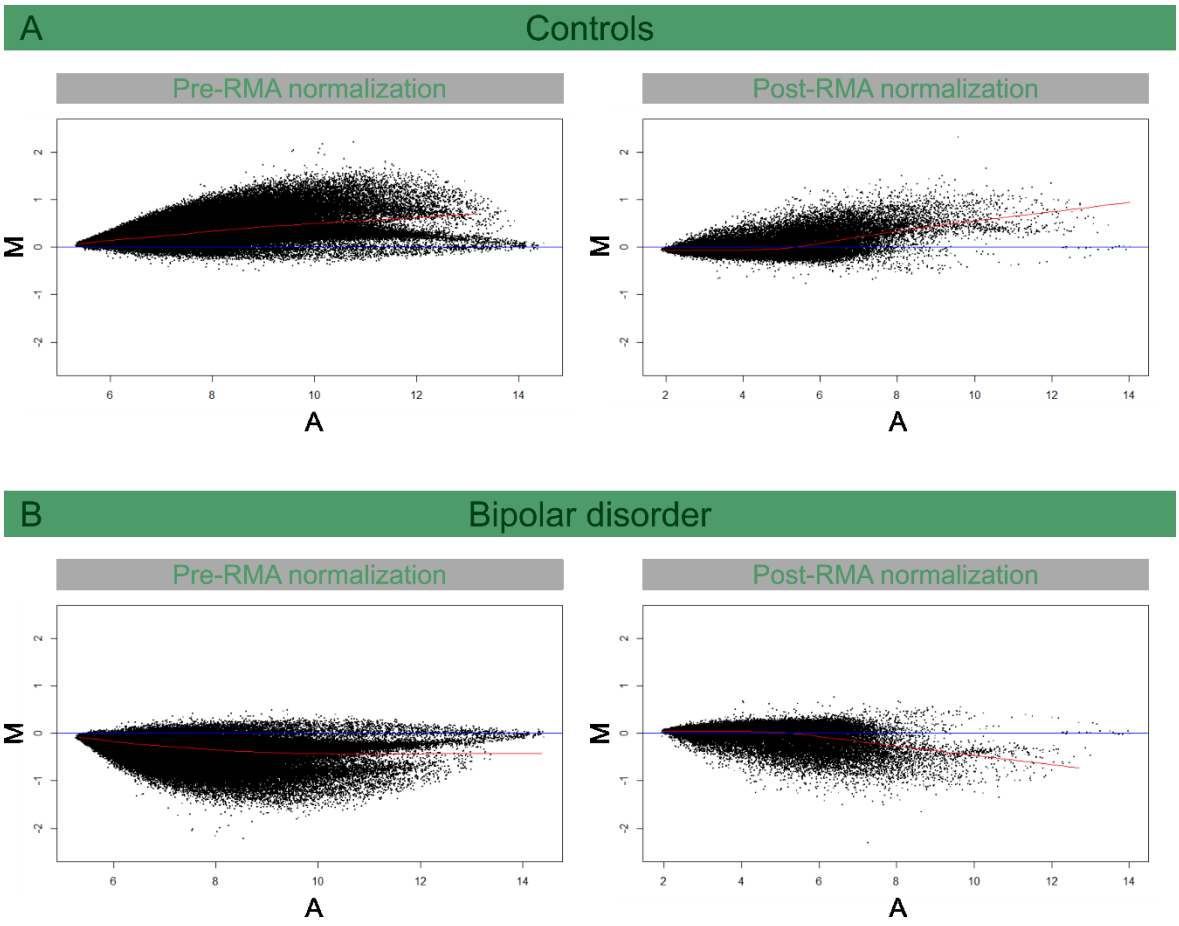

Figure 5. **MA-plots of raw data prior to RMA normalization and after RMA normalization for bipolar disorder and controls referenced to all samples.** Each dot represents one probe. In panel A, the averaged $\log_2$ intensity ratio of the controls (M) were compared to the averaged $\log_2$ intensity of all samples (A). In panel B, the averaged $\log_2$ intensity ratio (M) of the bipolar disorder samples are compared to the averaged $\log_2$ intensity of all samples (A). Non-differentially expressed probes are distributed tightly to M = 0 (blue line). With increasing average intensity, the spread of probe intensities increases.

3.2.5 Assessment of sample substructures based on gene expression

The principal component analysis of the preprocessed, normalized and pre-filtered gene expression data uncovered biological substructures enabling the differentiation of liver tissue of bipolar disorder samples from control samples. The percentage of explained variance of the top 10 principal components based on the gene expression was evaluated and plotted as scree plot (***Figure 6***).

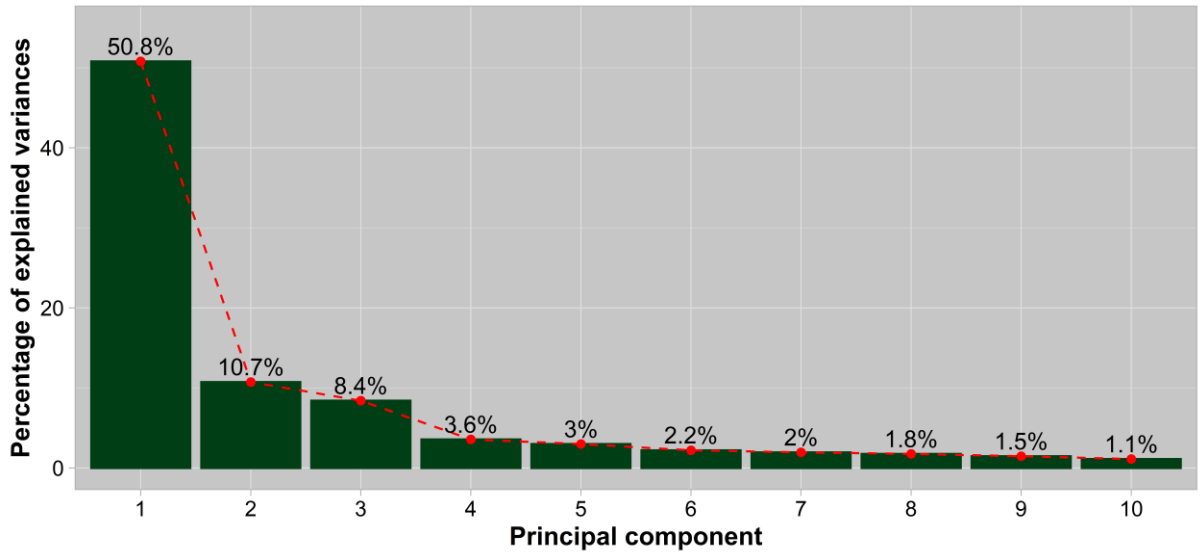

Figure 6. **Scree plot of principal components.** The percentage of the explained variance (y-axis) based on gene expression data is given for the principal components 1 to 10 (x-axis). Principal components 1, 2 and 3 explain the main variance in the groups amounting to 69.9%.

The principal components 1, 2 and 3 are contrasted (***Figure 7***). A clear separation was seen particularly for principal component 1 and 2 representing in total 61.5% of variance in the dataset.

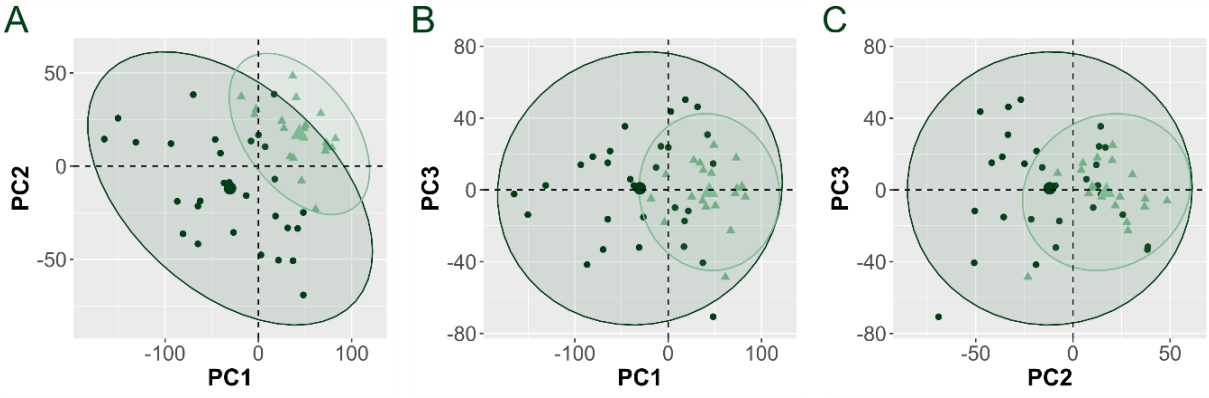

Figure 7. **Differences in gene expression profiles based on the principal component analysis.** The differences in gene expression profiles were indicated by the distance between the samples. Each dot represents one sample of the bipolar disorder (dark green) and control (light green) group representing the principal components (PC) of normalized and filtered $\log_2$ gene expression values. In (A-C), two of first three principal components are plotted against each other. [Based on [90]]

Of the 54675 probes included in the preprocessing and normalization, 7280 probes remained after non-specific filtering and were used for the differential gene expression analysis.

3.3 Differential gene expression in bipolar disorder

Differential gene expression profiles were investigated by comparing non-specific filtered probes of the bipolar disorder group with the control group. Based on an adjusted *p*-value of <0.05 and a fold change of >1.5, a total of 648 DEGs were obtained between samples with bipolar disorder and controls. Among those DEGs, only 25 genes were overexpressed, whereas 623 DEGs were found to be underexpressed. An extensive list of all DEGs with their annotation, as well as the corresponding fold change, $\log_2$ fold change and the adjusted significance value is given in the Appendix (***Table A1***). The top five upregulated genes included three genes belonging to the S100 calcium binding protein family, namely S100 calcium binding protein A12 (*S100A12)*, S100 calcium binding protein A9 (*S100A9*) and S100 calcium binding protein (*S100A8*), as well as the genes coding for the serum amyloid A2 (*SAA2*) and the interleukin-1 receptor antagonist (*IL1RN*). The top five downregulated genes identified were the flavin containing dimethylaniline monooxygenase 3 (*FMO3*), the solute carrier family 38 member 4 (*SLC38A4*), the TNF superfamily member 10 (*TNFSF10*), the catalase (*CAT*) and

the tubulin epsilon 1 (*TUBE1*). The volcano plot depicts the fold change and the adjusted significance level of the DEGs (***Figure 8***).

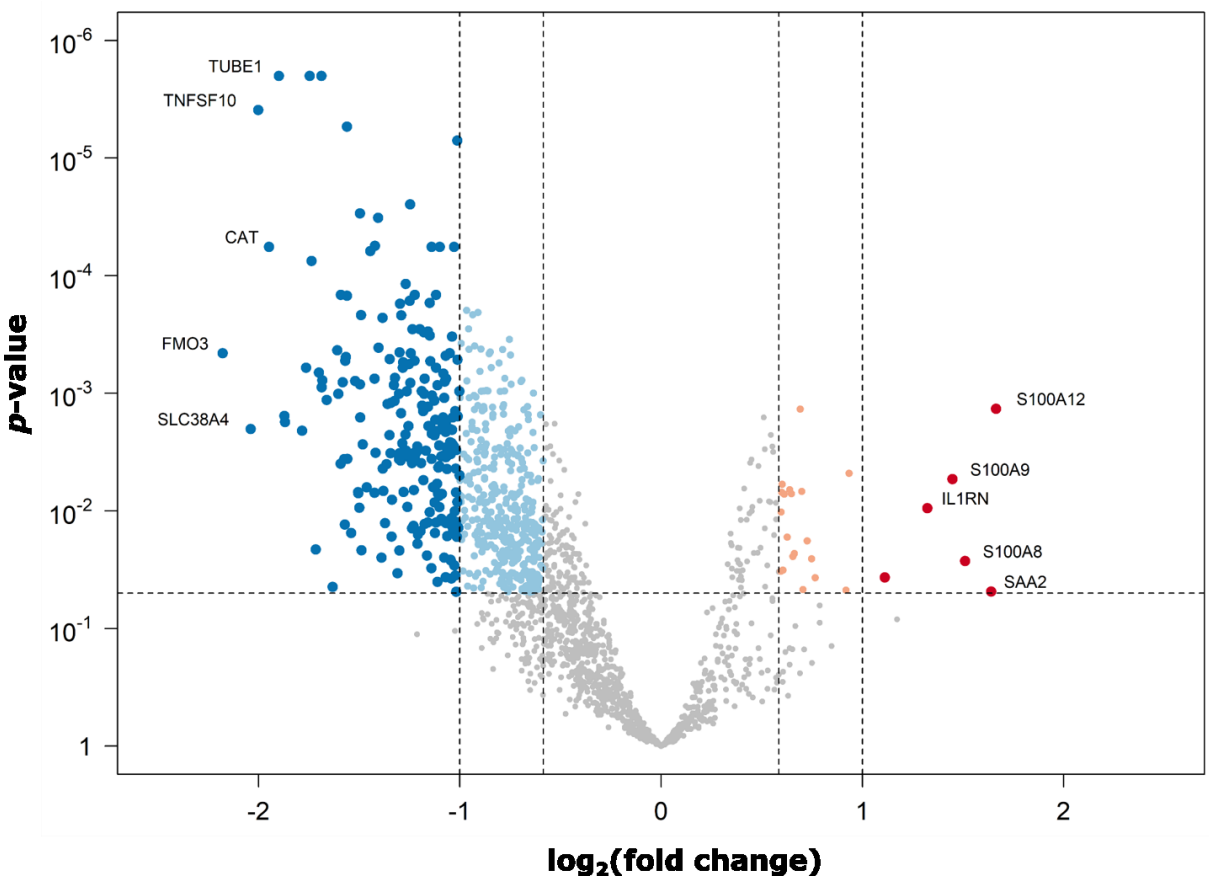

Figure 8. **Volcano plot highlighting underexpressed and overexpressed DEGs in bipolar disorder.** For each DEG, the $\log_2$ fold change (x-axis) is plotted against the corresponding adjusted *p*-value (y-axis). Thresholds for significance (adjusted *p*-value = 0.05; horizontal dashed line) and for expression (fold change >1.5 or >2; vertical dashed lines) are shown. Significant underexpressed genes with a fold change >1.5 or >2 are displayed as dots in light blue or dark blue, respectively. Significant overexpressed genes with a fold change of >1.5 or >2 are displayed as dots in light red or dark red, respectively. The five most underexpressed and overexpressed genes are labeled with their corresponding gene names. Gray dots represent genes with no significant difference. [Based on [90]]

3.4 Identified protein-protein interaction network

Underexpressed and overexpressed DEGs with reliable protein data were investigated using STRING. The protein-protein interaction network generated with a confidence level score of 0.7 included 610 nodes representing the proteins and 1229 edges representing interactions between proteins (***Figure 9***).

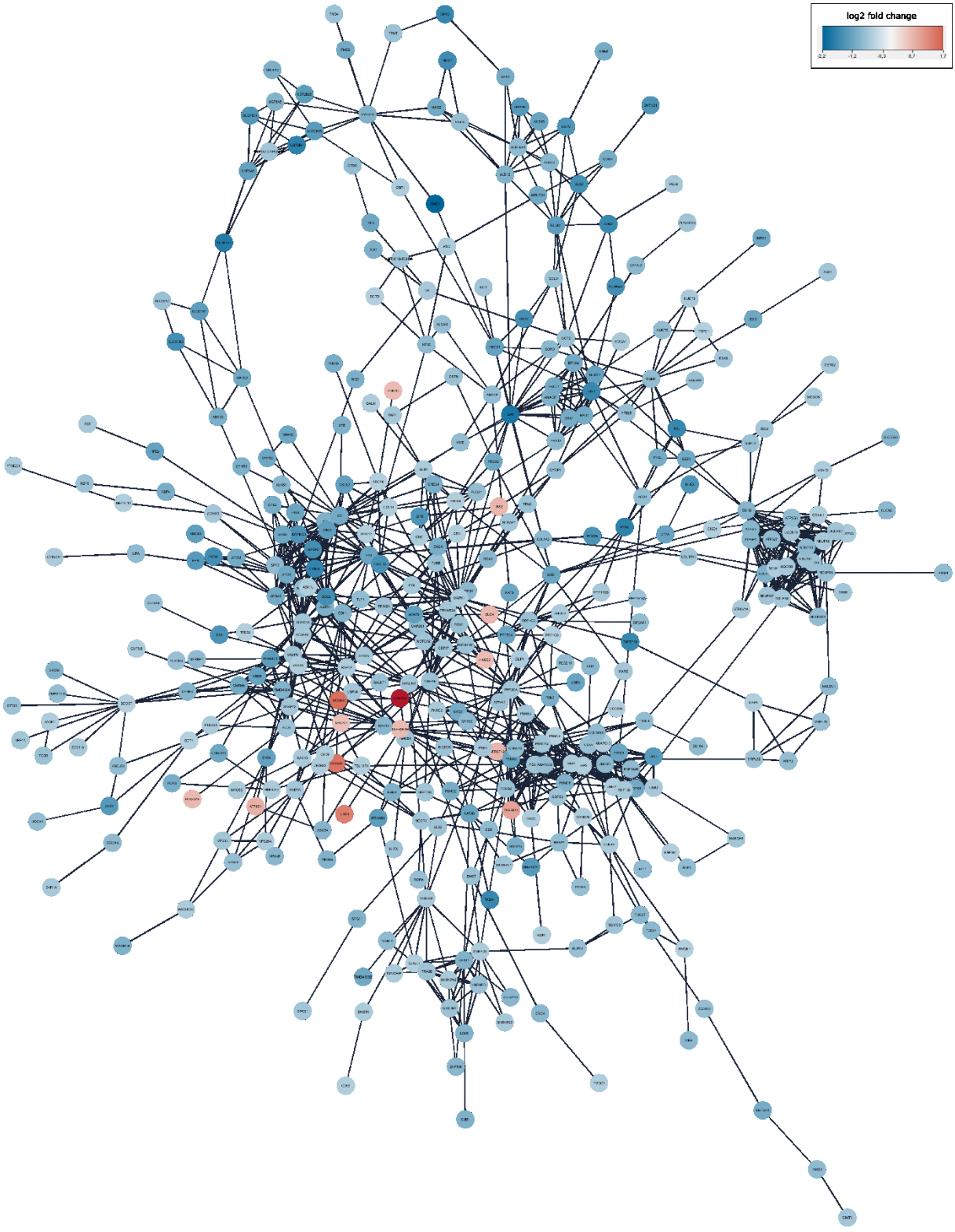

Figure 9. **Protein-protein interaction network of corresponding DEGs.** The overall protein-protein network generated by Cytoscape using the underexpressed and overexpressed DEGs with reliable protein data of the STRING database is displayed. The network included 610 connected nodes (proteins) and 1229 edges (interactions) shown as circles and lines, respectively. The coloring of the nodes corresponds to the $\log_2$ fold change of the gene expression microarray analysis.

3.5 Determined key regulators of protein-protein interaction network

The top 20 hub proteins or key regulators of the overall protein-protein interaction network generated from the corresponding DEGs were identified and mapped (***Figure 10***).

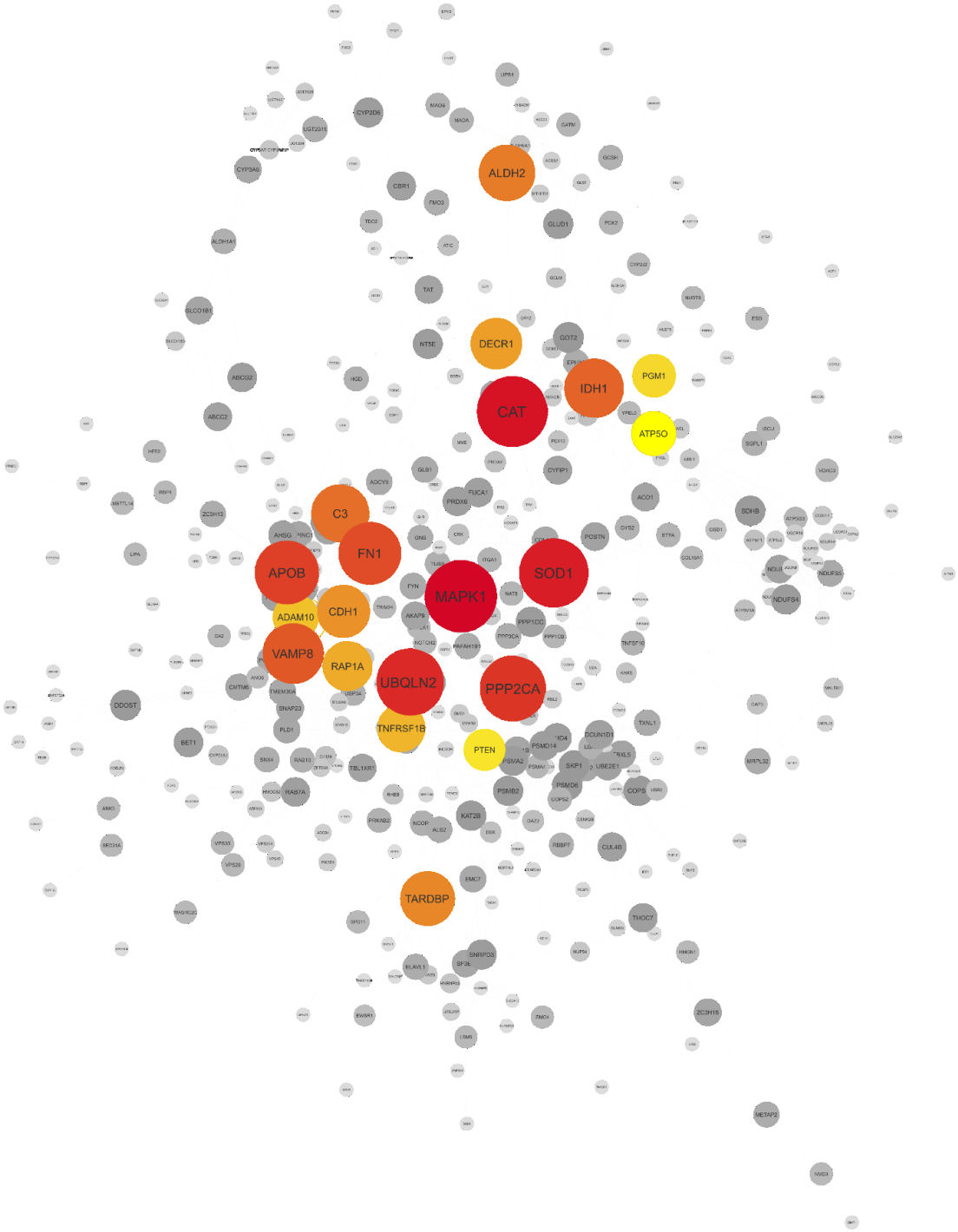

Figure 10. **Hub proteins of the protein-protein interaction network.** The nodes layout including circle size and color correspond to the betweenness centrality values. The 20 hub proteins with the highest betweenness scores are shown in nuances from red to yellow and all other nodes in nuances of gray. Dark red indicates the highest betweenness score. Full names are listed in ***Table A1*** in the Appendix.

Those hub proteins indicating a pivotal role for the network's structure and function and their corresponding betweenness score were listed (***Table 5***). The three hubs with the highest degrees were identified as mitogen-activated protein kinase 1 (MAPK1), a crucial part of the MAP kinase signal transduction pathway involved in numerous biological cell functions, followed by CAT, a crucial antioxidant enzyme mitigating the harmful effect of hydrogen peroxide, and superoxide dismutase 1 (SOD1), an isoenzyme abolishing detrimental superoxide radicals.

Table 5. **Hub proteins of the protein-protein interaction network.** The top 20 hub proteins with the corresponding betweenness scores are given.

Protein	Betweenness score	Protein	Betweenness score
MAPK1	26129.1	ALDH2	7611.9
CAT	21152.4	TARDBP	7560.8
SOD1	15946.9	CDH1	7523.5
UBQLN2	12262.7	DECR1	6808.1
PPP2CA	12249.0	RAP1A	6714.6
APOB	11510.8	TNFRSF1B	6657.2
FN1	10986.4	ADAM10	6581.8
VAMP8	9714.5	ATP5O	6523.2
IDH1	7953.7	PGM1	6433.7
C3	7821.5	PTEN	6227.6

MAPK1 - mitogen-activated protein kinase 1; *CAT* - catalase; *SOD1* - superoxide dismutase 1; *UBQLN2* – ubiquilin 2; *PPP2CA* - protein phosphatase 2 catalytic subunit alpha; *APOB* - apolipoprotein B; *FN1* - fibronectin 1; *VAMP8* - vesicle associated membrane protein 8; *IDH1* - isocitrate dehydrogenase (NADP(+)) 1; *C3* - complement 3; *ALDH2* - aldehyde dehydrogenase 2 family member; *TARDBP* - TAR DNA binding protein; *CDH1* - cadherin 1; *DECR1* - 2,4-dienoyl-CoA reductase 1; *RAP1A* - RAP1A, member of RAS oncogene family; *TNFRSF1B* - TNF receptor superfamily member 1B; *ADAM10* - ADAM metallopeptidase domain 10; *ATP5O* - ATP synthase peripheral stalk subunit OSCP; *PGM1* - phosphoglucomutase 1; *PTEN* - phosphatase and tensin homolog;

3.6 Identified modules of protein-protein interaction network

Functional module analysis of the protein-protein interaction network using ClusterViz and the MCODE algorithm was performed and identified 8 modules with a MCODE score higher than 4. Module 1 with a MCODE score of 14.00 consisted of 14 nodes and 91 edges, whereas complement 3 (C3) was identified as the seed, classified as the highest-weighted node (***Figure 11***).

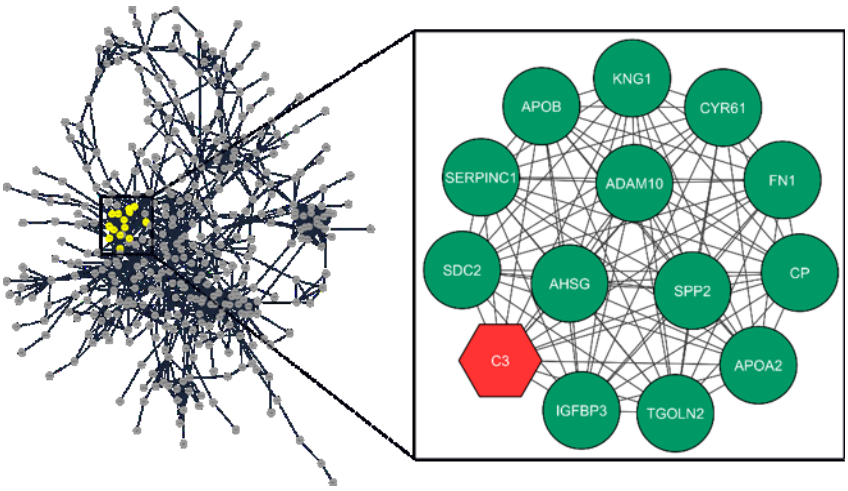

Figure 11. **Module 1 of the protein-protein interaction network.** Module 1 included 14 nodes and 91 edges and reach a score of 14. The seed and the other proteins included in the module are shown as red hexagon and green ellipses, respectively. The connecting lines indicate the edges representing protein interactions between the nodes. Full names are given in ***Table A1*** in the Appendix.

Module 2 with a MCODE score of 12.17 consisted of 13 nodes and 73 edges, where NADH:ubiquinone oxidoreductase subunit A9 (NDUFA9), a complex I subunit contributing to the respiratory chain, was determined as seed (***Figure 12***).

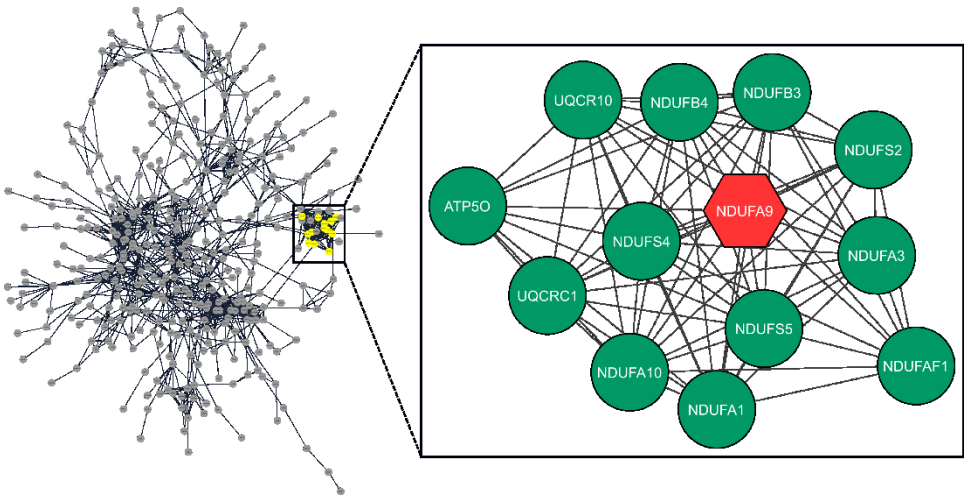

Figure 12. **Module 2 of the protein-protein interaction network.** Module 2 included 13 nodes and 73 edges and reach a score of 12.2. The seed protein and the other proteins included in the module are shown as red hexagon and green ellipses, respectively. The connecting lines indicate the edges representing protein interactions between the nodes. Full names are given in ***Table A1*** in the Appendix.

Module 3 with a MCODE score of 9.79 comprised 20 nodes and 93 edges (***Figure 13***). The seed in module 3 was identified as anaphase promoting complex subunit 13 (ANAPC13), a component of an ubiquitin ligase in the anaphase promoting complex regulating cell cycle progression.

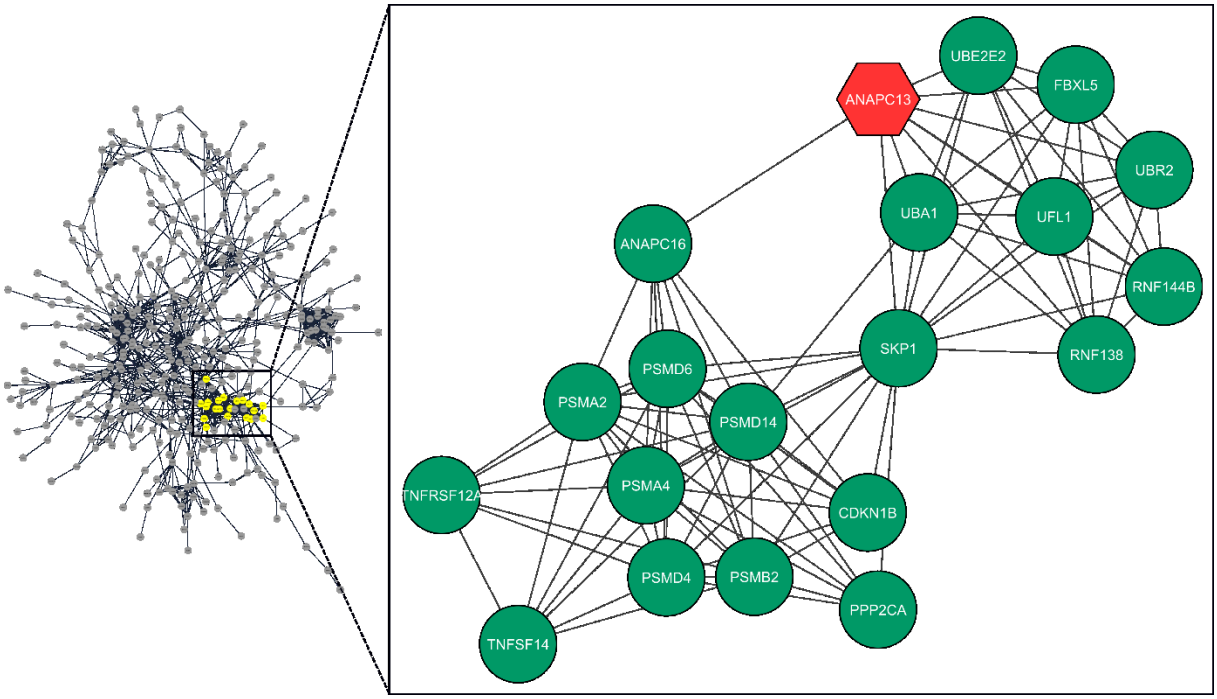

Figure 13. **Module 3 of the protein-protein interaction network.** Module 3 included 20 nodes and 93 edges and reach a score of 9.8. The seed protein and the other proteins included in the module are shown as red hexagon and green ellipses, respectively. The connecting lines indicate the edges representing protein interactions between the nodes. Full names are given in ***Table A1*** in the Appendix.

Module 4 with a MCODE score of 8.00 consisting of 8 nodes and 28 edges, whereas vesicle associated membrane protein 8 (VAMP8) was determined as seed, a membrane protein involved in the fusion process of cellular membranes such as synaptic vesicles (***Figure 14***).

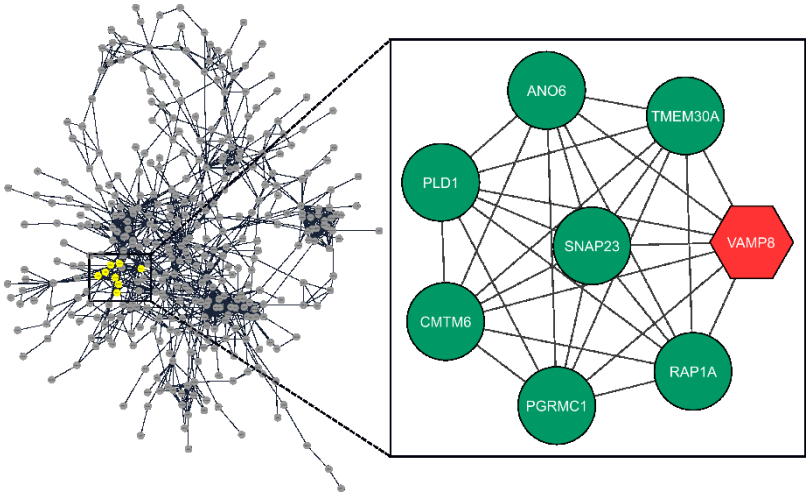

Figure 14. **Module 4 of the protein-protein interaction network.** Module 4 included 8 nodes and 28 edges and reach a score of 8.0. The seed protein and the other proteins included in the module are shown as red hexagon and green ellipses, respectively. The connecting lines indicate the edges representing protein interactions between the nodes. Full names are given in ***Table A1*** in the Appendix.

Module 5 with a MCODE score of 7.71 consisted of 8 nodes and 27 edges, and LSM5 homolog, U6 small nuclear RNA and mRNA degradation associated (LSM5), a component of a snRNP complex involved in spliceosome, was representing the seed (***Figure 15***).

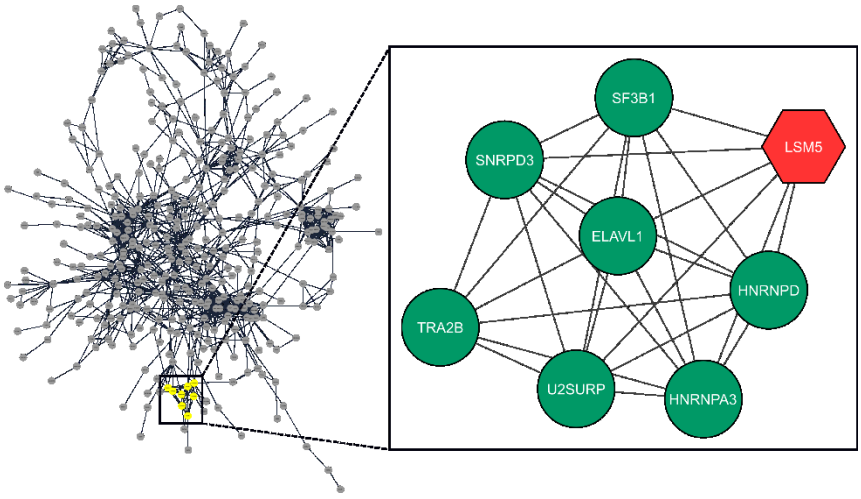

Figure 15. **Module 5 of the protein-protein interaction network.** Module 5 included 8 nodes and 27 edges and reach a score of 7.7. The seed protein and the other proteins included in the module are shown as red hexagon and green ellipses, respectively. The connecting lines indicate the edges representing protein interactions between the nodes. Full names are given in ***Table A1*** in the Appendix.

Module 6 with a MCODE score of 7.00 comprised 21 nodes and 70 edges, whereas hydroxyacid oxidase 1 (HAO1), an oxidase associated with glycolate and fatty acid oxidase activity, was revealed as seed (***Figure 16***).

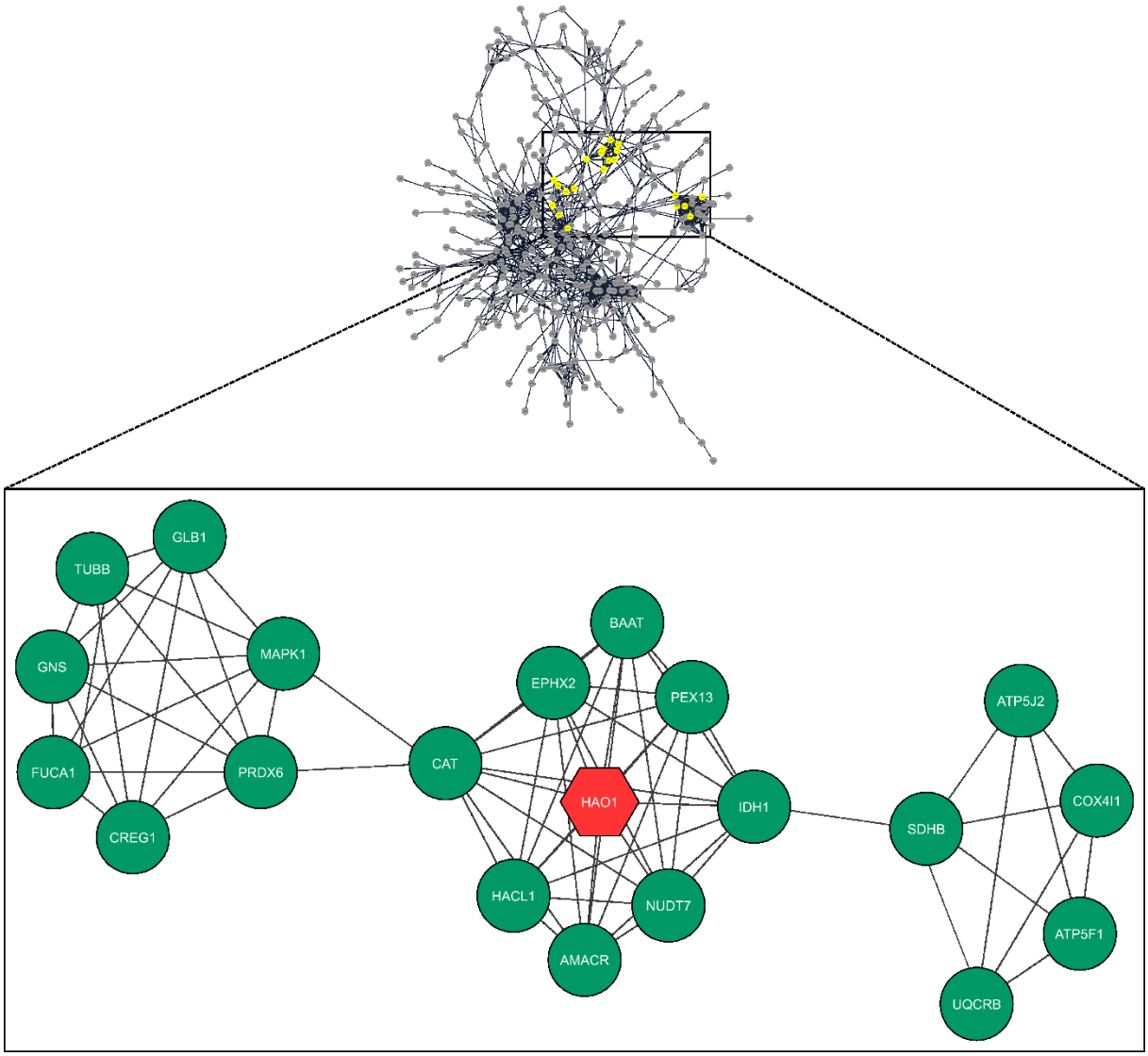

Figure 16. **Module 6 of the protein-protein interaction network.** Module 6 included 21 nodes and 70 edges and reach a score of 7.0. The seed protein and the other proteins included in the module are shown as red hexagon and green ellipses, respectively. The connecting lines indicate the edges representing protein interactions between the nodes. Full names are given in ***Table A1*** in the Appendix.

Module 7 with a MCODE score of 5.43 contained 8 nodes and 19 edges, and as seed centrosomal protein 57 (CEP57), which is supposed to interact with microtubules for their attachment to the centrosomes, was found (***Figure 17***).

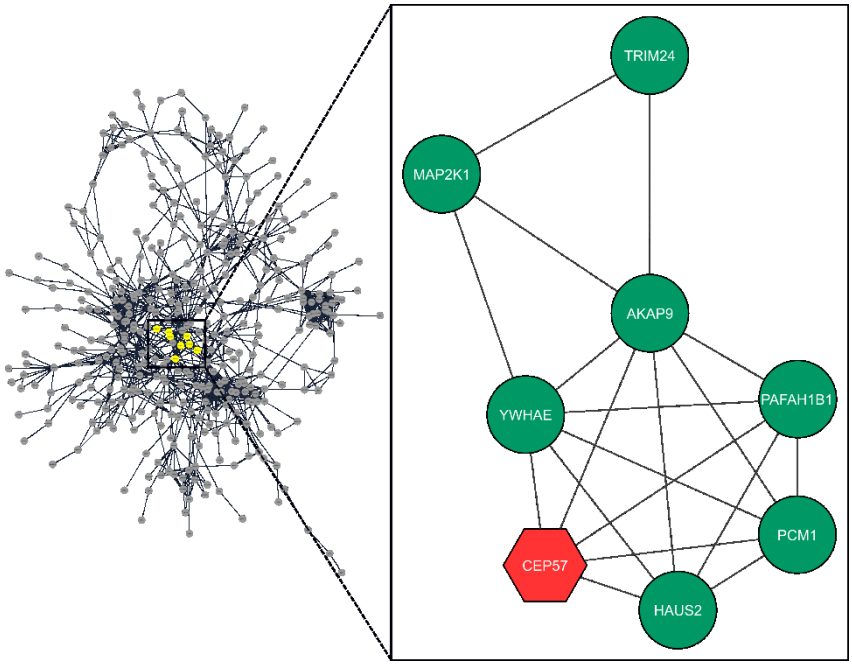

Figure 17. **Module 7 of the protein-protein interaction network.** Module 7 included 8 nodes and 19 edges and reach a score of 5.4. The seed protein and the other proteins included in the module are shown as red hexagon and green ellipses, respectively. The connecting lines indicate the edges representing protein interactions between the nodes. Full names are given in ***Table A1*** in the Appendix.

Module 8 with a MCODE score of 4.67 consisted of 10 nodes and 21 edges, whereas angiotensin II receptor type 1 (AGTR1), which is involved in a G-protein mediated phosphatidylinositol-calcium second messenger system, was revealed as seed (***Figure 18***).

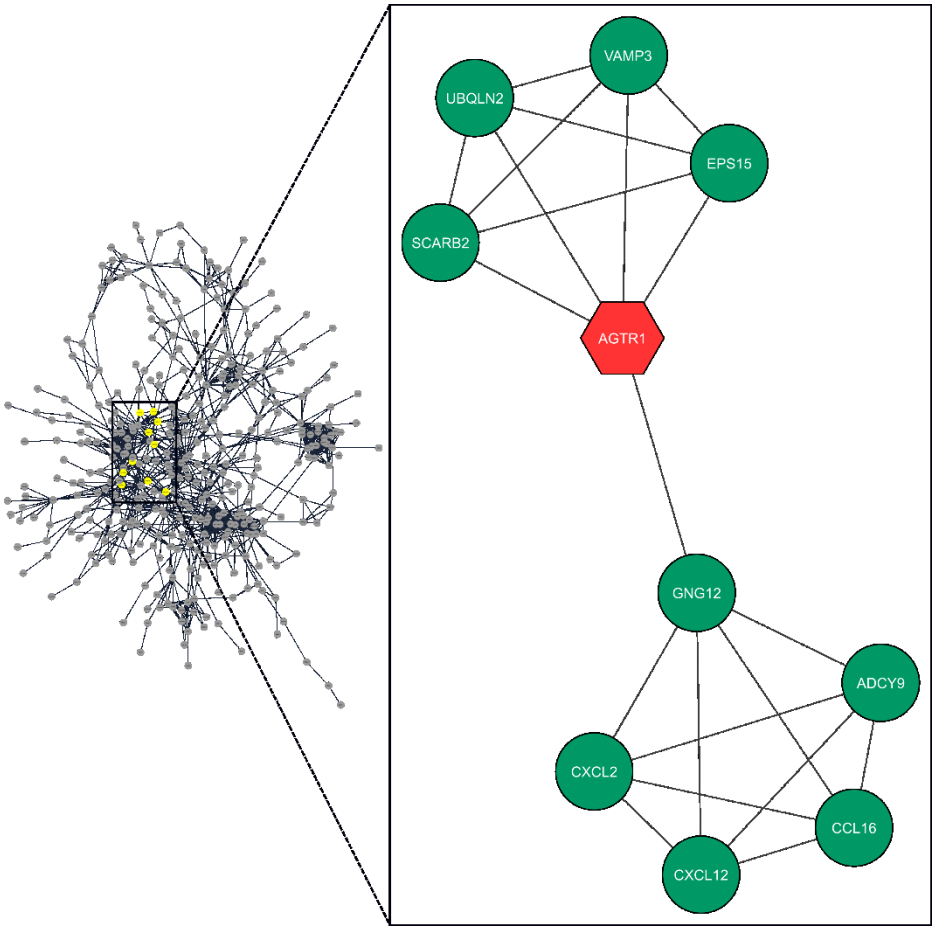

Figure 18. **Module 8 of the protein-protein interaction network.** Module 8 included 10 nodes and 21 edges and reach a score of 4.7. The seed protein and the other proteins included in the module are shown as red hexagon and green ellipses, respectively. The connecting lines indicate the edges representing protein interactions between the nodes. Full names are given in ***Table A1*** in the Appendix.

3.7 Functional enrichment analysis

3.7.1 Determination of gene ontology terms

The GO terms for cellular components (***Figure 19***), biological processes (***Figure 20***) and molecular functions (***Figure 21***) were assessed for the 648 DEGs. With regard to the cellular component, the majority of the DEGs was present at the membrane followed by the cytosol and the nucleus. Most of the underexpressed DEGs were involved in metabolic process, biological regulation and stimulus response with regard to biological processes. In relation to the molecular function, upregulated DEGs and a large number of downregulated DEGs were predominantly involved in protein and ion binding.

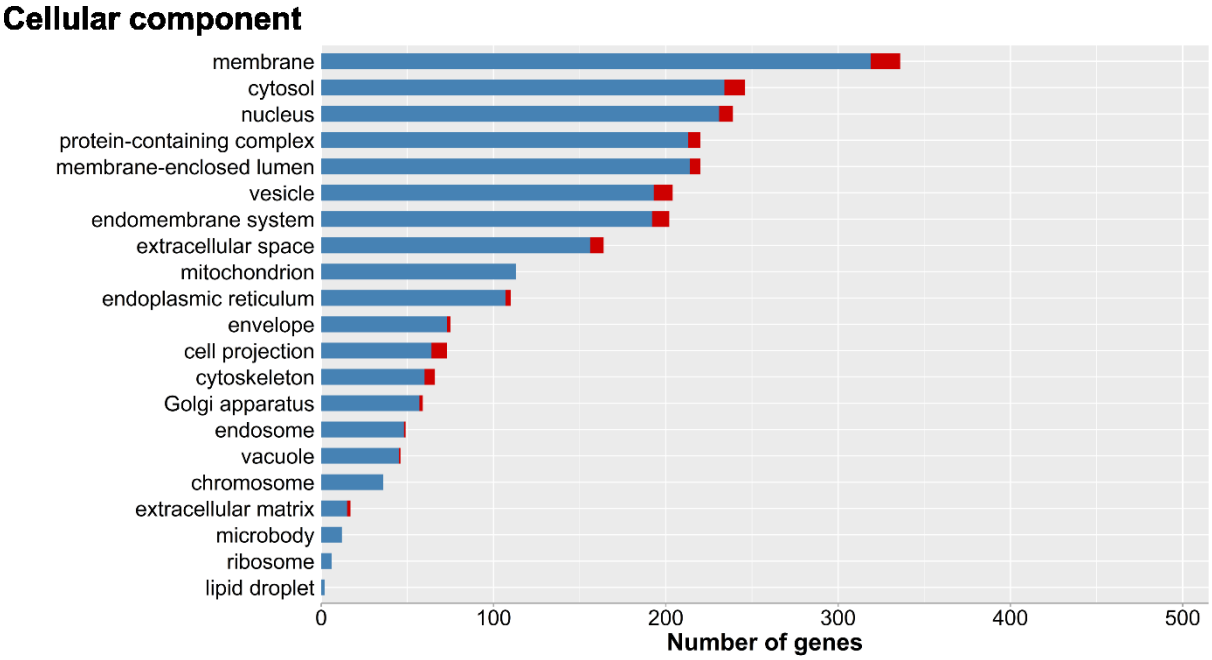

Figure 19. **Ranking of the cellular component terms based on the GO analysis.** The portion of under- and overexpressed genes based on the microarray analysis are shown in blue and red, respectively.

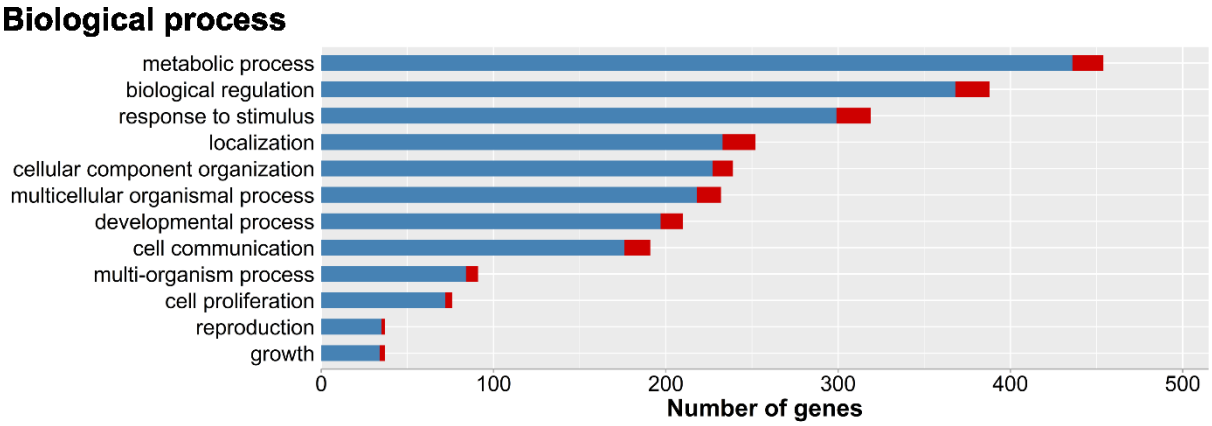

Figure 20. **Ranking of biological process terms based on the GO analysis.** The portion of under- and overexpressed genes based on the microarray analysis are shown in blue and red, respectively.

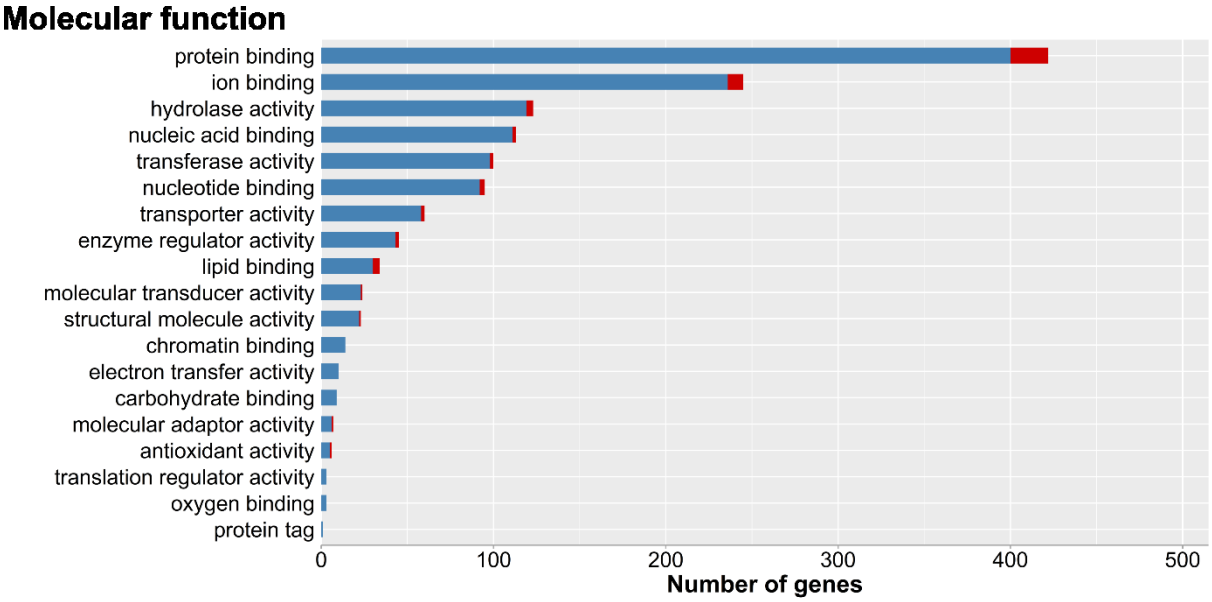

Figure 21. **Ranking of molecular function terms based on the GO analysis.** The portion of under- and overexpressed genes based on the microarray analysis are shown in blue and red, respectively.

3.7.2 Identification of over-represented functional pathways

The over-represented functional pathway analysis revealed nine functional pathways included in the Reactome database with statistical significance. A marked over-representation of DEGs was present for the respiratory electron transport chain (RETC) involving four pathways. The four pathways were as follows: Respiratory electron transport, ATP synthesis by chemiosmotic coupling, and heat production by uncoupling proteins (R-HSA-163200, number of DEGs in pathway: 21, FDR = <0.001); Respiratory electron transport (R-HSA-611105, number of DEGs in pathway: 17, FDR = <0.001); The citric acid cycle and respiratory electron transport (R-HSA-1428517, number of DEGs in pathway: 22, FDR = <0.001); and Complex I biogenesis (R-HSA-6799198, number of DEGs in pathway: 10, FDR = <0.014). Other significantly over-represented pathways were found to be involved in the innate immune system with the pathway Neutrophil degranulation (R-HSA-6798695, number of DEGs in pathway: 42, FDR = <0.001), in the lipid metabolism with the pathway Metabolism of lipids and lipoproteins (R-HSA-556833, number of DEGs in pathway: 21, FDR = <0.001), in the biotransformation of endogenous compounds and xenobiotics with the pathway Biological oxidations (R-HSA-211859, number of DEGs in pathway: 21, FDR = <0.015), and the cellular amino acid and polyamine metabolism with the pathways Metabolism of amino acids and derivatives (R-HSA-

71291, number of DEGs in pathway: 21, FDR = <0.020) and Regulation of ornithine decarboxylase (R-HSA-350562, number of DEGs in pathway: 21, FDR = <0.027). The pathway allocation of the corresponding DEGs in the pathways is given in the Appendix (***Table A1***).

3.8 Gene expression validation of microarray data

The expression of 14 genes were evaluated in bipolar disorder and the controls to validate the microarray results. The amplicon size of the endogenous controls and each validation gene were verified by agarose gel electrophoresis (***Figure 22***). The gene specific amplicons showed the expected size and the absence of unspecific products.

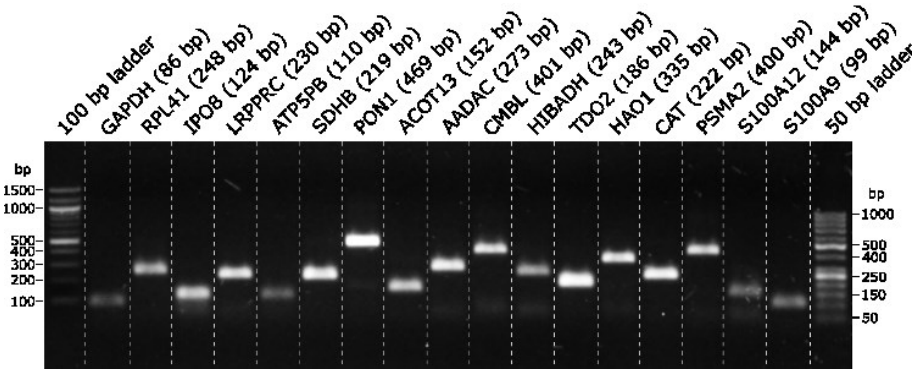

Figure 22. **Verification of gene specific products by amplicon size determination.** Gene specific amplicons were separated by gel electrophoresis using a 2% agarose gel. Each lane corresponds to one gene of interest. Gene name and amplicon size are given above the image. Molecular sizes of the 100 and 50 bp ladder are indicated on the left and right side of the image, respectively. Full names are given in ***Table A1*** in the Appendix. [Published in [90]]

As endogenous controls, *RPL41* and *IPO8* were used. Gene expression of *GAPDH* was not properly detected in all tested samples and therefore excluded as endogenous control gene. Despite the variation in the differential expression between bipolar disorder and controls, both, microarray and quantitative real-time PCR analyses showed comparable gene expression in most of the examined genes. A statistical significant difference in gene expression between bipolar disorder and controls was confirmed for 11 of the tested genes.

For the enriched RETC pathway, the genes *LRPPRC*, *ATP5PB* and *SDHB* were validated (***Figure 23***). No difference was revealed for *LRPPRC* between the groups. The genes *ATP5PB*

($p = 0.032$) and *SDHB* ($p = 0.007$) were significantly underexpressed in bipolar disorder. A reduction of 46.5% and 56.3% was observed for *ATP5PB* and *SDHB*, respectively.

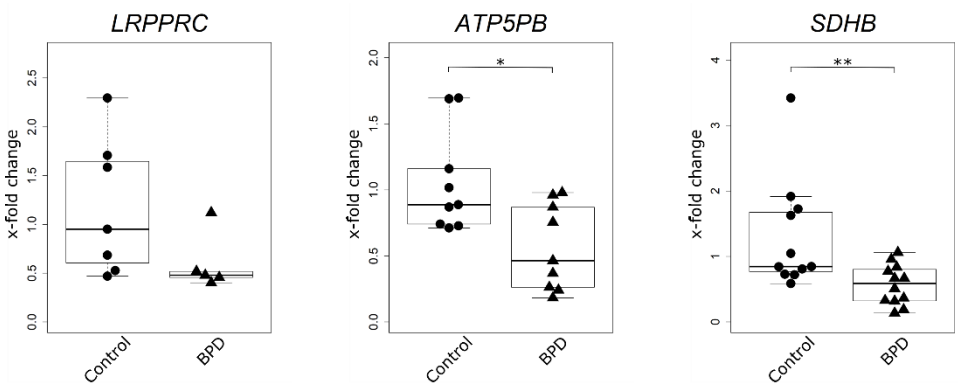

Figure 23. **Validation of selected DEGs allocated to the RETC pathway.** Relative gene expression is given as x-fold change assessed by sample triplicates and normalized using *RPL41* and *IPO8* as endogenous controls for the bipolar disorder (BPD) and control (Control) samples. Statistical analyses: Mann Whitney U test; * $p = <0.05$, ** $p = <0.01$ [Published in [90]]

The genes *PON1* and *ACOT13* allocated to the metabolism of lipids and lipoproteins were examined (***Figure 24***). For *PON1*, a difference was absent between the groups. The gene *ACOT13* ($p = 0.013$) was significantly downregulated by 45.9% in bipolar disorder.

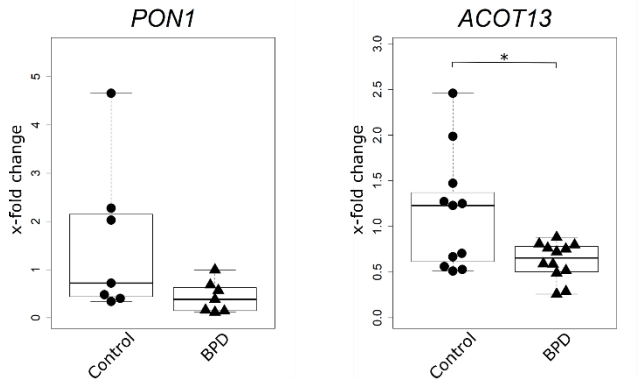

Figure 24. **Validation of selected DEGs allocated to the metabolism of lipids and lipoproteins.** Relative gene expression is given as x-fold change assessed by sample triplicates and normalized using *RPL41* and *IPO8* as endogenous controls for the bipolar disorder (BPD) and control (Control) samples. Statistical analyses: Mann Whitney U test (*PON1*) and unpaired t-test (*ACOT13*); * $p = <0.05$ [Published in [90]]

For the enriched pathway of biological oxidations, the gene expression of *AADAC* and carboxymethylenebutenolidase homolog (*CMBL*) were investigated (***Figure 25***). A statistically significant lower expression for both genes, *AADAC* ($p = 0.007$) and *CMBL* ($p = 0.013$), was shown. The reduction accounted for 92.0% and 73.6%, respectively.

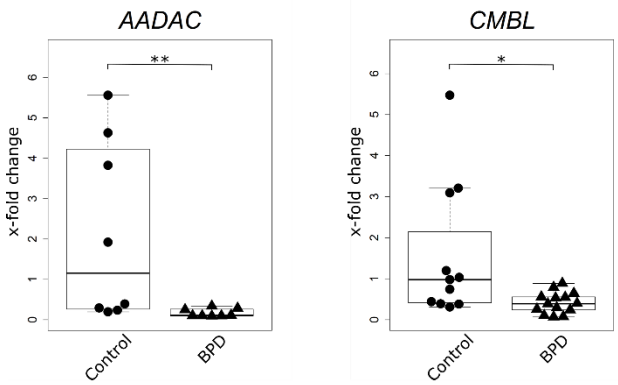

Figure 25. **Validation of selected DEGs allocated to biological oxidations.** Relative gene expression is given as x-fold change assessed by sample triplicates and normalized using *RPL41* and *IPO8* as endogenous controls for the bipolar disorder (BPD) and control (Control) samples. Statistical analyses: Mann Whitney U test; * p = <0.05, ** p = <0.01 [Published in [90]]

Diminished gene expression of the three tested genes related to the amino acid metabolism, *HIBADH* (p = 0.032), *TDO2* (p = 0.002) and *HAO1* (p = 0.037) was observed with a decrease of 49.3%, 56.4% and 62.5%, respectively (***Figure 26***).

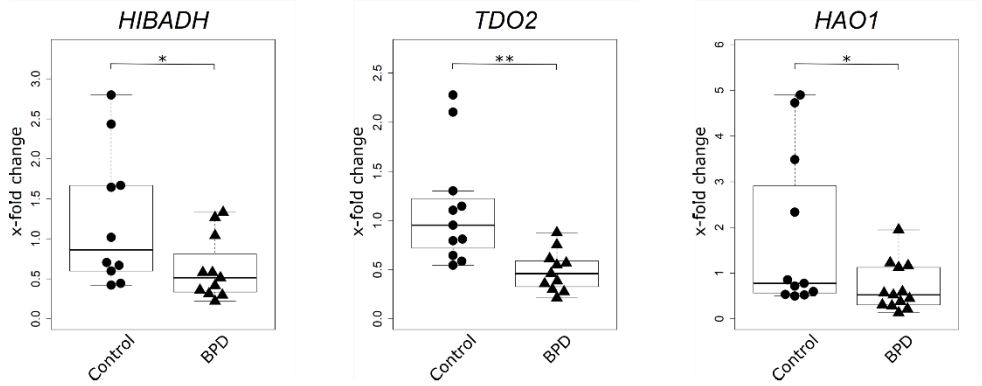

Figure 26. **Validation of selected DEGs allocated to the metabolism of amino acids.** Relative gene expression is given as x-fold change assessed by sample triplicates and normalized using *RPL41* and *IPO8* as endogenous controls for the bipolar disorder (BPD) and control (Control) samples. Statistical analyses: Mann Whitney U test; * p = <0.05, ** p = <0.01 [Published in [90]]

For the enriched pathway of neutrophil degranulation, the genes *CAT*, *PSMA2*, *S100A9* and *S100A12* were examined (***Figure 27***). The gene expression of *CAT* decreased by 62.5% (p = 0.004) and increased for *S100A9* (p = 0.003) and *S100A12* (p = 0.003) by 189.1% and 574.1%, respectively, in the bipolar disorder samples compared to the controls. *PSMA2* gene expression did not differ between the groups.

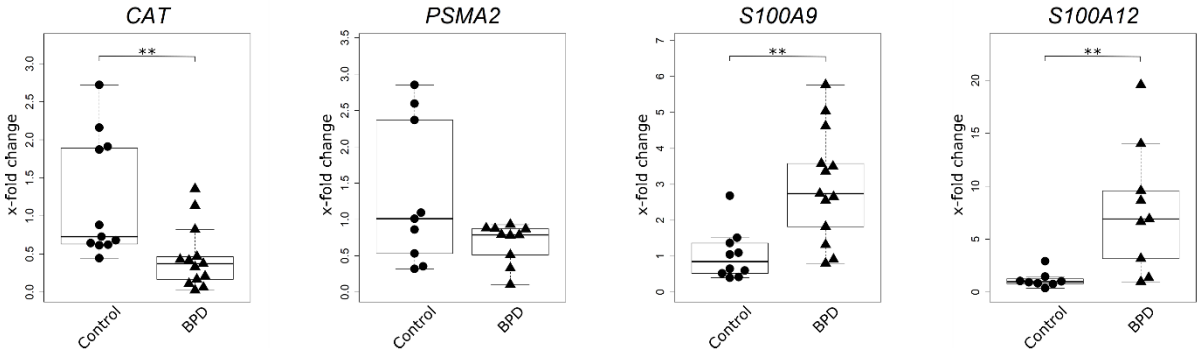

Figure 27. **Validation of selected DEGs allocated to neutrophil degranulation.** Relative gene expression is given as x-fold change assessed by sample triplicates and normalized using *RPL41* and *IPO8* as endogenous controls for the bipolar disorder (BPD) and control (Control) samples. Statistical analyses: Mann Whitney U test; ** $p = <0.01$ [Published in [90]]

3.9 Frequency distributions of histopathological features in the liver

The presence of steatosis in liver tissue did not differ between patients with bipolar disorder and controls, whereby all bipolar disorder samples and 94.1% of the controls showed steatosis ($p = 0.405$). The bipolar disorder group revealed a considerably higher percentage of steatohepatitis compared to the controls (68.0% and 35.3%, respectively), however, statistical significance was absent ($p = 0.059$).

The assessed histopathological liver features were assigned to six categories. The first category termed as degenerative changes comprised features of reactive-degenerative changes, hepatocellular ballooning, hepatocellular accumulation of rough endoplasmic reticulum at the apical pole also known as basophilia of the biliary pole, as well as glycogen inclusions of the nucleus, and cytoplasmic inclusion and deposits of metals, such as iron, and endogenous pigments, such as ceroid and lipofuscin both formed by the degradation of lipids. The corresponding frequency distributions of histopathological features in this category were assessed (***Figure 28***). Comparable frequency distributions were observed for most of the features. The bipolar disorder group revealed a less severe iron pigment storage compared to the controls, where the majority of the control samples had moderate (41.2%) to severe (29.4%) stored iron pigments in the parenchymal cells.

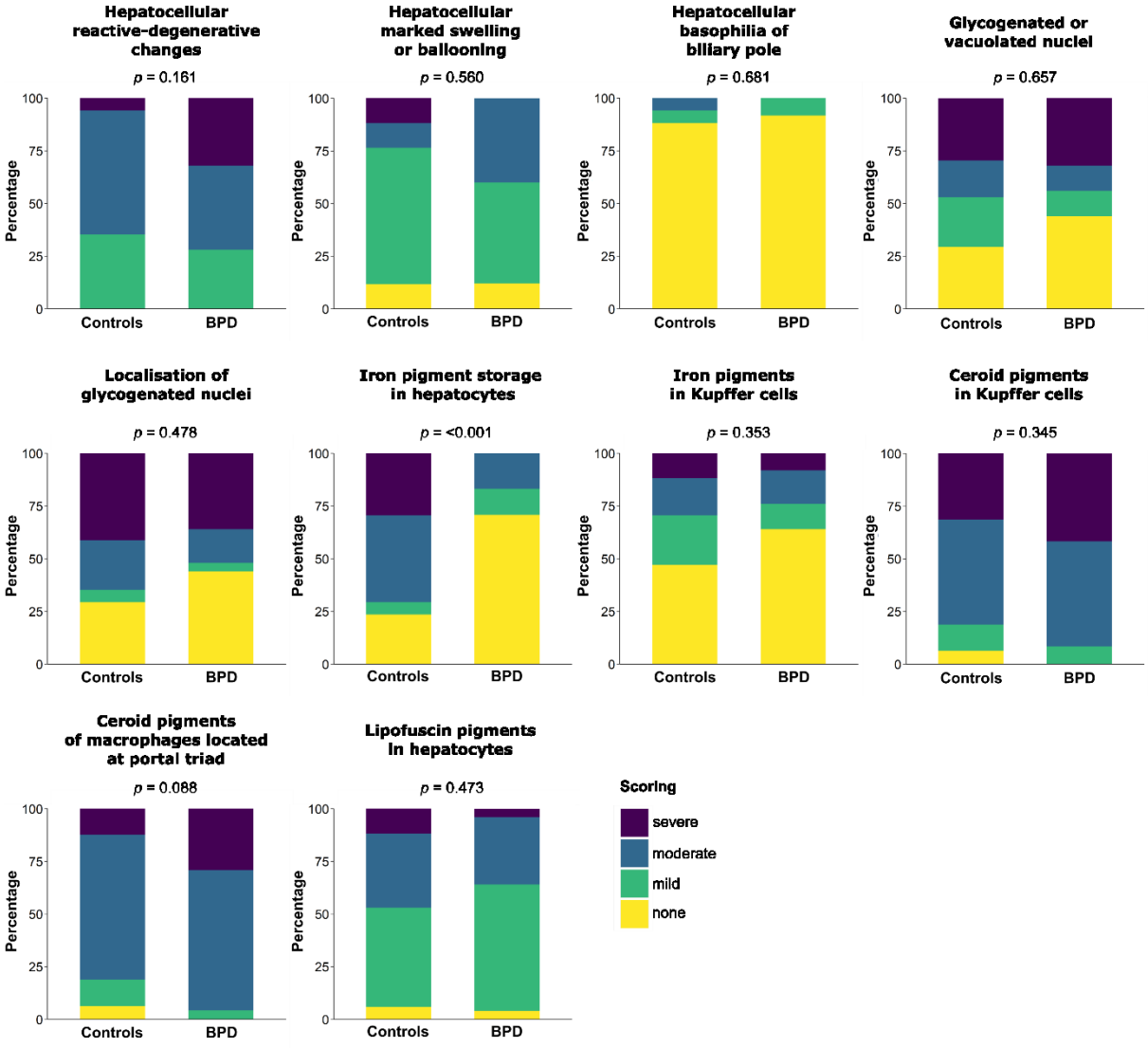

Figure 28. **Frequency distribution of assessed histopathological features categorized to degenerative changes.** The percentage of the respective histopathological feature score for the patients with bipolar disorder (BPD) and the control group (Controls) are given. Statistical analyses: Mann Whitney U test; [Based on [90]]

The second category comprised histopathological features assigned to hepatic reactivity. Frequency distributions describing the pathology of necrosis and inflammation according to the Ishak's modified histological activity index [111] including the presence of interface hepatitis, confluent and focal necroses and inflammation at portal areas were assessed (***Figure 29***). No statistically significant frequency distribution differences for all features were observed between the groups.

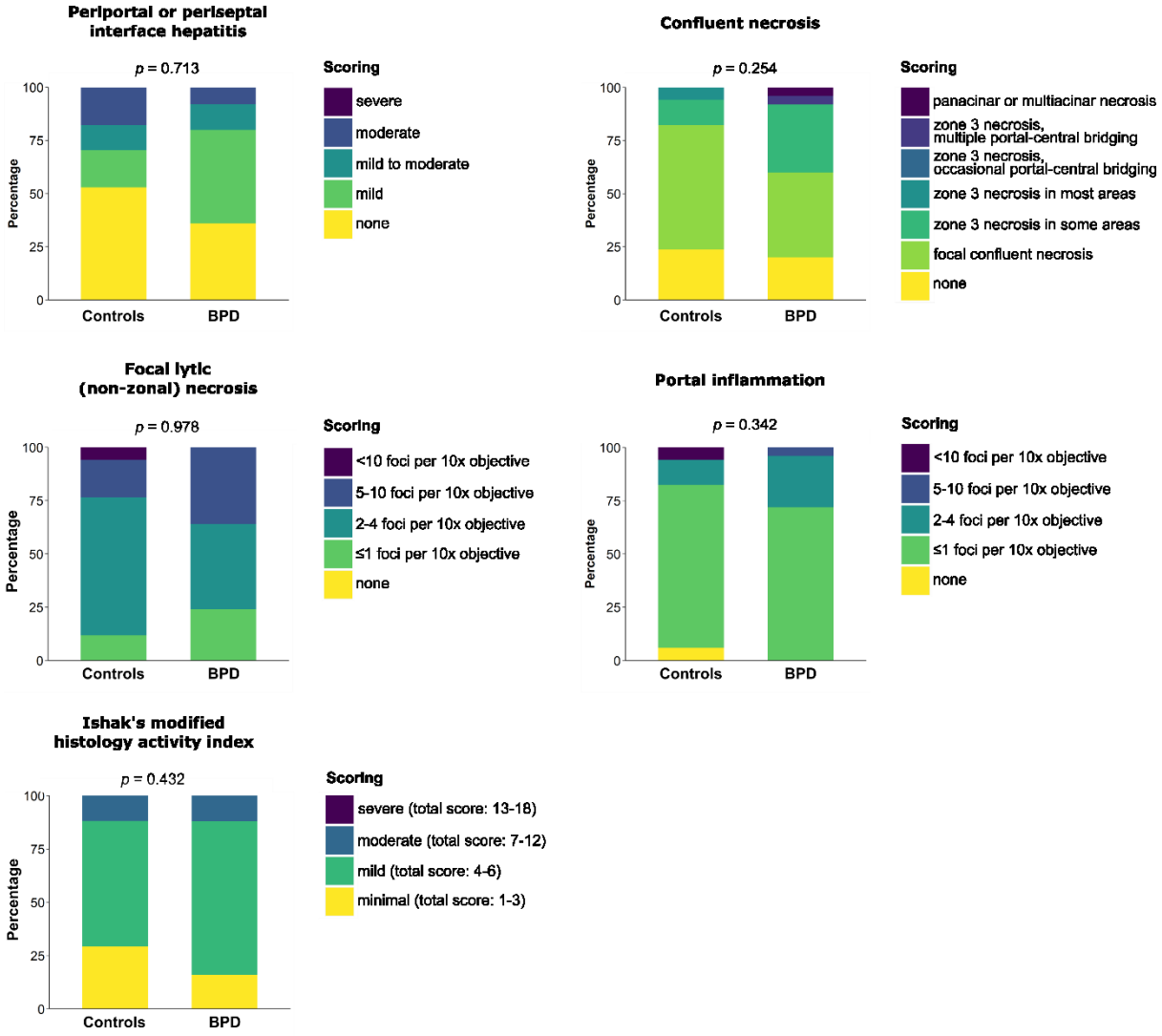

Figure 29. **Frequency distribution of assessed histopathological features categorized to hepatic reactivity.** The percentage of the respective histopathological feature score for the patients with bipolar disorder (BPD) and the control group (Controls) are given. Statistical analyses: Mann Whitney U test; [Based on [90]]

Frequency distributions of histopathological features of inflammation were assessed including features such as the presence of portal inflammation, zonal necrosis, lobular activity according to Scheurer [112], and lymph follicles, as well as the presence of chronic cholangitis and bile duct injury, the accumulation of immune cells such as macrophages including Kupffer cells and histiocytes, as well as hepatic stellate cells termed as Ito cells and granulocytes (***Figure 30***). The majority of bipolar disorder samples, 92.0%, revealed severe histiocytes presence in lobular areas, compared to 58.8% of the controls ($p = 0.10$). The presence of granulocytes in portal areas was more dominant in liver samples of patients with bipolar disorder ($p = 0.025$).

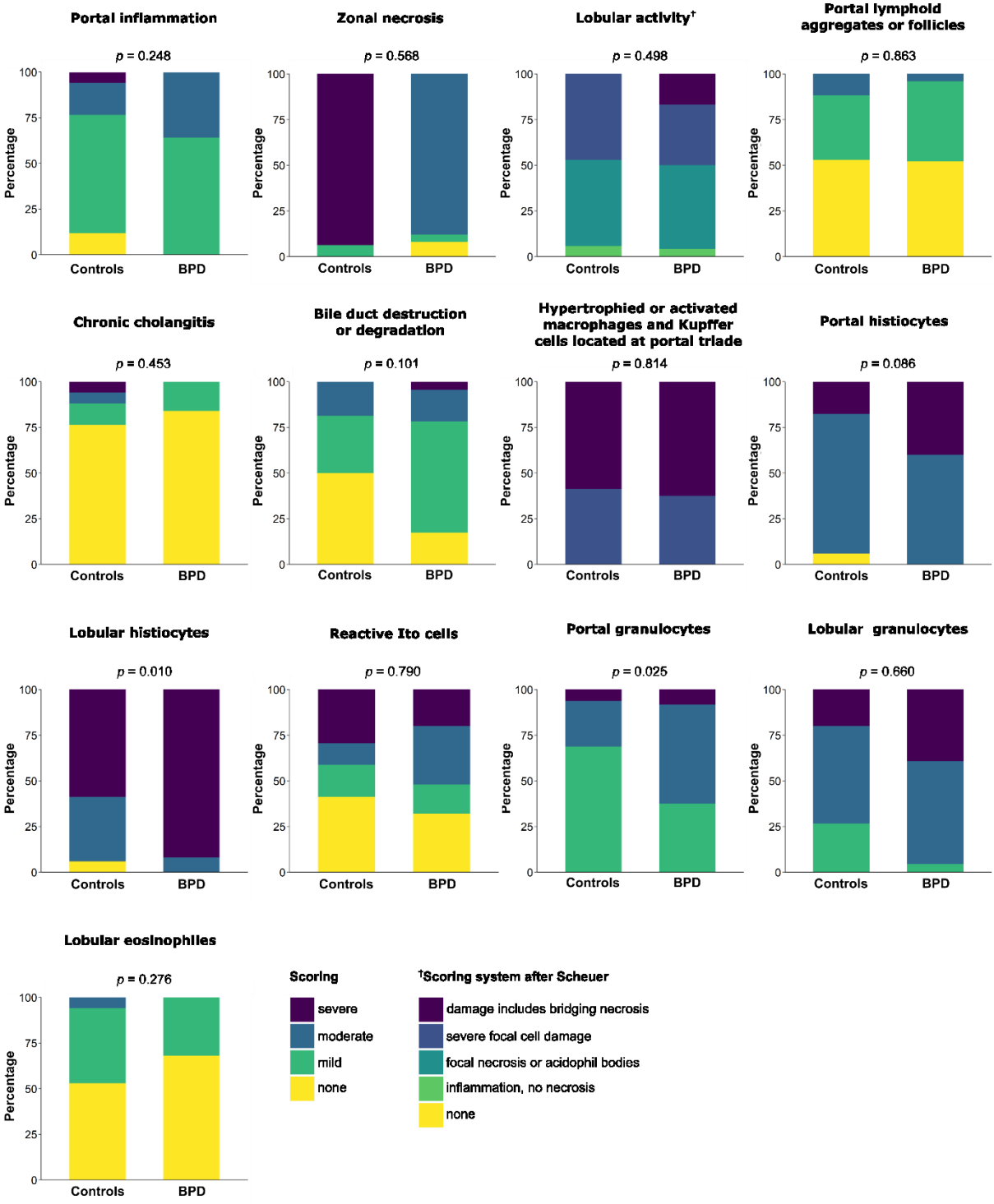

Figure 30. **Frequency distribution of assessed histopathological features categorized to inflammation, part I.** The percentage of the respective histopathological feature score for the patients with bipolar disorder (BPD) and the control group (Controls) are given. Statistical analyses: Mann Whitney U test; [Based on [90]]

Further, the portal and lobular appearance of lymphocytes was assessed (***Figure 31***). Mainly, none or mild appearance of cytotoxic T-lymphocytes ($CD8^+$) in lobular areas was observed in

the group of bipolar disorder (83.4%) as compared to a moderate to severe appearance in 81.3% of the controls ($p = 0.001$). None of the other assessed inflammation features revealed statistical significant difference of the frequency distributions.

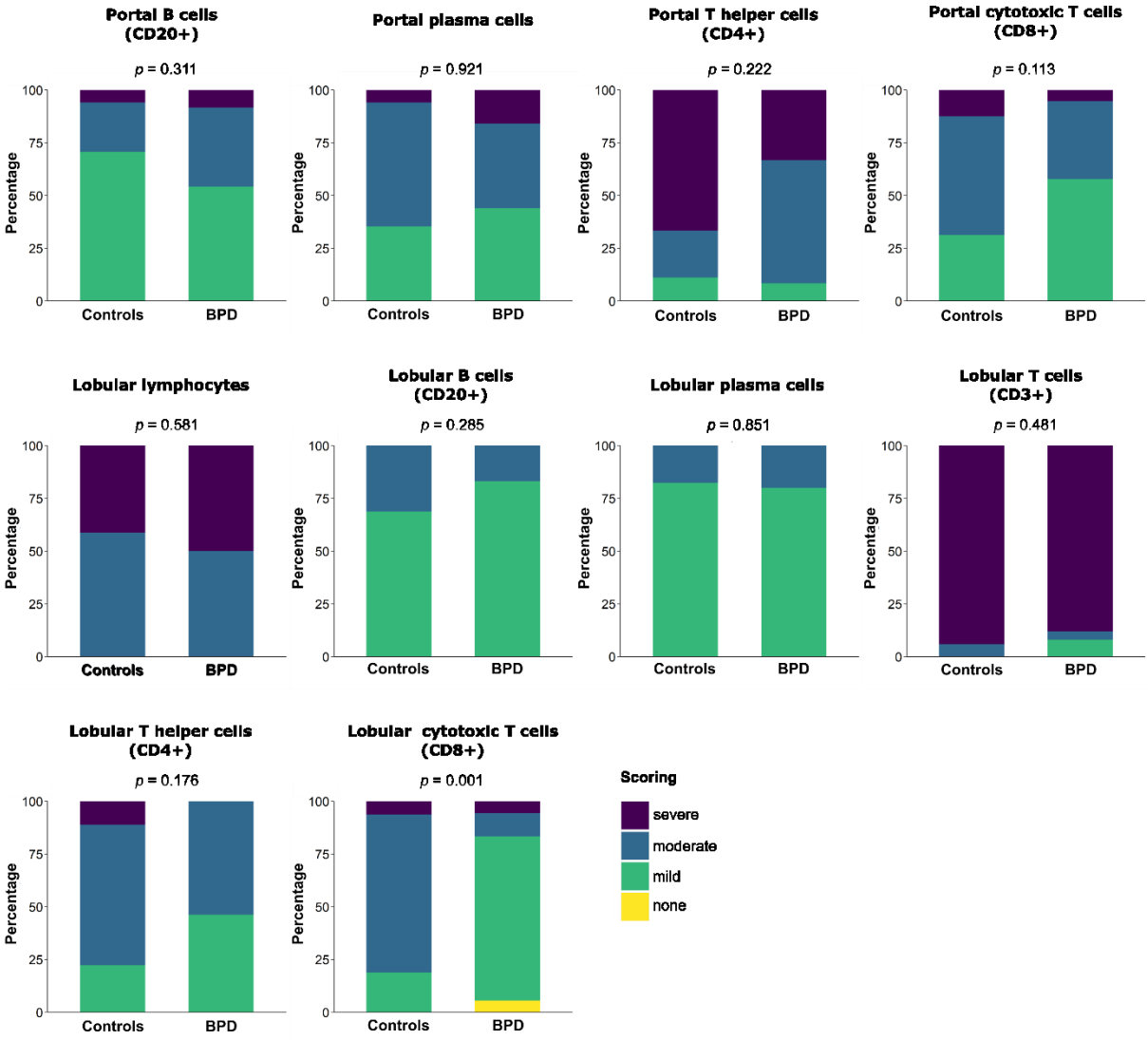

Figure 31. **Frequency distribution of assessed histopathological features categorized to inflammation, part II.** The percentage of the respective histopathological feature score for the patients with bipolar disorder (BPD) and the control group (Controls) are given. Statistical analyses: Mann Whitney U test; [Based on [90]]

The histopathological features of fibrosis were assessed with respect to their frequency distribution for the presence of fibrosis in perisinsoidal and perivenular areas, as well as the appearance of fibrosis at areas surrounding the central vein (***Figure 32***). A statistical significant difference in these features was absent.

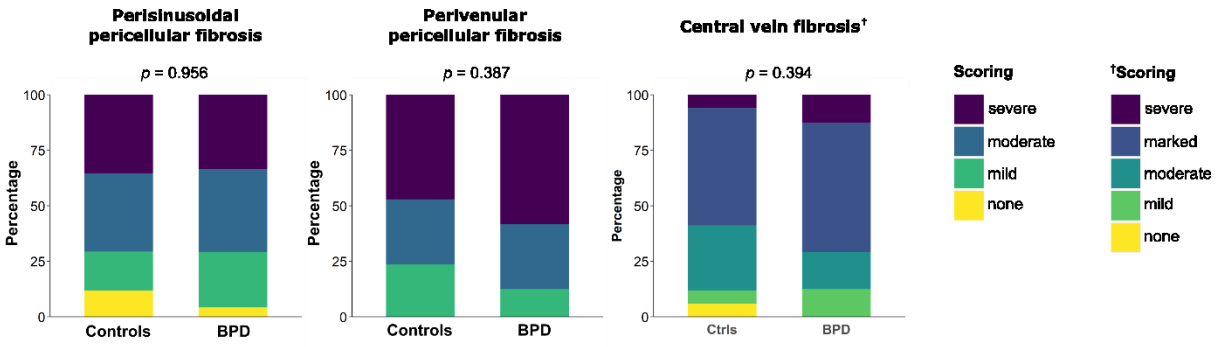

Figure 32. **Frequency distribution of assessed histopathological features categorized to fibrosis.** The percentage of the respective histopathological feature score for the patients with bipolar disorder (BPD) and the control group (Controls) are given. Statistical analyses: Mann Whitney U test; [Based on [90]]

Frequency distributions of the category of endogenous reaction describing a possible cholestatic reaction including features for typical and atypical ductular proliferation, as well as bile duct metaplasia were assessed (***Figure 33***). Both groups revealed comparable frequencies of the respective scores for all features. For none of the features, statistical significant difference was observed between the bipolar disorder and the controls.

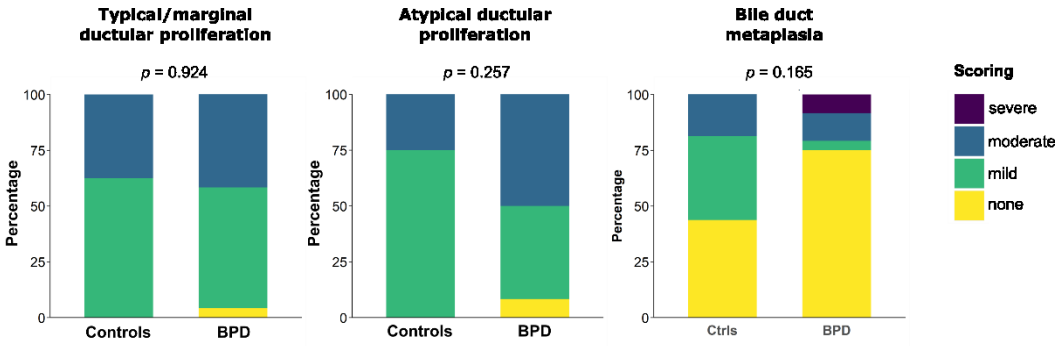

Figure 33. Frequency distribution of assessed histopathological features categorized to endogenous reaction. The percentage of the respective histopathological feature score for the patients with bipolar disorder (BPD) and the control group (Controls) are given. Statistical analyses: Mann Whitney U test; [Based on [90]]

For the category of steatosis, frequency distributions were assessed for histopathological features of intracytoplasmic accumulation of lipids, namely macrovesicular and microvesicular steatosis and the combination of both types, as well as the zonal distribution of the lipid

accumulation (***Figure 34***). No statistical significant differences were observable for all features of this category between the groups.

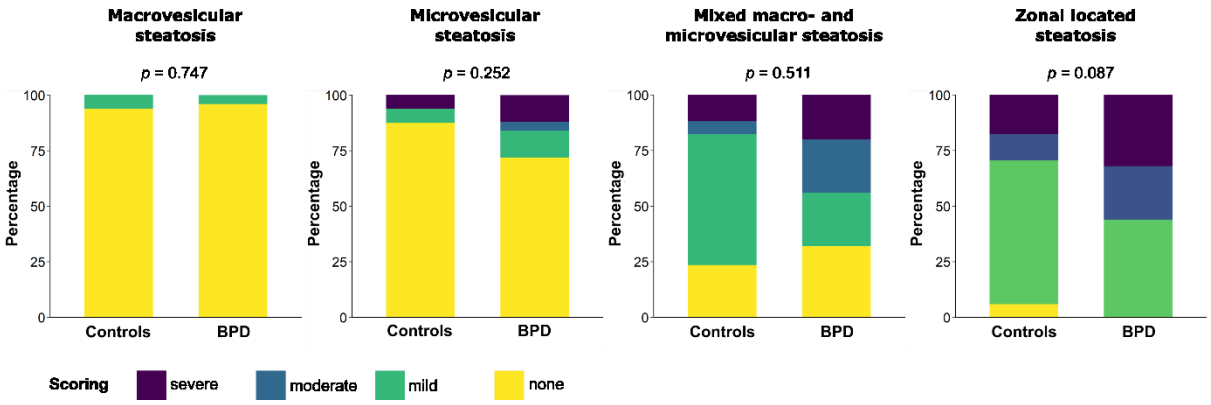

Figure 34. Frequency distribution of assessed histopathological features categorized to steatosis. The percentage of the respective histopathological feature score for the patients with bipolar disorder (BPD) and the control group (Controls) are given. Statistical analyses: Mann Whitney U test; [Based on [90]]

3.10 Associations between gene expression and histopathological features

Feature-expression heatmaps were generated in order to visualize the association between assessed histopathological characteristics and gene expression.

The associations between genes belonging to the RETC and histological features of the liver were depicted in the RETC feature-expression heatmap (***Figure 35***). Although an overall clustering of associations was absent between RETC genes and degenerative changes, the positive associations between the presence of glycogenated or vacuolated nuclei, located glycogenated nuclei and the presence of iron pigments in Kupffer cells were notable. A clustering of negative associations between RETC gene expression and hepatic activity was present. Prominent negative associations were observed for periportal or periseptal interface hepatitis and the Ishak grading. The heatmap showed a cluster of strong negative association between RETC genes and histological features of inflammation including the presence of portal inflammation, portal granulocytes, $CD20^+$ B-cells and $CD4^+$ T-cells, lobular plasma cells and histiocytes and biliary duct destruction. A cluster of weaker negative associations were found between RETC genes and the presence of portal lymphoid aggregates or follicles and plasma cell infiltrates, reactive Ito cells and lobular $CD3^+$, $CD4^+$ and $CD8^+$ T-cells. Positive association

cluster were observed between RETC genes and the presence of lobular granulocytes, eosinophils and $CD20^+$ B-cells. Association clustering between genes of the RETC and fibrosis was absent. Strong positive associations were present between RETC genes and biliary duct metaplasia in the category of endogenous reaction. Clustering of associations were absent between RETC genes and the histological features of steatosis. After FDR correction, none of the individual analyses were statistically significant.

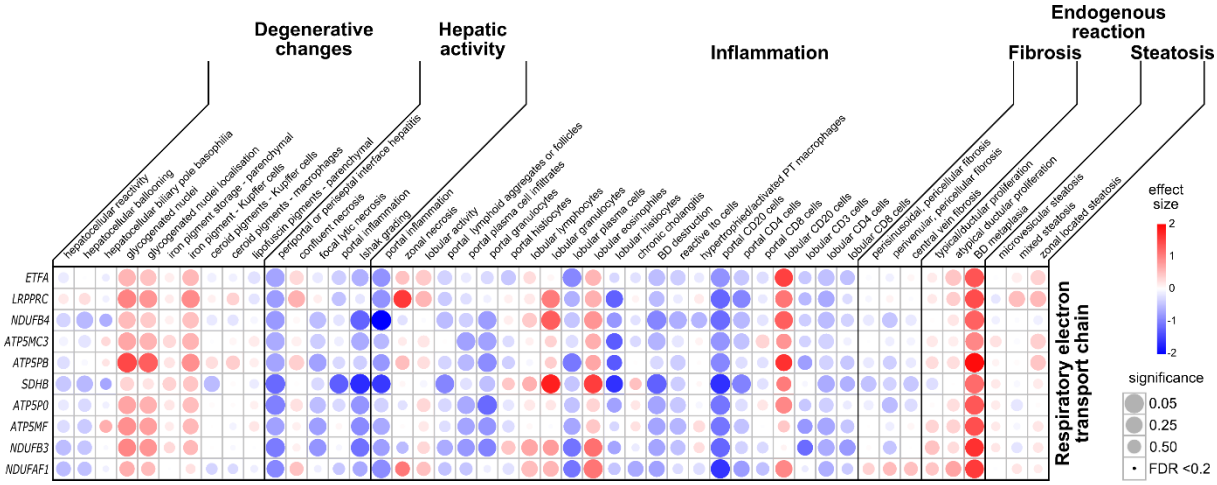

Figure 35. **Feature-expression heatmap depicting the association between genes related to respiratory electron transport chain (RETC) and histologically assessed characteristics of the liver.** Histological characteristics were ordinally or binary measured. Gene expression was expresses as $\log_2$ intensity values. The color code (red = positive, blue = negative) and color intensity represent the regression coefficient. The circle radius represent the statistical significance of the regression analysis, whereas dotted circles represent a false discovery rate (FDR) below 0.2 for multiple testing. Blank squares correspond to a small regression coefficient and statistical probability or an analysis with insufficient observations. Full names are listed in ***Table A1*** in the Appendix. [Published in [90]]

The lipid metabolism feature-expression heatmap was created from associations between genes belonging to the lipid metabolism and histological features of the liver (***Figure 36***). A clustering of positive associations was observed between lipid metabolism genes and degenerative changes. Especially the association analyses between the presence of glycogenated or vacuolated nuclei, located glycogenated nuclei, and the presence of iron pigments in Kupffer cells revealed strong positive associations. Four associations were significant after FDR correction, corresponding to the acyl-CoA binding domain containing 5 (*ACBD5*) gene and the protein kinase AMP-activated non-catalytic subunit beta 2 (*PRKAB2*) gene. An overall clustering of associations between lipid metabolism genes and hepatic activity could not be

identified, however, the negative association between the *ACOT13* gene and periportal or periseptal interface hepatitis was significant after FDR correction. Although an overall clustering of associations was absent between lipid metabolism genes and inflammation, negative associations were revealed for portal inflammation and positive associations for lobular histiocytes and $CD20^+$ B-cells, and chronic cholangitis. A clustering of associations was absent between lipid metabolism genes and fibrosis, endogenous reaction and steatosis and none of the individual analyses was significant after FDR correction.

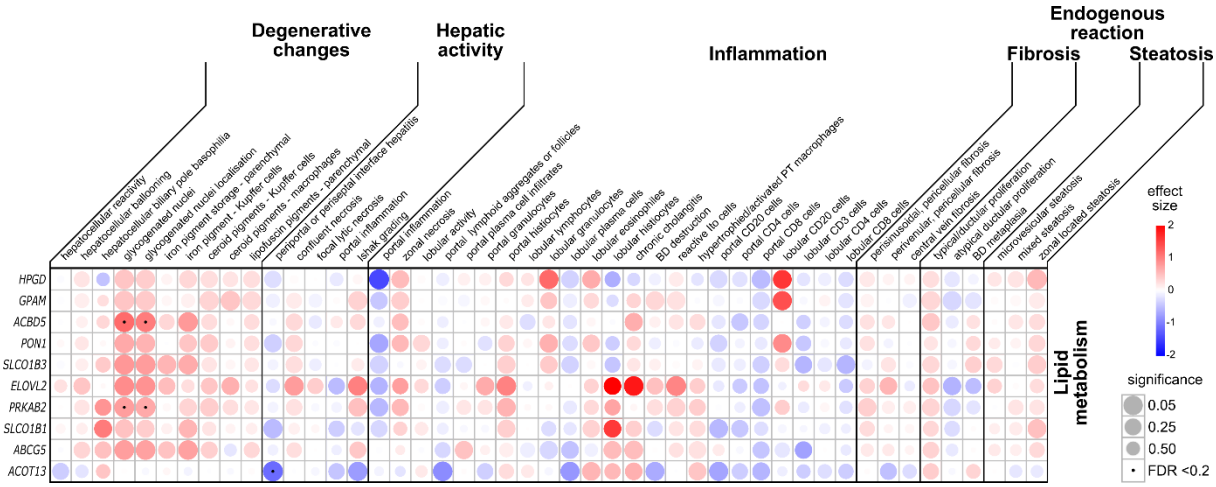

Figure 36. **Feature-expression heatmap depicting the association between the expression of genes related to lipid metabolism and histologically assessed characteristics of the liver.** Histological characteristics were ordinally or binary measured. Gene expression was expresses as $\log_2$ intensity values. The color code (red = positive, blue = negative) and color intensity represent the regression coefficient. The circle radius represents the statistical significance of the regression analysis, whereas dotted circles depict a false discovery rate (FDR) below 0.2 for multiple testing. Blank squares correspond to a small regression coefficient and statistical probability or an analysis with insufficient observations. Full names are listed in ***Table A1*** in the Appendix. [Published in [90]]

The biological oxidations feature-expression heatmap was generated from associations between genes belonging to biological oxidations and histological features of the liver (***Figure 37***). A clustering of positive associations was observed between biological oxidations genes and degenerative changes. A strong positive associations was observed between present glycogenated or vacuolated nuclei, located glycogenated nuclei and the presence of iron pigments in Kupffer cells. The association between the expression of gene coding for the *CMBL* and the presence of glycogenated or vacuolated nuclei was significant after FDR correction. A pronounced clustering of associations was absent for hepatic activity, inflammation, fibrosis, endogenous reaction and steatosis. However, a strong positive association was observed

between sulfotransferase family 1E member 1 (*SULT1E1*) and portal zonal necrosis in the inflammation category. A strong negative association was revealed between *SULT1E1* expression and the presence of microvesicular steatosis in the steatosis category. After FDR correction, none of the other individual analyses were statistically significant.

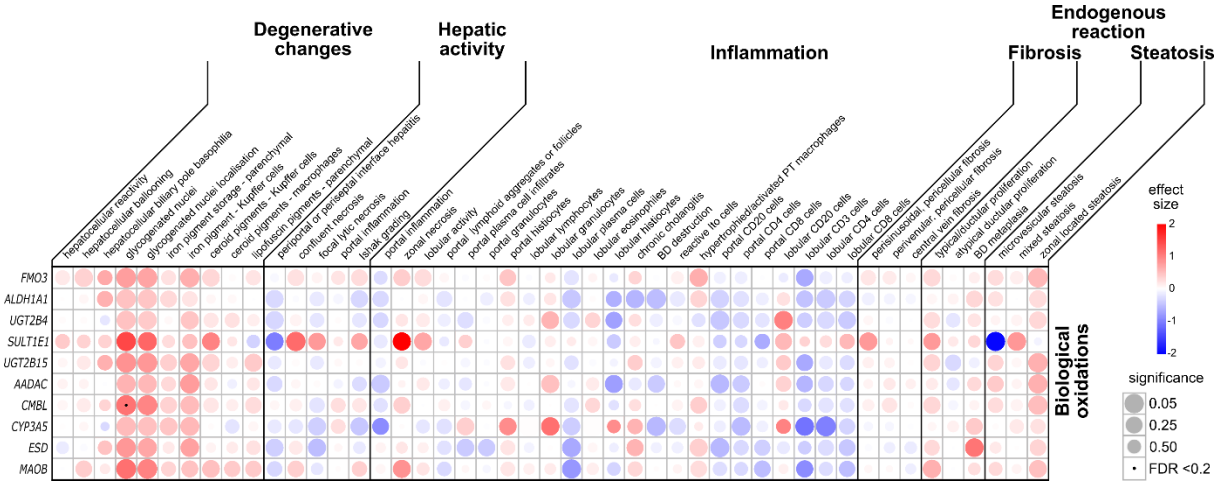

Figure 37. **Feature-expression heatmap depicting the association between the expression of genes related to biological oxidations and histologically assessed characteristics of the liver.** Histological characteristics were ordinally or binary measured. Gene expression was expresses as $\log_2$ intensity values. The color code (red = positive, blue = negative) and color intensity represent the regression coefficient. The circle radius represent the statistical significance of the regression analysis, whereas dotted circles depict a false discovery rate (FDR) below 0.2 for multiple testing. Blank squares correspond to a small regression coefficient and statistical probability or an analysis with insufficient observations. Full names are listed in ***Table A1*** in the Appendix. [Published in [90]]

The associations between genes belonging to the metabolism of amino acids and histological features of the liver were depicted in the amino acid metabolism feature-expression heatmap (***Figure 38***). Association analyses revealed a clustering of associations between amino acid metabolism genes and degenerative changes. Particularly strong positive associations were discovered between presence of glycogenated or vacuolated nuclei, located glycogenated nuclei, and the presence of iron pigments in Kupffer cells. Three associations were significant after FDR correction, corresponding to the genes coding for dehydrogenase E1 and transketolase domain containing 1 (*DHTKD1*) and glycine amidinotransferase (*GATM*). An overall clustering of associations between amino acid metabolism genes and hepatic activity could not be identified. Although an overall clustering of associations was absent between amino acid metabolism genes and inflammation, negative associations were revealed for portal inflammation and portal $CD3^+$ T-cells, and positive associations for zonal necrosis and lobular histiocytes. A clustering of associations was absent between amino metabolism genes and

fibrosis, as well as endogenous reaction. Weak associations were found between neutrophil degranulation genes and zonal located steatosis in the steatosis category.

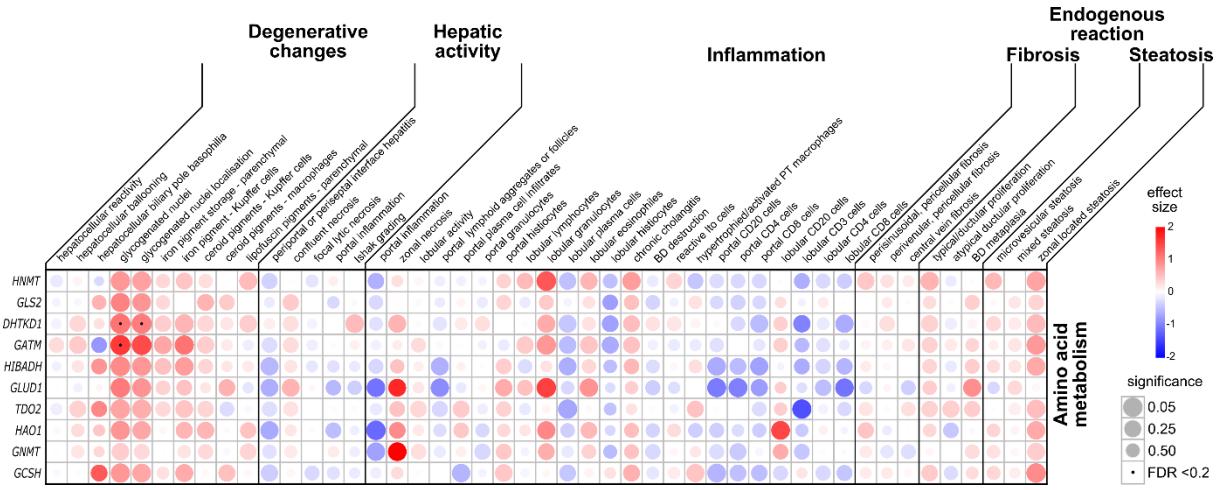

Figure 38. **Feature-expression heatmap depicting the association between the expression of genes related to amino acid metabolism and histologically assessed characteristics of the liver.** Histological characteristics were ordinally or binary measured. Gene expression was expresses as $\log_2$ intensity values. The color code (red = positive, blue = negative) and color intensity represent the regression coefficient. The circle radius represent the statistical significance of the regression analysis, whereas dotted circles depict a false discovery rate (FDR) below 0.2 for multiple testing. Blank squares correspond to a small regression coefficient and statistical probability or an analysis with insufficient observations. Full names are listed in ***Table A1*** in the Appendix. [Published in [90]]

The associations between genes belonging to the neutrophil degranulation and histological features of the liver were depicted in the neutrophil degranulation feature-expression heatmap (***Figure 39***). A clustering of positive associations was observed between neutrophil degranulation genes and degenerative changes. Strong positive associations were observed between present glycogenated or vacuolated nuclei and located glycogenated nuclei, weaker positive associations for the presence of iron pigments in Kupffer cells. The associations between the expression of the genes coding for amylo-alpha-1, 6-glucosidase, 4-alpha-glucanotransferase (*AGL*) and high mobility group box 1 (*HMGB1*) and the presence of glycogenated or vacuolated nuclei were significant after FDR correction. An overall clustering of associations between amino acid metabolism genes and hepatic activity could not be identified. A weak clustering of negative associations was observed between neutrophil degranulation genes and inflammation, whereas the negative associations between the genes coding for *S100A9* and *S100A12* and the presence of reactive Ito cells were significant after FDR correction. Clustering of associations could not be identified for fibrosis and steatosis

features. A weak clustering of associations was present between neutrophil degranulation genes and biliary duct metaplasia.

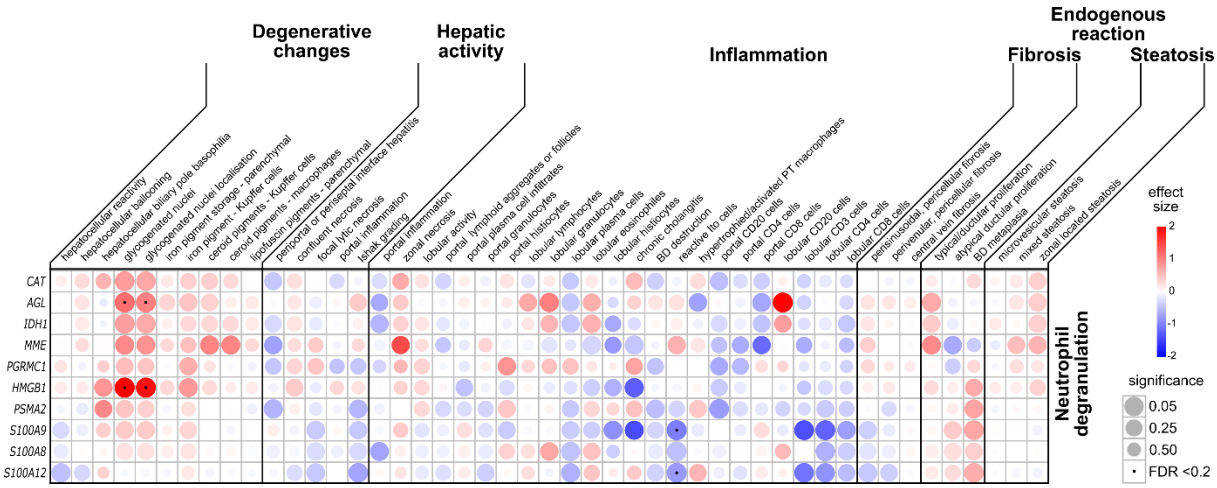

Figure 39. **Feature-expression heatmap depicting the association between the expression of genes related to neutrophil degranulation and histologically assessed characteristics of the liver.** Histological characteristics were ordinally or binary measured. Gene expression was expresses as $\log_2$ intensity values. The color code (red = positive, blue = negative) and color intensity represent the regression coefficient. The circle radius represent the statistical significance of the regression analysis, whereas dotted circles depict a false discovery rate (FDR) below 0.2 for multiple testing. Blank squares correspond to a small regression coefficient and statistical probability or an analysis with insufficient observations. Full names are listed in ***Table A1*** in the Appendix. [Published in [90]]

4 Discussion

Parts of the discussion resemble the discussion section in Birkl-Toeglhofer et al. 2019 [90].

Psychotropic drugs, such as antipsychotics, antidepressants and mood stabilizers, represent a substantial treatment option in bipolar disorder. Despite their positive treatment effects and improved drug safety, potential adverse effects of the required acute and long-term drug treatment in the liver have to be considered. However, consequences on hepatic gene expression upon psychotropic drug treatment in bipolar disorder remain to be fully elucidated. Here, a genome-wide approach of gene expression with advanced comprehensive bioinformatical analyses was applied to address the influence of psychotropic drugs in bipolar disorder on the hepatic function. In addition, possible associations between gene expression and the presence of histopathological features of liver disease were examined.

4.1 Presence of an altered hepatic expression in bipolar disorder

Differential gene expression was present in hepatic tissue of patients with bipolar disorder and psychotropic drug treatment. The differential expression analysis revealed only a few upregulated genes, whereas the larger portion were identified as downregulated genes. This suggests that psychotropic drug treatment rather turns off genes than shifting to an increased expression state of various genes. After annotation of the DEGs, assumptions on the individual gene level were feasible. The majority of downregulated genes were found to be associated with membranes in context to their subcellular localization and are involved in processes related to the metabolism. Resulting disturbances in energy metabolism, as well as lipid and glucose metabolism have already been shown for psychotropic drugs [113,114]. Psychotropic drugs for treating depression and mood disorders were shown to affect enzyme activity and respiration in the mitochondria [113]. Both, lipid and glucose metabolism were supposed to be affected by antipsychotics, such as clozapine, olanzapine, risperidone and quetiapine [114]. A higher estimated prevalence was shown for obesity and diabetes in patients with bipolar disorder and schizophrenia. These observations supported the assumption that psychotropic drug treatment possibly adversely effects metabolic pathways in the liver tissue of patients with bipolar disorder.

Beside the possible impairment of metabolic processes, the individual gene analysis revealed that the five respective major over- and underexpressed genes were found to play a role in immune response, oxidative stress response, apoptosis, and maintenance of the cell structure. Those genes are discussed and interpreted in accordance with recent literature.

4.1.1 Upregulated genes involved in inflammatory response

Revealing of the top five upregulated genes suggested the presence of increased inflammatory features in hepatic tissue of patients with bipolar disorder treated with psychotropic drugs. Those upregulated genes included the calgranulin genes *S100A8*, *S100A9* and *S100A12*, which are known to be abundantly expressed in neutrophils and associated with acute and chronic inflammatory disorders and various cancer types [115–118]. Altered levels of S100 genes and proteins were found in various tissue types of psychiatric disorders, such as bipolar disorder and schizophrenia [119–122]. It has been shown that increased *S100A8* and *S100A9* expression was present in the hippocampus of patients with bipolar disorder and schizophrenia [119]. Additionally, altered *S100A9* expression in blood were reported in a microarray approach of patients with bipolar disorder and schizophrenia [120]. Increased *S100A9* mRNA levels were found in both psychiatric disorder groups when compared to control subjects. With regard to *S100A12*, altered protein levels and mRNA expression have been observed in patients with bipolar disorder and patients with schizophrenia [121,122]. In both disorders, non-invasively measured S100A12 levels were found to be increased in saliva samples in comparison to healthy controls [121].With regard to hepatic pathology, higher serum levels of S100A8 and S100A9 were present in patients with NASH and fibrotic features [123]. In HCC, malignancy progression was supposed to be promoted by an increase of S100A8 and S100A9 on gene and protein level [124]. A recent study investigating the knockout of *S100A9* in a mouse model of HCC observed reduced tumor size and a lower number of high-graded tumors in comparison to wild type mice [125]. The overexpression of S100 genes indicated a possible prominent inflammatory component in hepatic tissue of bipolar disorder. Probably, overexpression of calgranulins is intrinsically prevalent in severe mental disorders and might not be restricted to brain tissue. The overlapping findings in bipolar disorder and schizophrenia would indicate a relationship between these psychiatric disorders, but to which extent patients with schizophrenia also show hepatic overexpression of these S100 genes has to be examined.

Another highly overexpressed gene was identified as *SAA2*. The gene encodes for the serum amyloid A2 protein and belongs with the serum amyloid A1 protein to the acute-phase serum amyloid protein (A-SAA) primarily synthesized in the liver [126]. The SAA2 protein level was found to be induced by proinflammatory cytokines, such as interleukin-1-beta, interleukin-6 and tumor necrosis factor-α [127]. SAA2 has been shown to serve as chemoattractant for monocytes [128] and neutrophils [129]. With regard to psychiatric disorders, increased A-SAA plasma levels were associated with symptoms of depression and depressive disorder in a population-based cohort study (36). Another study showed that higher A-SAA levels were found in individuals with moderate to severe depressive symptoms [131]. The increased A-SAA levels correlated with several psychiatric rating scales items pointing to fatigue. In context to hepatic function, it has been shown that elevated A-SAA levels were present in primary hepatic stellate cells of healthy human livers and in an animal model investigating hepatic fibrosis [132]. It was proposed that A-SAA modulates fibrogenesis by its pro-proliferative effect on hepatic stellate cell at the sites of injury. These findings suggest that the presence of generally higher A-SAA levels in patients with bipolar disorder might entails a higher susceptibility to fibrogenesis during liver injury.

The *IL1RN* gene encoding for the protein interleukin-1 receptor antagonist (IL-1Rα) was found to be upregulated in bipolar disorder. This protein represents an anti-inflammatory cytokine which binds specifically to the interleukin-1 receptors leading to the inhibition of interleukin-1 downstream signaling and thereby functioning immunosuppressive [133]. In non-medicated patients with bipolar disorder, a state-dependent cytokine pattern was observed in manic and depressive phases [134]. A meta-analysis showed that patients with bipolar disorder revealed higher circulating IL-1Rα levels during a manic episode and in euthymic patients compared to healthy controls [135]. Additionally, associations between increased IL-1Rα levels and psychotic symptoms [136], as well as cognitive function in psychiatric disorders [137] were reported. Furthermore, a recent study revealed increased plasma IL-1Rα levels in patients with NASH and correlate with markers for hepatic inflammation and damage [138]. Another study showed an association between increased serum IL-1Rα levels and histologically assessed features, as well as a correlation between hepatic *IL1RN* expression and NASH [139]. In summary, these findings would suggest that patients with psychiatric disorders, such as bipolar disorder, have higher levels of IL-1Rα per se. This could probably lead to a more detrimental effect in the context of hepatic injury.

4.1.2 Downregulated genes involved in oxidative stress response, apoptosis and regeneration

FMO3 was identified as the most underexpressed gene in the bipolar disorder group. Aside from CYPs, the FMO3 enzyme reduces oxidative stress by metabolizing a broad variety of endogenous compounds and xenobiotics including plant alkaloids and synthetic therapeutic drugs [140]. Decreased *FMO3* expression has been observed in a mouse model of hepatoxicity using carbon tetrachloride for oxidative stress induction [141]. Recently, a study analyzed the effect of epigenetically silenced *FMO3* expression in HCC-derived cell lines and further analyzed the effect on the HCC survival probability in the publicly available liver hepatocellular carcinoma data set of The Cancer Genome Atlas (TCGA LIHC) [142]. Cells of the HCC cell lines showed increased cell viability and invasion capability, as well as decreased apoptosis when *FMO3* was epigenetically silenced. The TCGA LIHC revealed that patients with HCC and a low *FMO3* expression indicated a poorer survival probability than those with higher expression. Another study showed detrimental effects on the hepatic antioxidative system by chronic administration of antidepressants, such as the SSRI fluoxetine, in an animal model for depression [143]. This leads to the suggestion that patients with bipolar disorder under psychotropic drug treatment probably have a higher rate of hepatic oxidative stress and would be more prone to develop liver disease, possibly even HCC. None of the analyzed patients with bipolar disorder were identified to suffer from HCC, but several histopathological features pointed to NAFLD or NASH, which are known to be precursors stages and can progress in unfavorable cases to HCC.

The amino acid transporter *SLC38A4* was found to be underexpressed in bipolar disorder upon psychotropic drug treatment. So far, less research has been performed on the effect of altered *SLC38A4* expression in the context of hepatic function, especially in context of psychiatric disorders. A genome-wide association study reported an association between the *SLC38A4* locus and cases of severe alcoholic hepatitis [144]. Genetic predispositions in *SLC38A4* were identified as potential risk to develop alcoholic hepatitis. However, as genetic variants were not explored in the bipolar disorder and control samples and a difference in alcohol intake between bipolar disorder and the control group was absent, the impact of such predisposition on the hepatic function under psychotropic drug treatment remains to be determined.

One of the top five underexpressed genes in bipolar disorder was *TNFSF10*. This gene encodes for the TNF-related apoptosis-inducing ligand super family member 10 or TRAIL, which is

mainly known in the context of apoptotic signaling [145]. It triggers the proapoptotic signaling cascade by binding to the death-signaling receptors followed by the activation of the caspase pathway [146]. A recent study reported that *TNFSF10* mRNA and protein levels were associated with NAFLD or NASH in humans, mice and *in vitro* [147]. Lower TNFSF10 plasma levels were shown in patients with NASH. *TNFSF10* knock-out mice developed more severe histopathological features of NAFLD and NASH than their wildtype littermates with high fat diet. Palmitate-treated HepG2 cells resembling an in vitro model of NAFLD showed increased lipid accumulation, inflammation and fibrosis, and about 50% reduced *TNFSF10* mRNA expression. Conversely, the palmitate-induced lipid uptake was reduced when treating the HepG2 cells with exogenous TNFSF10. These findings suggests a protective effect of *TNFSF10* expression in liver tissue. Therefore, it can be concluded that a detrimental effect of psychotropic drugs in bipolar disorder probably exists and leads to lowered *TNFSF10* expression and, hence, contributes to hepatic injury. In context of psychiatric disorders, decreased *TNFSF10* expression was observed in prefrontal brain tissue of patients with bipolar disorder and patients with schizophrenia [148]. An effect of antipsychotic treatment on *TNFSF10* expression in both groups was excluded by regression analysis. All of which indicates that decreased *TNFSF10* expression might rather be generally linked to bipolar disorder than affected by drug treatment.

Another top downregulated gene in bipolar disorder was found to be *CAT*. The protein is mainly located in peroxisomes and acts as antioxidative enzyme essential for decomposing hydrogen peroxide to water and oxygen in the setting of intracellular oxidative stress [149]. An altered CAT activity was reported in psychiatric disorders [150–152]. Lower levels of CAT were observed in blood samples of male patients with bipolar disorder and schizophrenia treated with psychotropic drugs suggesting increased oxidative stress [152]. A case report of identical twins with bipolar disorder showed lower CAT activity levels in serum samples in comparison to a matched control [150]. Decreased CAT activity remained even after psychotropic drug treatment in one of the twins. Additionally, another study showed reduced CAT activity in plasma red blood cells of patients with bipolar disorder and schizophrenia, whereas lowest activity was present in the schizophrenia samples [151]. The function of antioxidant enzymes including *CAT* has been extensively reviewed in the context of NAFLD pathogenesis [153]. It has been proposed that increased oxidative stress triggers the development of NAFLD and NASH, whereas CAT was shown to suppress hydrogen peroxide accumulation and, hence,

plays a prominent role in the cellular antioxidant defense system. In an early study, *CAT* overexpression was shown to have a beneficial effect by protecting cells from cytotoxicity arising by oxidative stress *in vitro* [154]. Another study investigated the hepatic gene expression of reactive oxygen species scavenging enzymes including *CAT* in NASH [155]. A significant downregulation of *CAT* and other genes encoding those scavenging enzymes was identified in NASH. Besides a decreased *CAT* expression, the activity of CAT was also reduced in human liver tissue samples [156]. The progression from steatosis to steatohepatitis showed a continuous decrease of the antioxidant capacity by CAT. All of this would suggest that patients with bipolar disorder and treated with psychotropic drugs are challenged with a higher level of oxidative stress and would be more prone to undergo the progress from simple fatty liver to NAFLD or NASH.

The fifth most downregulated gene was identified as *TUBE1*, encoding the ε-tubulin protein a member of the tubulin superfamily. The protein is specifically localized at the centrosomes and is thought to be an integral centrosomal component [157]. The ε-tubulin presented distinct spatial and temporal cell cycle-dependent localizations compared to the other tubulin family members. A pivotal role for TUBE1 has been identified in the organization of the microtubule cytoskeleton [158]. An *in vitro* study has shown that after silencing *TUBE1* in *Paramecium* a progressive worsening of the cell structure was observable which was induced by an impaired basal body duplication [159]. This impaired basal body duplication revealed a phenotype presenting a diminished cell size and a more rounded cell shape, whereas cell death occurred after three to four cell divisions. With regard to hepatic cells in patients with bipolar disorder upon drug treatment this might suggest a lower regeneration rate of injured hepatic sites which remains to be determined.

4.2 Affected biological pathways upon psychotropic drug treatment

As biological processes rely rather on intricate networks of interacting genes and proteins than individual gene or protein function, the application of extensive computational biological approaches was indispensable to capture and investigate the underlying mechanism in liver tissue of psychotropic drug treated patients with bipolar disorder. An intricate network of interacting proteins has been confirmed by the protein-protein network analyses. The

investigation of affected functional processes and networks included the comprehensive analyses of probable key regulators and underlying molecular complexes, as well as the determination of enriched biological pathways.

4.2.1 Mitochondrial dysfunction upon psychotropic drug treatment

The most affected biological process in bipolar disorder was found to be the cellular energy supply. Several energy-related genes and their corresponding proteins were found to be decreased. Based on betweenness centrality, the hub protein analysis revealed the ATP synthase subunit ATP5O as considerable key regulator. ATP5O was also found in module 2 alongside with various NADH dehydrogenases, where NDUFA9 was determined as the module's seed protein. Some of the module 6 proteins referred to mitochondrial proteins related to the energy supply. Furthermore, the enrichment analysis strengthened the possible functional deterioration of cellular energy supply. Several highly significant enriched pathways were related to the RETC. All proteins of module 2 overlapped with the queried and RETC-allocated DEGs. In addition, all RETC-allocating DEGs were underexpressed in the liver tissue of the investigated psychotropic drug-treated bipolar disorder group. Recent studies showed impairing effects on the energy metabolism and mitochondrial function upon psychotropic drug treatment [160–162]. One of those studies revealed reduced expression levels of mitochondria related genes in brain tissue of patients with bipolar disorder and antipsychotic treatment [160]. This observation was concluded as effect of the drug treatment, since untreated patients with bipolar disorder revealed rather an upregulation of those genes. Another study revealed decreased expression of mitochondria-related genes in blood samples of patients with bipolar disorder and known response to the mood stabilizer lithium [163]. Downregulated genes included genes encoding for the RETC and the oxidative phosphorylation pathway. Another study showed that patients with schizophrenia treated with antipsychotics revealed lower gene expression of mitochondria enzymes in peripheral blood mononuclear cells [161]. The antipsychotics, clozapine and olanzapine, showed the strongest decreasing effect on those genes, followed by quetiapine and risperidone. A recent study showed that bupropion, an antidepressant, decreased cellular ATP content at non-cytotoxic drug concentrations in two human hepatocyte cell lines [162]. The bupropion-treated cells presented the inhibition of complex I and II of the RETC, as well as increased reactive oxygen production. Among other antipsychotics and antidepressants,

all of the aforementioned antipsychotics and bupropion were under those psychotropic drugs recorded in the investigated patients with bipolar disorder. The previous findings have now been confirmed also in human liver tissue of patients with bipolar disorder and psychotropic drug treatment, since the decreased expression of RETC-genes was present in the bipolar disorder group. An animal study showed NAFLD features upon antipsychotic treatment [164]. Wistar albino rats treated with olanzapine or aripiprazole revealed increased hepatic steatosis, ballooned hepatocytes and inflammatory infiltrates. Therefore a diminished energy supply upon psychotropic drug treatment in liver cells, but obviously also in the periphery, and the resulting consequences, such as liver injury, have to be taken into consideration.

4.2.2 Altered lipid metabolism upon psychotropic drug treatment

In addition, diminished expression levels of all genes allocated to the enriched pathway metabolism of lipids and lipoproteins have been observed in the bipolar disorder group. As the catabolism of lipids produces substrates, such as pyruvate, for the citric acid cycle and thus for the RETC, it further suggest that psychotropic drugs could lead to a severe interference of the cell's energy supply. Several proteins of module 6 overlapped with the genes enriched in the lipid and lipoprotein metabolism. Further overlaps were present for module 1 and 4. In total, four supposed hub proteins were also present among the enriched pathway. Those included IDH1, DECR1, APOB and PTEN.

IDH1, coding for a peroxisomal and cytoplasmic enzyme, was one of the most underexpressed genes in this enriched pathway. A comprehensive gene expression profiling study searching for symptom-depending blood biomarkers in schizophrenia showed associations with *IDH1* [165]. Decreased *IDH1* expression was observed in blood samples of patients with schizophrenia and delusions and was confirmed in additional human tissue of schizophrenia patients, such as post-mortem brain tissue and fibroblasts, as well as in a schizophrenia mouse model treated with phencyclidine. Unfortunately, a possible association with psychotropic drug treatment in bipolar disorder still remains to be determined. In context of hepatic IDH1 function, *Idh1* knockout mice showed increased oxidative stress by accumulation of reactive oxygen species in the liver [166]. This led to the assumption that IDH1 might play a role in the antioxidant defense and probably suppress hepatic inflammation.

The enzyme encoded by *DECR1* is known to play a role in the mitochondrial β-oxidation of unsaturated fatty acids as auxiliary enzyme. In terms of psychiatric disorder and effects of psychotropic drug treatment, less is known about this gene. An *in silico* study of published data investigating a gene expression study using an animal model of NASH induced by high fat diet showed a possible fundamental role in NASH development [167]. It was suggested that altered *DECR1* levels possibly affect the development of NASH at later stage. To which extent decreased *DECR1* expression due to psychotropic drug treatment might affect liver injury in bipolar disorder remains to be solved.

The ApoB protein, where the isoform ApoB-100 is synthesized in the liver, is involved in transporting lipids in very low density lipoproteins [168]. A study investigating lipid metabolism upon antipsychotic treatment observed altered ApoB-100 secretion levels in several human hepatic cell lines [169]. The clozapine treatment did not alter ApoB-100 secretion, but after omitting clozapine increased ApoB-100 secretion was shown. It has been assumed that the antipsychotic-dependent effect entailing increased triglycerides levels regulates the ApoB secretion. If the decreased *APOB* gene expression in bipolar disorder, represent an adequate ApoB level after protein translation has not been investigated. So far, an effect of long-term psychotropic drug treatment on ApoB levels was absent in cell culture. It has to be taken into account that psychotropic drug treatment is generally a long-term treatment in patients meaning that effects of long-term drug exposure might be apparent only after a longer time period. In addition, possible compensating effects have to be considered where ApoB levels would be decreasing when fat accumulation in the cell exceeds a certain threshold. In context of *APOB* gene and protein expression in liver injury, an early study could show that patients with NASH have reduced ApoB-100 synthesis rates [170]. This has been shown when comparing the ApoB-100 synthesis rates in patients with NASH to lean and obese individuals. Due to reduced ApoB-100 availability, it has been suggested that fat accumulation in the liver might be more likely. Additionally, there might be an association between PTEN and APOB levels. The lipid phosphatase PTEN is primarily known as tumor suppressor mutated in various cancer entities, however, it plays an apparent pivotal role in liver metabolism too [171]. The investigation of hepatic *Pten* deficiency in mice demonstrated an increased fatty acid synthesis and hepatic steatosis [173]. It was supposed that hepatic *Pten* deficiency results in a constitutive insulin signaling. Another study showed that PTEN activity possibly regulates the availability of APOB in the liver [172]. Hepatic *Pten* deficiency in mice indicated a reduced lipid transport in

and from the cell and probably result in steatosis due to diminished APOB availability. Thus, all of this points to an increased probability for lipid accumulation in the liver due to underexpressed genes related to the lipid metabolism.

4.2.3 Altered amino acid metabolism upon psychotropic drug treatment

The impairment of adequate energy supply in cells of the liver in patients with bipolar disorder and psychotropic drug treatment was further emphasized by the reduced and enriched pathway of amino acid metabolism. Apart from glucose and lipids, amino acids can also serve as substrate for the citric acid cycle and further for energy generation. Every gene of this enriched pathway was underexpressed which implies an impaired amino acid metabolism. Further analyses revealed that several proteins of module 3 were overlapping with the enriched pathway. All of these were annotated as subunits of the proteolytic 26S proteasome complex or rather to the 19S and 20S proteasome. A gene expression study of brain tissue of patients with bipolar disorder showed decreased levels of genes related to protein degradation [174]. The GO results included processes associated to protein degradation including the 26S and 20S proteasome. Further analysis revealed that most genes of the proteasome were underexpressed in brain tissue of patients with bipolar disorder. In addition, gene expression related to the proteasome was also decreased in hippocampal tissue of patients with schizophrenia [175] and in blood samples of patients with psychosis [176], whereby both studies included patients under psychotropic drug treatment. These studies support the findings in the herein examined bipolar disorder group and indicated that an adequate protein degradation might be hampered by the underexpression of proteasomal subunits. Detrimental effects of an impaired protein degradation on hepatic cells have been observed in *in vitro* and *in vivo* studies [177–179]. Studies of hepatic cell lines showed that cytoplasmic inclusions were present upon proteasome inhibition [177,178]. One study showed that those cytoplasmatic inclusion consisted of keratin 8 and 18, ubiquitin, heat-shock protein 70 and p62, which are typically found in Mallory-Denk bodies [178]. Similar results have been observed in an animal study investigating Mallory-Denk body formation in mice overexpressing keratin 8 upon proteasome inhibition [179]. It has been supposed that cytoplasmatic inclusions have a higher occurrence in patients with NAFLD and obese individuals. Consequently, an increased susceptibility to develop Mallory-Denk bodies would exist for patients with psychotropic drug treatment. However, for none of the herein investigated individuals, Mallory-Denk bodies were observed. This does not exclude a possible detrimental effect of psychotropic drug treatment in bipolar disorder on proteasomal function.

The implication of accumulating ubiquitinated proteins in liver cells by proteasomal impairment in bipolar disorder remains to be elucidated.

4.2.4 Reduced biotransformation upon psychotropic drug treatment

The biotransformation of xenobiotics, such as drugs, and endogenous compounds was found to be disturbed in bipolar disorder. The pathway of biological oxidations was enriched based on the queried DEGs. This pathway includes the functionalization and conjugation of compounds, the so called phase I and phase II of biotransformation, respectively. The top downregulated gene *FMO3* and other enzymes of the phase I reaction were allocated to this pathway, such as enzymes belonging to the CYP450 family, such as cytochrome P450 family 3 subfamily A member 5 (CYP3A5) belonging to the subfamily of CYP3A. The subfamily CYP3A was determined to metabolize a high number of clinical drugs including psychotropic drugs [59]. The expression of *CYP3A5* seems to be largely dependent on genetic polymorphism. A study investigating hepatic CYP3A5 protein levels based on the three known *CYP3A5* genotypes revealed that CYP3A5 protein levels could represent up to 50% of total CYP3A protein levels [180]. With regard to psychotropic drugs, genetic polymorphism in *CYP3A5* were also shown to influence the clearance of olanzapine [181]. A higher olanzapine clearance was suggested for individuals carrying at least one of the *CYP3A5*1* allele. Further, a study revealed a possible relationship between homozygous genotypes of *CYP3A5*3* and another CYP450 gene, namely *CYP2D6*10*, resulting in obviously high exposure and active moiety of risperidone [182]. It was supposed that the combined homozygous genotypes could be more prone to potential detrimental effects of psychotropic drug treatment. Unfortunately, genotype data was not available for the herein investigated samples. However, the genotype studies suggest that lower CYP3A5 levels probably lead to higher drug exposure due to an impaired first-pass metabolism. Furthermore, an increased exposure might also result in enhanced toxic effects on the liver in those individuals.

Beside enzymes of the phase I reaction, genes of phase II conjugation enzymes were also allocated to the biological oxidations pathway in bipolar disorder including transferases for glucuronidation and sulfonation, such as the UDP glucuronosyltransferase family 2 member B15 (*UGT2B15*) and *SULT1E1*, respectively. The conjugation of glucuronide is a major metabolizing pathway of psychotropic drugs, such as lamotrigine, olanzapine and others [183]. A study investigating inhibitory effects on uridine diphosphate (UDP)-glucuronosyltransferases

(UGT) by valproic acid treatment revealed impeded UGT2B15 activity in human liver microsomes and in a cell culture model [184]. The mode of inhibition could not be clarified, but an inhibition by valproic acid was supposed to be due to competitive inhibition. With regard to sulfate conjugation by sulfotransferases in liver disease, it has been shown that sulfotransferase activity decreased with increased liver disease severity [185]. Gene expression levels of *SULT1E1* were reduced in human diabetic liver cirrhosis tissue. A diminished phase II enzyme capacity could result in a reduced psychotropic drug metabolization, and, hence, a decreased clearing followed by a potential increase in their toxicity. Thus, impaired biotransformation of therapeutic drugs might induce detrimental effects on the liver and affect physiological liver function.

4.2.5 Altered neutrophil degranulation upon psychotropic drug treatment

The detected overexpressed S100 genes, *S100A8*, *S100A9* and *S100A12*, already indicated an involvement of the immune system in hepatic tissue of patients with bipolar disorder and psychotropic drug treatment. The pathway analysis revealed an enrichment of genes assigned to neutrophil degranulation, which is considered as response mechanism of the innate immune system. All genes in this pathway were underexpressed with the exception of the aforementioned overexpressed S100 genes. The S100A8 and S100A9 were determined to be involved in neutrophil chemotaxis [186]. This would lead to the suggestion that an accumulation of neutrophils, though with low degranulation potential, was supposed to be present in the hepatic tissue of patients with bipolar disorder and drug treatment. Indeed, patients with bipolar disorder revealed higher grades of portal and lobular granulocytes indicating an increased number of granulocytes. However, a differentiation in granulocytic subtypes was absent. Recent studies revealed an increased neutrophil to lymphocytes ratio in peripheral blood samples of patients with bipolar disorder [187] and in a meta-analysis of patients with non-affective psychosis [188]. The latter study considered that drug treatment could possibly influence the increased neutrophil amount, although not statistically significant. With regard to hepatic neutrophil presence upon psychotropic drug treatment, a study reported that atypical antipsychotic treatment caused hepatic injury defined by steatosis, fibrosis and features of inflammation [164]. Clozapine-treated animals showed mainly infiltrates of neutrophils and lymphocytes at sites of lobular inflammatory. This was also observed in the

herein studied bipolar disorder group. Patients with bipolar disorder revealed a higher percentage of portal and lobular granulocyte compared to the controls. But still, whether and how psychotropic drug treatment affects the neutrophil degranulation despite increased neutrophil presence, remains unclear. Early studies proposed that treatment with phenothiazines, which are used as antipsychotics, inhibit neutrophil degranulation [189,190]. Phenothiazine was supposed to prevent neutrophil degranulation by binding to calmodulin and, hence, altering the essential receptor binding property to fulfill degranulation [190]. It seems that psychotropic drug treatment probably result in an involvement of various molecular subclusters with regard to neutrophil degranulation. A large number of hub proteins overlapped with genes queried and allocated to this pathway, such as *CAT*, *MAPK1*, *C3* and *VAMP8*. Whereas the latter two were also determined as seeds in module 1 and module 4. Predominantly, proteins of module 4 and module 6 overlapped with this pathway. The gene encoding for the antioxidant enzyme *CAT* was revealed as one of the most underexpressed genes in the bipolar disorder group. With regard to its activity in inflammatory cells, it has been shown that CAT revealed high activity in neutrophils [191]. In neutrophils, CAT has been suggested to be responsible for the oxidant resistance upon the respiratory burst and its resulting oxidative stress due to the cell's activation. The underexpression of *CAT* in bipolar disorder with psychotropic drug treatment implies that neutrophils seem to be more vulnerable for oxidative stress and that the present liver injury in bipolar disorder may partly be based on the drug-treatment.

For the hub protein MAPK1, the highest betweenness score was revealed in the bipolar disorder group. As member of the MAPK family, it belongs to the subfamily of extracellular signal-regulated kinases (ERKs) and is also known as ERK2 [192]. The ERK signaling has been determined as important response mechanism to extracellular signals. It has been shown that neutrophil activation was influenced by MAPK signaling in an *in vitro* study of isolated human neutrophils [193]. Inhibition of MAPK1/MAPK3 signaling resulted in reduced respiratory burst of the neutrophils upon activation reflected by diminished generation of reactive oxygen species. Similar to the detected probable pivotal role in the bipolar disorder group with psychotropic drug treatment, MAPK1 was supposed to have a central role in the molecular response of psychotropic drug treatment. In a study investigating biological interaction networks, MAPK1 was reported to act as one of the key regulators of the cellular response upon lithium and valproate treatment [194]. In addition, altered ERK signaling was shown in several psychiatric disorders. In *post mortem* brain tissue of suicide subjects with major depression,

decreased *ERK1* and *ERK2* levels on gene and protein level have been shown [195]. Another study revealed altered levels of proteins involved in the ERK pathway in psychiatric disorders [196]. Reduced levels for the MAPK1-upstream signal RAP1, which is a member of the Ras family, were observed in major depression and schizophrenia. In the herein studied bipolar disorder group, the underexpressed gene *RAP1A*, encoding for an isoform of RAP1, was allocated to the neutrophil degranulation pathway and was determined as hub protein in the bipolar disorder group with psychotropic drug treatment. All of this indicates a reduced MAPK signaling in neutrophils and, thus, a diminished neutrophil activation rate in bipolar disorder with psychotropic drug treatment.

The determined hub protein and seed of module 1, C3, was underexpressed in the bipolar disorder group. The C3 protein was found to be the most abundant complement protein [197]. The cleavage of C3 was shown to be involved in inflammatory response, phagocytosis and pathogen lysis. In an early study, C3 plasma levels were reported to be different in medicated patients with psychiatric disorders [198]. The combined analysis of patients with schizophrenia, mania or depression revealed decreased levels upon psychotropic drug treatment compared to the non-medicated group of patients. It was proposed that psychotropic drug treatment might suppresses the active phase response of the immune system. In contrast, the cleaved C3 component C3a and other complement components were defined to be increased in a sample of patients with bipolar disorder [199]. However, at the time of investigation all patients were in the euthymic state. A study of patients with bipolar disorder and drug treatment in the acute and chronic phase presented decreased serum levels of complement components [200]. Therefore, a possible effect of psychotropic drugs on complement activation and a potential dependency on the mood state cannot be excluded. With regard to liver injury, an animal study has reported the involvement of C3 in liver regeneration and that xenobiotic-induced liver injury led to the cleavage of C3 and further to the activation of the complement cascade [201]. C3-deficient mice revealed impaired liver regeneration upon toxic injury. This leads to the suggestion that complement activation or rather C3 cleavage might be impaired in bipolar disorder with psychotropic drug treatment and, so, liver regeneration after hepatic injury might be diminished.

Another possibly central gene allocated to the neutrophil degranulation pathway was *VAMP8*. It was identified as hub protein and seed of module 6 and was underexpressed in the bipolar disorder group. The membrane fusion catalyzing protein VAMP8 located on granules or vesicles was proposed to be involved in exocytosis of neutrophil-derived mediators [202]. For

VAMP8, it has been shown that an interaction with synaptosome associated protein 23 (SNAP23) exist during exocytosis. Apart from the underexpression of *VAMP8*, a decreased mRNA expression was observed in the bipolar disorder group for *SNAP23*. Unfortunately, VAMP8 and SNAP23 were less investigated in context of psychiatric disorders, psychotropic drug treatment and liver injury, therefore, their role in developing potential detrimental effects remains inconclusive.

4.3 Associations between genes expression and features of liver injury

Most of the histopathological features assigned to the six categories characterizing liver injury, revealed comparable frequency distributions between patients with bipolar disorder and controls. Based on these findings, a similar liver histopathology was assumed in the studied groups. However, the detected altered gene expression between the studied groups and the assignment to various overrepresented biological pathways indicated separate underlying mechanism initiating or triggering hepatic injury. Therefore, a drug-induced etiology could exist. Further, a more intense effect on gene expression might be observable when comparing liver tissue of patients with bipolar disorder and liver tissue of healthy individuals. The association studies between gene expression and histopathological features of the liver in patients with bipolar disorder revealed a potential contribution of all enriched pathways to degenerative changes. All other histopathological feature groups and enriched pathways revealed weak overall association clustering with the exception of the RETC and hepatic activity, inflammation and endogenous reaction.

In context of degenerative changes, particularly, the histopathological features of glycogenated nuclei were found to be positively associated with nearly all genes of each pathway. An abundant presence of glycogenated nuclei is usually found in NAFL and NASH, but is typically absent in alcoholic steatohepatitis [84,86,203]. However, this histopathological feature is thought to be irrelevant for the diagnosis of these diseases. Until now, the pathophysiology of glycogenated nuclei is unknown. Though, a recent study revealed a possible association between the presence of glycogenated nuclei and cellular senescence [204]. This was suggested by the observation of absent cytoplasmatic apoptosis marker and present DNA damage marker in hepatocytes with glycogenated nuclei. Another study observed an impaired lipid metabolism

in senescent hepatocytes [205]. An involvement of mitochondrial dysfunction and a resulting decreased lipid metabolism was supposed to be related to the development of the senescent phenotype. This leads to the suggestion that glycogenated nuclei might represent a possible liver-specific senescence marker. Further, senescent cells could be associated with a decreased ability of lipid metabolism which possibly result in a diminished cellular energy supply accompanied by increased reactive oxygen species production. This is in line with observed enriched pathways of the herein studied bipolar disorder group, such as lipid metabolism and respiratory electron transport chain, and indicates a possible involvement of psychotropic drug treatment in the development of senescence in hepatocytes. Up to now, specific studies determining the impact of psychotropic drug treatment on senescence in hepatocytes are absent. Since both, the bipolar disorder group and the controls, revealed no difference between their frequency distribution of the presence of glycogenated nuclei in the examined liver sections, an obvious effect of psychotropic drugs influencing the development of glycogen inclusions could not be verified. A transition to a senescent phenotype could also originate from injured liver tissue in general leading to a decreased regeneration capability. This has already been observed during progression of fibrosis during cirrhosis in hepatocytes, suggesting a persistent liver damage with lowered regeneration rate [206]. Hepatic stellate cells, triggering hepatic fibrosis when activated following parenchymal damage, affect the fibrogenic response upon cell-cycle arrest [207]. A limiting effect has been proposed for senescent activated hepatic stellate cells where a restrained secretion of extracellular matrix proteins could probably regulate liver fibrosis. Hence, senescence of hepatic cells could have beneficial or detrimental effects during liver injury. Whether and how psychotropic drugs influence senescence in hepatic cells has to be evaluated in future.

A decreased function of the mitochondrial respiration has been observed to influence various features of liver injury. In NAFLD, mitochondrial dysfunction has been raised to a central pathogenic event [208–210]. The mitochondrial respiratory chain has already been shown to be involved in NASH [211]. Its dysfunction, has been shown to trigger extensive reactive oxygen species production, whereas the presence of increased reactive oxygen species can lead to the occurrence of cell death, inflammation and fibrosis [209,212]. In addition, mitochondrial dysfunction in brain tissue has been linked to bipolar disorder [174]. Moreover, inhibiting effects on mitochondrial respiration induced by various psychotropic drugs used in the treatment of mood disorders and depression have been observed in an animal study [113].

Therefore, patients with bipolar disorder might innately have a mitochondrial dysfunction, which probably exists also in other tissue than the brain. Furthermore, the treatment with psychotropic drugs induce additional detrimental effects on mitochondria and, hence, the energy supply of cells. In conclusion, the reduced RETC function might have a devastating impact on the pathogenesis of liver injury in bipolar disorder. All of this highlights the crucial aspect of mitochondrial function, where a diminished energy supply and increased oxidative stress are the suspected main drivers of hepatic injury upon psychotropic drug treatment.

4.4 Approaches and limitations of the study

The usage of global gene expression data implied intense bioinformatical processing of the data. To ensure proper and valuable data, an adequate pre-processing preceded the post-analyses. Despite the extensive application of gene expression microarrays, a strict guideline on pre-processing is unavailable and is rather based on recommendations [213]. Human *post mortem* tissue serves as fundamental resource for biological investigations, though effects on RNA integrity have to be considered in subsequent experiments. In *post mortem* tissue, increased PMI typically effects tissue autolysis and is associated with lower RNA quality values [214]. Low RIN values of the herein studied samples were present. However, the low RIN values were comparable with other studies investigating *post mortem* tissue of the liver [214,215]. The pre-processing revealed that despite a difference in PMI comparable quality metrics were present in the investigated groups. In addition, RMA normalization resulted in a between array noise reduction resting on non-biological differences. This lead to the suggestion that the pre-processing and normalization of the raw gene expression data was successful and further analyses were feasible. However, to overcome adverse effects of prolonged PMI, it was included in the linear model for the analysis of DEGs.

Already the substructure analysis discovered differences in the groups based on pre-processed and normalized gene expression data excluding a pure clustering due to confounding effects. Especially, principal component 1 and 2 were enabling a distinction between bipolar disorder and control samples. The exposed group clustering strengthened the assumption that differential gene expression was present in bipolar disorder with psychotropic drug treatment compared to the controls. The subsequent differential expression analysis confirmed the presence of

differences in gene expression and was successfully validated by examining a subset of genes by quantitative real-time PCR. All of the determined pre-processing and normalization metrics, as well as the validation of the detected DEGs, emphasized further structured *in silico* analyses covering the evaluation of subclusters, as well as the functional analyses of the corresponding proteins influenced by psychotropic drug treatment in bipolar disorders.

In addition, it has to be considered that human tissue has a high degree of cellular heterogeneity. So, the herein examined transcriptomes were based on tissue containing an assembly of different liver cells and not on hepatocytes solely. This study, like other gene expression studies, was limited by providing key insights into gene expression, but not at the level of post-transcriptional regulation or translation *in vivo*. Unfortunately, the sample size and the present mixed medication history of the included patients with bipolar disorder limited explicit statements of the effect on hepatic gene expression by individual psychotropic drugs. To clarify the effects of single psychotropic drugs on liver tissue in psychiatric disorders, cell culture and animal studies besides human studies are inevitable. Residual biological and non-biological factors, such as genetic predispositions and non-registered clinical characteristics, influencing an individual's gene expression may not be negligible. In particular, genetic predispositions were shown to influence drug metabolism and response with a high degree of heterogeneity [18,216]. Therefore, a potential influence of pharmacogenomics on adverse effects of psychotropic drugs can be assumed and might be included in future studies.

4.5 Conclusion

In summary, the findings of this study revealed altered gene expression upon psychotropic drug treatment in liver tissue of patients with bipolar disorder. Different biological pathways were found to be enriched, whereas predominantly an effect was observed for the cellular energy supply. It might be that the observed downregulation of RETC-related genes could result in cellular senescence, while senescence possibly could be detected in hepatic histopathology. Further affected biological pathways included the metabolism of lipids, amino acids and xenobiotics. All of this probably lead to increased oxidative stress in the cells entailing serious cell damage. In addition, the innate immune system response was found to be enriched. On the one hand, the accumulation of neutrophils was supposed to exist, but on the other hand, a

reduced neutrophil activation was assumed. To which extent a reduced neutrophil degranulation contributes to liver injury in bipolar disorder remains unclear.

Further investigations are necessary to clarify possible detrimental effects of psychotropic drugs on hepatic function in patients with bipolar disorder, whereas the inclusion of genetic factors should be considered in particular, as well as the impact of Western diet. An additional dietary intervention focusing on lipid, glucose and antioxidants intake might contribute to mitigate side effects of psychotropic drug treatment. In order to reveal the fundamental physiology behind complex biological function and dysfunction, the application of bioinformatical analyses of transcriptomics and other '-omics' technologies in combination with wet lab experiments is crucial. Advanced computational analyses are necessary to extract and integrate essential information from the vast amount of such data. All of which could improve the understanding of hepatic function and dysfunction upon psychotropic drug treatment and promote the development of clinically innovative psychotropic drugs with enhanced safety for their therapeutic usage in psychiatric disorders.

5 Bibliography

[1] McKee J, Brahm N. Medical mimics: Differential diagnostic considerations for psychiatric symptoms. Ment Heal Clin 2016;6:289–96. doi:10.9740/mhc.2016.11.289.

[2] Alonso J, Petukhova M, Vilagut G, Chatterji S, Heeringa S, Üstün TB, et al. Days out of role due to common physical and mental conditions: results from the WHO World Mental Health surveys. Mol Psychiatry 2011;16:1234–46. doi:10.1038/mp.2010.101.

[3] Alonso J, Angermeyer MC, Bernert S, Bruffaerts R, Brugha TS, Bryson H, et al. Prevalence of mental disorders in Europe: results from the European Study of the Epidemiology of Mental Disorders (ESEMeD) project. Acta Psychiatr Scand 2004;109:21–7. doi:10.1111/j.1600-0047.2004.00327.x.

[4] Chang C-K, Hayes RD, Perera G, Broadbent MTM, Fernandes AC, Lee WE, et al. Life expectancy at birth for people with serious mental illness and other major disorders from a secondary mental health care case register in London. PLoS One 2011;6:e19590. doi:10.1371/journal.pone.0019590.

[5] Nordentoft M, Wahlbeck K, Hällgren J, Westman J, Osby U, Alinaghizadeh H, et al. Excess mortality, causes of death and life expectancy in 270,770 patients with recent onset of mental disorders in Denmark, Finland and Sweden. PLoS One 2013;8:e55176. doi:10.1371/journal.pone.0055176.

[6] Laursen TM, Musliner KL, Benros ME, Vestergaard M, Munk-Olsen T. Mortality and life expectancy in persons with severe unipolar depression. J Affect Disord 2016;193:203–7. doi:10.1016/j.jad.2015.12.067.

[7] Kessing LV, Vradi E, McIntyre RS, Andersen PK. Causes of decreased life expectancy over the life span in bipolar disorder. J Affect Disord 2015;180:142–7. doi:10.1016/j.jad.2015.03.027.

[8] Stevens AJ, Rucklidge JJ, Kennedy MA. Epigenetics, nutrition and mental health. Is there a relationship? Nutr Neurosci 2018;21:602–13. doi:10.1080/1028415X.2017.1331524.

[9] Sullivan PF, Kendler KS, Neale MC. Schizophrenia as a Complex Trait: Evidence from a Meta-analysis of Twin Studies. Arch Gen Psychiatry 2003;60:1187–92. doi:10.1001/archpsyc.60.12.1187.

[10] McGuffin P, Rijsdijk F, Andrew M, Sham P, Katz R, Cardno A. The heritability of bipolar affective disorder and the genetic relationship to unipolar depression. Arch Gen Psychiatry 2003;60:497–502. doi:10.1001/archpsyc.60.5.497.

[11] Anderson IM, Haddad PM, Scott J. Bipolar disorder. BMJ 2012;345:e8508. doi:10.1136/bmj.e8508.

[12] Sullivan PF, Daly MJ, O'Donovan M. Genetic architectures of psychiatric disorders: The emerging picture and its implications. Nat Rev Genet 2012;13:537–51. doi:10.1038/nrg3240.

[13] Ripke S, O'Dushlaine C, Chambert K, Moran JL, Kähler AK, Akterin S, et al. Genome-

wide association analysis identifies 13 new risk loci for schizophrenia. Nat Genet 2013;45:1150–9. doi:10.1038/ng.2742.

[14] Stahl EA, Breen G, Forstner AJ, McQuillin A, Ripke S, Trubetskoy V, et al. Genome-wide association study identifies 30 loci associated with bipolar disorder. Nat Genet 2019;51:793–803. doi:10.1038/s41588-019-0397-8.

[15] Wray NR, Ripke S, Mattheisen M, Trzaskowski M, Byrne EM, Abdellaoui A, et al. Genome-wide association analyses identify 44 risk variants and refine the genetic architecture of major depression. Nat Genet 2018;50:668–81. doi:10.1038/s41588-018-0090-3.

[16] Lee SH, Ripke S, Neale BM, Faraone S V., Purcell SM, Perlis RH, et al. Genetic relationship between five psychiatric disorders estimated from genome-wide SNPs. Nat Genet 2013;45:984–94. doi:10.1038/ng.2711.

[17] Coleman JRI, Gaspar HA, Bryois J, Bipolar Disorder Working Group of the Psychiatric Genomics Consortium, Major Depressive Disorder Working Group of the Psychiatric Genomics Consortium, Breen G. The Genetics of the nood disorder spectrum: Genome-wide association analyses of more than 185,000 cases and 439,000 controls. Biol Psychiatry 2020;88:169–84. doi:10.1016/j.biopsych.2019.10.015.

[18] Bousman C, Maruf A Al, Müller DJ. Towards the integration of pharmacogenetics in psychiatry. Curr Opin Psychiatry 2018;32:1. doi:10.1097/YCO.0000000000000465.

[19] Grande I, Berk M, Birmaher B, Vieta E. Bipolar disorder. Lancet 2016;387:1561–72. doi:10.1016/S0140-6736(15)00241-X.

[20] Global Burden of Disease Collaborative Network. Global Burden of Disease Study 2017 (GBD 2017) Incidence, Prevalence, and Years Lived with Disability 1990-2017 2018.

[21] American Psychiatric Association. Diagnostic and statistical manual of mental disorders. Fifth edit. Washington, DC: American Psychiatric Ass.; 2013.

[22] Vieta E, Berk M, Schulze TG, Carvalho AF, Suppes T, Calabrese JR, et al. Bipolar disorders. Nat Rev Dis Prim 2018;4:18008. doi:10.1038/nrdp.2018.8.

[23] Tondo L, Vazquez G, Baldessarini R. Depression and mania in bipolar disorder. Curr Neuropharmacol 2016;15:353–8. doi:10.2174/1570159x14666160606210811.

[24] Angst J, Sellaro R. Historical perspectives and natural history of bipolar disorder. Biol Psychiatry 2000;48:445–57. doi:10.1016/S0006-3223(00)00909-4.

[25] Coryell W, Endicott J, Maser JD, Mueller T, Lavori P, Keller M. The likelihood of recurrence in bipolar affective disorder: the importance of episode recency. J Affect Disord 1995;33:201–6. doi:10.1016/0165-0327(94)00091-M.

[26] Gitlin MJ, Swendsen J, Heller TL, Hammen C. Relapse and impairment in bipolar disorder. Am J Psychiatry 1995;152:1635–40. doi:10.1176/ajp.152.11.1635.

[27] Geddes JR, Miklowitz DJ. Treatment of bipolar disorder. Lancet 2013;381:1672–82. doi:10.1016/S0140-6736(13)60857-0.

[28] McCormick U, Murray B, McNew B. Diagnosis and treatment of patients with bipolar

disorder: A review for advanced practice nurses. J Am Assoc Nurse Pract 2015;27:530–42. doi:10.1002/2327-6924.12275.

[29] Yatham LN, Kennedy SH, Parikh S V., Schaffer A, Beaulieu S, Alda M, et al. Canadian Network for Mood and Anxiety Treatments (CANMAT) and International Society for Bipolar Disorders (ISBD) collaborative update of CANMAT guidelines for the management of patients with bipolar disorder: Update 2013. Bipolar Disord 2013;15:1–44. doi:10.1111/bdi.12025.

[30] Virupaksha HS, Shashidhara B, Thirthalli J, Kumar CN, Gangadhar BN. Comparison of electroconvulsive therapy (ECT) with or without anti-epileptic drugs in bipolar disorder. J Affect Disord 2010;127:66–70. doi:10.1016/j.jad.2010.05.008.

[31] Bailine S, Fink M, Knapp R, Petrides G, Husain MM, Rasmussen K, et al. Electroconvulsive therapy is equally effective in unipolar and bipolar depression. Acta Psychiatr Scand 2009;121:431–6. doi:10.1111/j.1600-0447.2009.01493.x.

[32] Grande I, Vieta E. Pharmacotherapy of acute mania: Monotherapy or combination therapy with mood stabilizers and antipsychotics? CNS Drugs 2015;29:221–7. doi:10.1007/s40263-015-0235-1.

[33] Baldessarini RJ, Tondo L, Vázquez GH. Pharmacological treatment of adult bipolar disorder. Mol Psychiatry 2019;24:198–217. doi:10.1038/s41380-018-0044-2.

[34] Zohar J, Stahl S, Moller HJ, Blier P, Kupfer D, Yamawaki S, et al. A review of the current nomenclature for psychotropic agents and an introduction to the Neuroscience-based Nomenclature. Eur Neuropsychopharmacol 2015;25:2318–25. doi:10.1016/j.euroneuro.2015.08.019.

[35] Keck PE, McElroy SL, Richtand N, Tohen M. What makes a drug a primary mood stabilizer? Mol Psychiatry 2002;7:S8–14. doi:10.1038/sj.mp.4001013.

[36] Søndergård L, Lopez AG, Andersen PK, Kessing LV. Mood-stabilizing pharmacological treatment in bipolar disorders and risk of suicide. Bipolar Disord 2008;10:87–94. doi:10.1111/j.1399-5618.2008.00464.x.

[37] Gould TD, Chen G, Manji HK. Mood stabilizer psychopharmacology. Clin Neurosci Res 2002;2:193–212. doi:10.1016/S1566-2772(02)00044-0.

[38] Schloesser RJ, Martinowich K, Manji HK. Mood-stabilizing drugs: mechanisms of action. Trends Neurosci 2012;35:36–46. doi:10.1016/j.tins.2011.11.009.

[39] Pisanu C, Papadima EM, Del Zompo M, Squassina A. Understanding the molecular mechanisms underlying mood stabilizer treatments in bipolar disorder: Potential involvement of epigenetics. Neurosci Lett 2018;669:24–31. doi:10.1016/j.neulet.2016.06.045.

[40] Jauhar S, Young AH. Controversies in bipolar disorder; role of second-generation antipsychotic for maintenance therapy. Int J Bipolar Disord 2019;7:10. doi:10.1186/s40345-019-0145-0.

[41] Scherk H, Pajonk FG, Leucht S. Second-generation antipsychotic agents in the treatment of acute mania. Arch Gen Psychiatry 2007;64:442. doi:10.1001/archpsyc.64.4.442.

[42] Tohen M, Vieta E, Calabrese J, Ketter TA, Sachs G, Bowden C, et al. Efficacy of olanzapine and olanzapine-fluoxetine combination in the treatment of bipolar I depression. Arch Gen Psychiatry 2003;60:1079. doi:10.1001/archpsyc.60.11.1079.

[43] Calabrese JR, Keck PE, Macfadden W, Minkwitz M, Ketter TA, Weisler RH, et al. A randomized, double-blind, placebo-controlled trial of quetiapine in the treatment of bipolar I or II depression. Am J Psychiatry 2005;162:1351–60. doi:10.1176/appi.ajp.162.7.1351.

[44] Yatham LN, Goldstein JM, Vieta E, Bowden CL, Grunze H, Post RM, et al. Atypical antipsychotics in bipolar depression: potential mechanisms of action. J Clin Psychiatry 2005;66 Suppl 5:40–8.

[45] Baldessarini RJ, Vázquez GH, Tondo L. Bipolar depression: a major unsolved challenge. Int J Bipolar Disord 2020;8. doi:10.1186/s40345-019-0160-1.

[46] Viktorin A, Lichtenstein P, Thase ME, Larsson H, Lundholm C, Magnusson PKE, et al. The risk of switch to mania in patients with bipolar disorder during treatment with an antidepressant alone and in combination with a mood stabilizer. Am J Psychiatry 2014;171:1067–73. doi:10.1176/appi.ajp.2014.13111501.

[47] Grunze H, Vieta E, Goodwin GM, Bowden C, Licht RW, Azorin J-M, et al. The World Federation of Societies of Biological Psychiatry (WFSBP) Guidelines for the Biological Treatment of Bipolar Disorders: Acute and long-term treatment of mixed states in bipolar disorder. World J Biol Psychiatry 2018;19:2–58. doi:10.1080/15622975.2017.1384850.

[48] Goodwin G, Haddad P, Ferrier I, Aronson J, Barnes T, Cipriani A, et al. Evidence-based guidelines for treating bipolar disorder: Revised third edition recommendations from the British Association for Psychopharmacology. J Psychopharmacol 2016;30:495–553. doi:10.1177/0269881116636545.

[49] Saddichha S, Chaturvedi SK. Clinical practice guidelines in psychiatry: more confusion than clarity? A critical review and recommendation of a unified guideline. ISRN Psychiatry 2014;2014:828917. doi:10.1155/2014/828917.

[50] Ghaemi SN, Wingo AP, Filkowski MA, Baldessarini RJ. Long-term antidepressant treatment in bipolar disorder: meta-analyses of benefits and risks. Acta Psychiatr Scand 2008;118:347–56. doi:10.1111/j.1600-0447.2008.01257.x.

[51] Moretti A, Gorini A, Villa RF. Affective disorders, antidepressant drugs and brain metabolism. Mol Psychiatry 2003;8:773–85. doi:10.1038/sj.mp.4001353.

[52] D'Sa C, Duman RS. Antidepressants and neuroplasticity. Bipolar Disord 2002;4:183–94. doi:10.1034/j.1399-5618.2002.01203.x.

[53] Neuroscience based Nomenclature Second Edition Revised (NbN2R) n.d. https://nbn2r.com/

[54] Shiloh R, Stryjer R, Weizman A, Nutt DJ. Atlas of Psychiatric Pharmacotherapy. 2nd ed. Milton, Abingdon, UK: Taylor & Francis; 2006. doi:10.1201/b14436.

[55] Telles-Correia D, Barbosa A, Cortez-Pinto H, Campos C, Rocha NBF, Machado S. Psychotropic drugs and liver disease: A critical review of pharmacokinetics and liver toxicity. World J Gastrointest Pharmacol Ther 2017;8:26–38.

doi:10.4292/wjgpt.v8.i1.26.

[56] Shen WW. The metabolism of psychoactive drugs: A review of enzymatic biotransformation and inhibition. Biol Psychiatry 1997;41:814–26. doi:10.1016/S0006-3223(96)00180-1.

[57] Wong YC, Qian S, Zuo Z. Regioselective biotransformation of CNS drugs and its clinical impact on adverse drug reactions. Expert Opin Drug Metab Toxicol 2012;8:833–54. doi:10.1517/17425255.2012.688027.

[58] Musenga A, Saracino M, Sani G, Raggi M. Antipsychotic and Antiepileptic Drugs in Bipolar Disorder: The Importance of Therapeutic Drug Monitoring. Curr Med Chem 2009;16:1463–81. doi:10.2174/092986709787909604.

[59] Zanger UM, Schwab M. Cytochrome P450 enzymes in drug metabolism: Regulation of gene expression, enzyme activities, and impact of genetic variation. Pharmacol Ther 2013;138:103–41. doi:10.1016/j.pharmthera.2012.12.007.

[60] Stingl J, Oesterheld J, Turpeinen M. Metabolism of psychotropic drugs. Encycl. Drug Metab. Interact., Hoboken, NJ, USA: John Wiley & Sons, Inc.; 2012, p. 1–16. doi:10.1002/9780470921920.edm130.

[61] Jancova P, Anzenbacher P, Anzenbacherova E. Phase II drug metabolizing enzymes. Biomed Pap 2010;154:103–16. doi:10.5507/bp.2010.017.

[62] Esteki M, Khayamian T. Mechanistic-Based Descriptors for QSAR Study of Psychotropic Drug Toxicity. Chem Biol Drug Des 2008;72:409–35. doi:10.1111/j.1747-0285.2008.00718.x.

[63] Young SL, Taylor M, Lawrie SM. "First do no harm." A systematic review of the prevalence and management of antipsychotic adverse effects. J Psychopharmacol 2015;29:353–62. doi:10.1177/0269881114562090.

[64] Murru A, Popovic D, Pacchiarotti I, Hidalgo D, León-Caballero J, Vieta E. Management of adverse effects of mood stabilizers. Curr Psychiatry Rep 2015;17:66. doi:10.1007/s11920-015-0603-z.

[65] Hayes JF, Marston L, Walters K, Geddes JR, King M, Osborn DPJ. Adverse renal, endocrine, hepatic, and metabolic events during maintenance mood stabilizer treatment for bipolar disorder: A population-based cohort study. PLOS Med 2016;13:e1002058. doi:10.1371/journal.pmed.1002058.

[66] Bak M, Fransen A, Janssen J, van Os J, Drukker M. Almost all antipsychotics result in weight gain: A meta-Analysis. PLoS One 2014;9:e94112. doi:10.1371/journal.pone.0094112.

[67] Sedky K, Nazir R, Joshi A, Kaur G, Lippmann S. Which psychotropic medications induce hepatotoxicity? Gen Hosp Psychiatry 2012;34:53–61. doi:10.1016/j.genhosppsych.2011.10.007.

[68] Selim K, Kaplowitz N. Hepatotoxicity of psychotropic drugs. Hepatology 1999;29:1347–51. doi:10.1002/hep.510290535.

[69] Jones JG. Hepatic glucose and lipid metabolism. Diabetologia 2016;59:1098–103.

doi:10.1007/s00125-016-3940-5.

[70] Carrier P, Debette-Gratien M, Girard M, Jacques J, Nubukpo P, Loustaud-Ratti V. Liver illness and psychiatric patients. Hepat Mon 2016;16:e41564. doi:10.5812/hepatmon.41564.

[71] Younossi ZM, Koenig AB, Abdelatif D, Fazel Y, Henry L, Wymer M. Global epidemiology of nonalcoholic fatty liver disease—Meta-analytic assessment of prevalence, incidence, and outcomes. Hepatology 2016;64:73–84. doi:10.1002/hep.28431.

[72] Younossi Z, Anstee QM, Marietti M, Hardy T, Henry L, Eslam M, et al. Global burden of NAFLD and NASH: trends, predictions, risk factors and prevention. Nat Rev Gastroenterol Hepatol 2018;15:11–20. doi:10.1038/nrgastro.2017.109.

[73] Kilbourne AM, Cornelius JR, Han X, Pincus HA, Shad M, Salloum I, et al. Burden of general medical conditions among individuals with bipolar disorder. Bipolar Disord 2004;6:368–73. doi:10.1111/j.1399-5618.2004.00138.x.

[74] Sicras A, Rejas J, Navarro R, Serrat J, Blanca M. Metabolic syndrome in bipolar disorder: a cross-sectional assessment of a Health Management Organization database. Bipolar Disord 2008;10:607–16. doi:10.1111/j.1399-5618.2008.00599.x.

[75] Ekstedt M, Hagström H, Nasr P, Fredrikson M, Stål P, Kechagias S, et al. Fibrosis stage is the strongest predictor for disease-specific mortality in NAFLD after up to 33 years of follow-up. Hepatology 2015;61:1547–54. doi:10.1002/hep.27368.

[76] Hsu J-H, Chien I-C, Lin C-H. Increased risk of chronic liver disease in patients with major depressive disorder: A population-based study. J Affect Disord 2019;251:180–5. doi:10.1016/J.JAD.2019.03.070.

[77] Fuller BE, Rodriguez VL, Linke A, Sikirica M, Dirani R, Hauser P. Prevalence of liver disease in veterans with bipolar disorder or schizophrenia. Gen Hosp Psychiatry 2011;33:232–7. doi:10.1016/j.genhosppsych.2011.03.006.

[78] Buzzetti E, Pinzani M, Tsochatzis EA. The multiple-hit pathogenesis of non-alcoholic fatty liver disease (NAFLD). Metabolism 2016;65:1038–48. doi:10.1016/j.metabol.2015.12.012.

[79] Bedossa P. Pathology of non-alcoholic fatty liver disease. Liver Int 2017;37:85–9. doi:10.1111/liv.13301.

[80] Brunt EM, Wong VW-S, Nobili V, Day CP, Sookoian S, Maher JJ, et al. Nonalcoholic fatty liver disease. Nat Rev Dis Prim 2015;1:15080. doi:10.1038/nrdp.2015.80.

[81] Mota M, Banini BA, Cazanave SC, Sanyal AJ. Molecular mechanisms of lipotoxicity and glucotoxicity in nonalcoholic fatty liver disease. Metabolism 2016;65:1049–61. doi:10.1016/j.metabol.2016.02.014.

[82] Tilg H, Moschen AR. Evolution of inflammation in nonalcoholic fatty liver disease: The multiple parallel hits hypothesis. Hepatology 2010;52:1836–46. doi:10.1002/hep.24001.

[83] Hübscher SG. Histological assessment of non-alcoholic fatty liver disease. Histopathology 2006;49:450–65. doi:10.1111/j.1365-2559.2006.02416.x.

[84] Brown GT, Kleiner DE. Histopathology of nonalcoholic fatty liver disease and nonalcoholic steatohepatitis. Metabolism 2016;65:1080–6. doi:10.1016/j.metabol.2015.11.008.

[85] Farrell GC, Larter CZ. Nonalcoholic fatty liver disease: From steatosis to cirrhosis. Hepatology 2006;43:S99–112. doi:10.1002/hep.20973.

[86] Kleiner D, Brunt E. Nonalcoholic fatty liver disease: pathologic patterns and biopsy evaluation in clinical research. Semin Liver Dis 2012;32:3–13. doi:10.1055/s-0032-1306421.

[87] Li B, Zhang C, Zhan Y-T. Nonalcoholic fatty liver disease cirrhosis: A review of its epidemiology, risk factors, clinical presentation, diagnosis, management, and prognosis. Can J Gastroenterol Hepatol 2018;2018:1–8. doi:10.1155/2018/2784537.

[88] Greco D, Kotronen A, Westerbacka J, Puig O, Arkkila P, Kiviluoto T, et al. Gene expression in human NAFLD. AJP Gastrointest Liver Physiol 2008;294:G1281–7. doi:10.1152/ajpgi.00074.2008.

[89] Ryaboshapkina M, Hammar M. Human hepatic gene expression signature of non-alcoholic fatty liver disease progression, a meta-analysis. Sci Rep 2017;7:12361. doi:10.1038/s41598-017-10930-w.

[90] Birkl-Toeglhofer AM, Birkl C, Llenos IC, Weis S, Haybaeck J. Hepatic gene expression explains primary drug toxicity in bipolar disorder. Transl Psychiatry 2019;9:331. doi:10.1038/s41398-019-0666-4.

[91] R Development Core Team. R: A language and environment for statistical computing. Vienna, Austria: R Foundation for Statistical Computing; 2008.

[92] Gautier L, Cope L, Bolstad BM, Irizarry RA. Affy - Analysis of Affymetrix GeneChip data at the probe level. Bioinformatics 2004;20:307–15. doi:10.1093/bioinformatics/btg405.

[93] Miller CJ. simpleaffy: Very simple high level analysis of Affymetrix data 2018.

[94] Irizarry RA, Bolstad BM, Collin F, Cope LM, Hobbs B, Speed TP. Summaries of Affymetrix GeneChip probe level data. Nucleic Acids Res 2003;31:e15.

[95] Gentleman R, Carey V, Huber W, Hahne F. Genefilter: Methods for filtering genes from high-throughput experiments. R package version 1.53.0. 2015.

[96] Ritchie ME, Phipson B, Wu D, Hu Y, Law CW, Shi W, et al. limma powers differential expression analyses for RNA-sequencing and microarray studies. Nucleic Acids Res 2015;43:e47–e47. doi:10.1093/nar/gkv007.

[97] Durinck S, Moreau Y, Kasprzyk A, Davis S, De Moor B, Brazma A, et al. BioMart and Bioconductor: a powerful link between biological databases and microarray data analysis. Bioinformatics 2005;21:3439–40. doi:10.1093/bioinformatics/bti525.

[98] Doncheva NT, Morris JH, Gorodkin J, Jensen LJ. Cytoscape StringApp: Network analysis and visualization of proteomics data. J Proteome Res 2019;18:623–32. doi:10.1021/acs.jproteome.8b00702.

[99] Shannon P, Markiel A, Ozier O, Baliga NS, Wang JT, Ramage D, et al. Cytoscape: A software Environment for integrated models of biomolecular interaction networks. Genome Res 2003;13:2498–504. doi:10.1101/gr.1239303.

[100] Snel B, Lehmann G, Bork P, Huynen M. STRING: a web-server to retrieve and display the repeatedly occurring neighbourhood of a gene. Nucleic Acids Res 2000;28:3442–4. doi:10.1093/nar/28.18.3442.

[101] Szklarczyk D, Gable AL, Lyon D, Junge A, Wyder S, Huerta-Cepas J, et al. STRING v11: Protein-protein association networks with increased coverage, supporting functional discovery in genome-wide experimental datasets. Nucleic Acids Res 2019;47:D607–13. doi:10.1093/nar/gky1131.

[102] Chin CH, Chen SH, Wu HH, Ho CW, Ko MT, Lin CY. cytoHubba: Identifying hub objects and sub-networks from complex interactome. BMC Syst Biol 2014;8:S11. doi:10.1186/1752-0509-8-S4-S11.

[103] Wang J, Zhong J, Chen G, Li M, Wu FX, Pan Y. ClusterViz: A Cytoscape APP for Cluster Analysis of Biological Network. IEEE/ACM Trans Comput Biol Bioinforma 2015;12:815–22. doi:10.1109/TCBB.2014.2361348.

[104] Bader GD, Hogue CWV. An automated method for finding molecular complexes in large protein interaction networks. BMC Bioinformatics 2003;4. doi:10.1186/1471-2105-4-2.

[105] Zhang B, Kirov S, Snoddy J. WebGestalt: an integrated system for exploring gene sets in various biological contexts. Nucleic Acids Res 2005;33:W741–8. doi:10.1093/nar/gki475.

[106] Wang J, Vasaikar S, Shi Z, Greer M, Zhang B. WebGestalt 2017: A more comprehensive, powerful, flexible and interactive gene set enrichment analysis toolkit. Nucleic Acids Res 2017;45:W130–7. doi:10.1093/nar/gkx356.

[107] Ye J, Coulouris G, Zaretskaya I, Cutcutache I, Rozen S, Madden TL. Primer-BLAST: a tool to design target-specific primers for polymerase chain reaction. BMC Bioinformatics 2012;13:134. doi:10.1186/1471-2105-13-134.

[108] Livak KJ, Schmittgen TD. Analysis of relative gene expression data using real-time quantitative PCR and the 2−ΔΔCT method. Methods 2001;25:402–8. doi:10.1006/meth.2001.1262.

[109] Haarman BCM (Benno), Riemersma-Van der Lek RF, Nolen WA, Mendes R, Drexhage HA, Burger H. Feature-expression heat maps – A new visual method to explore complex associations between two variable sets. J Biomed Inform 2015;53:156–61. doi:10.1016/J.JBI.2014.10.003.

[110] WHO/Europe | Nutrition - Body mass index - BMI n.d. http://www.euro.who.int/en/health-topics/disease-prevention/nutrition/a-healthy-lifestyle/body-mass-index-bmi

[111] Ishak ' K, Baptista2 A, Bianchi3 L, Callea4 F, De Grootes J, Gudat6 F, et al. Histological grading and staging of chronic hepatitis. J Hepatol 1995;22:696–9. doi:10.1016/0168-8278(95)80226-6.

[112] Brunt EM. Grading and staging the histopathological lesions of chronic hepatitis: The

Knodell histology activity index and beyond. Hepatology 2000;31:241–6. doi:10.1002/hep.510310136.

[113] Cikánková T, Fišar Z, Hroudová J. In vitro effects of antidepressants and mood-stabilizing drugs on cell energy metabolism. Naunyn Schmiedebergs Arch Pharmacol 2020;393:797–811. doi:10.1007/s00210-019-01791-3.

[114] Newcomer JW. Antipsychotic medications: Metabolic and cardiovascular risk. J Clin Psychiatry 2007;68:8–13.

[115] Goyette J, Geczy CL. Inflammation-associated S100 proteins: new mechanisms that regulate function. Amino Acids 2011;41:821–42. doi:10.1007/s00726-010-0528-0.

[116] Bresnick AR, Weber DJ, Zimmer DB. S100 proteins in cancer. Nat Rev Cancer 2015;15:96–109. doi:10.1038/nrc3893.

[117] Gebhardt C, Németh J, Angel P, Hess J. S100A8 and S100A9 in inflammation and cancer. Biochem Pharmacol 2006;72:1622–31. doi:10.1016/j.bcp.2006.05.017.

[118] Srikrishna G. S100A8 and S100A9: new insights into their roles in malignancy. J Innate Immun 2012;4:31–40. doi:10.1159/000330095.

[119] Lanz TA, Reinhart V, Sheehan MJ, Rizzo SJS, Bove SE, James LC, et al. Postmortem transcriptional profiling reveals widespread increase in inflammation in schizophrenia: a comparison of prefrontal cortex, striatum, and hippocampus among matched tetrads of controls with subjects diagnosed with schizophrenia, bipolar or major depressive disorder. Transl Psychiatry 2019;9:151. doi:10.1038/s41398-019-0492-8.

[120] Tsuang MT, Nossova N, Yager T, Tsuang M-M, Guo S-C, Shyu KG, et al. Assessing the validity of blood-based gene expression profiles for the classification of schizophrenia and bipolar disorder: A preliminary report. Am J Med Genet Part B Neuropsychiatr Genet 2005;133B:1–5. doi:10.1002/ajmg.b.30161.

[121] Iavarone F, Melis M, Platania G, Cabras T, Manconi B, Petruzzelli R, et al. Characterization of salivary proteins of schizophrenic and bipolar disorder patients by top-down proteomics. J Proteomics 2014;103:15–22. doi:10.1016/j.jprot.2014.03.020.

[122] Gardiner EJ, Cairns MJ, Liu B, Beveridge NJ, Carr V, Kelly B, et al. Gene expression analysis reveals schizophrenia-associated dysregulation of immune pathways in peripheral blood mononuclear cells. J Psychiatr Res 2013;47:425–37. doi:10.1016/j.jpsychires.2012.11.007.

[123] Serhal R, Hilal G, Boutros G, Sidaoui J, Wardi L, Ezzeddine S, et al. Nonalcoholic steatohepatitis: Involvement of the telomerase and proinflammatory mediators. Biomed Res Int 2015;2015:1–9. doi:10.1155/2015/850246.

[124] Németh J, Stein I, Haag D, Riehl A, Longerich T, Horwitz E, et al. S100A8 and S100A9 are novel nuclear factor kappa B target genes during malignant progression of murine and human liver carcinogenesis. Hepatology 2009;50:1251–62. doi:10.1002/hep.23099.

[125] De Ponti A, Wiechert L, Schneller D, Pusterla T, Longerich T, Hogg N, et al. A pro-tumorigenic function of S100A8/A9 in carcinogen-induced hepatocellular carcinoma. Cancer Lett 2015;369:396–404. doi:10.1016/j.canlet.2015.09.005.

[126] Uhlar CM, Whitehead AS. Serum amyloid A, the major vertebrate acute-phase reactant. Eur J Biochem 1999;265:501–23. doi:10.1046/j.1432-1327.1999.00657.x.

[127] Thorn CF, Lu ZY, Whitehead AS. Regulation of the human acute phase serum amyloid A genes by tumour necrosis factor-α, interleukin-6 and glucocorticoids in hepatic and epithelial cell lines. Scand J Immunol 2004;59:152–8. doi:10.1111/j.0300-9475.2004.01369.x.

[128] Badolato R, Johnston JA, Wang JM, McVicar D, Xu LL, Oppenheim JJ, et al. Serum amyloid A induces calcium mobilization and chemotaxis of human monocytes by activating a pertussis toxin-sensitive signaling pathway. J Immunol 1995;155:4004–10.

[129] Badolato R, Wang JM, Murphy WJ, Lloyd AR, Michiel DF, Bausserman LL, et al. Serum amyloid A is a chemoattractant: Induction migration, adhesion, and tissue infiltration of monocytes and polymorphonuclear leukocytes. J Exp Med 1994;180:203–9. doi:10.1084/jem.180.1.203.

[130] van Dooren FEP, Schram MT, Schalkwijk CG, Stehouwer CDA, Henry RMA, Dagnelie PC, et al. Associations of low grade inflammation and endothelial dysfunction with depression - The Maastricht Study. Brain Behav Immun 2016;56:390–6. doi:10.1016/j.bbi.2016.03.004.

[131] Bryleva EY, Keaton SA, Grit J, Madaj Z, Sauro-Nagendra A, Smart L, et al. The acute-phase mediator serum amyloid A is associated with symptoms of depression and fatigue. Acta Psychiatr Scand 2017;135:409–18. doi:10.1111/acps.12730.

[132] Siegmund S V., Schlosser M, Schildberg FA, Seki E, De Minicis S, Uchinami H, et al. Serum amyloid A induces inflammation, proliferation and cell death in activated hepatic stellate cells. PLoS One 2016;11. doi:10.1371/journal.pone.0150893.

[133] Tan Q, Hu J, Yu X, Guan W, Lu H, Yu Y, et al. The role of IL-1 family members and Kupffer cells in liver regeneration 2016. doi:10.1155/2016/6495793.

[134] Ortiz-Domínguez A, Hernández ME, Berlanga C, Gutiérrez-Mora D, Moreno J, Heinze G, et al. Immune variations in bipolar disorder: phasic differences. Bipolar Disord 2007;9:596–602. doi:10.1111/j.1399-5618.2007.00493.x.

[135] Modabbernia A, Taslimi S, Brietzke E, Ashrafi M. Cytokine alterations in bipolar disorder: A meta-analysis of 30 studies n.d. doi:10.1016/j.biopsych.2013.01.007.

[136] Hope S, Ueland T, Steen NE, Dieset I, Lorentzen S, Berg AO, et al. Interleukin 1 receptor antagonist and soluble tumor necrosis factor receptor 1 are associated with general severity and psychotic symptoms in schizophrenia and bipolar disorder. Schizophr Res 2013;145:36–42. doi:10.1016/j.schres.2012.12.023.

[137] Lotrich FE, Butters MA, Aizenstein H, Megan M, Marron M, Gildengers AG. The relationship between interleukin-1 receptor antagonist and cognitive function in older adults with bipolar disorder NIH Public Access. Int J Geriatr Psychiatry 2014;29:635–44. doi:10.1002/gps.4048.

[138] Hendrikx T, Walenbergh SMA, Jeurissen MLJ, Houben T, Van Gorp PJ, Lindsey PJ, et al. Plasma IL-1 receptor antagonist levels correlate with the development of non-alcoholic steatohepatitis. Biomark Med 2015;9:1301–9. doi:10.2217/bmm.15.71.

[139] Pihlajamäki J, Kuulasmaa T, Kaminska D, Simonen M, Kärjä V, Grönlund S, et al. Serum interleukin 1 receptor antagonist as an independent marker of non-alcoholic steatohepatitis in humans. J Hepatol 2012;56:663–70. doi:10.1016/j.jhep.2011.10.005.

[140] Krueger SK, Williams DE. Mammalian flavin-containing monooxygenases: structure/function, genetic polymorphisms and role in drug metabolism. Pharmacol Ther 2005;106:357–87. doi:10.1016/j.pharmthera.2005.01.001.

[141] Rudraiah S, Moscovitz JE, Donepudi AC, Campion SN, Slitt AL, Aleksunes LM, et al. Differential Fmo3 gene expression in various liver injury models involving hepatic oxidative stress in mice. Toxicology 2014;325:85–95. doi:10.1016/j.tox.2014.08.013.

[142] Hlady RA, Sathyanarayan A, Thompson JJ, Zhou D, Wu Q, Pham K, et al. Integrating the epigenome to identify drivers of hepatocellular carcinoma. Hepatology 2019;69:639–52. doi:10.1002/hep.30211.

[143] Zlatković J, Todorović N, Tomanović N, Bošković M, Djordjević S, Lazarević-Pašti T, et al. Chronic administration of fluoxetine or clozapine induces oxidative stress in rat liver: A histopathological study. Eur J Pharm Sci 2014;59:20–30. doi:10.1016/j.ejps.2014.04.010.

[144] Atkinson S, Way M, McQuillin A, Morgan M, Thursz M. A genome-wide association study identifies PNPLA3 and SLC38A4 as risk loci for alcoholic hepatitis. J Hepatol 2016;64:S134. doi:10.1016/s0168-8278(16)01634-2.

[145] Pitti RM, Marsters SA, Ruppert S, Donahue CJ, Moore A, Ashkenazi A. Induction of apoptosis by Apo-2 ligand, a new member of the tumor necrosis factor cytokine family. J Biol Chem 1996;271:12687–90. doi:10.1074/jbc.271.22.12687.

[146] Sheridan JP, Marsters SA, Pitti RM, Gurney A, Skubatch M, Baldwin D, et al. Control of TRAIL-induced apoptosis by a family of signaling and decoy receptors. Science 1997;277:818–21. doi:10.1126/science.277.5327.818.

[147] Cartland SP, Harith HH, Genner SW, Dang L, Cogger VC, Vellozzi M, et al. Non-alcoholic fatty liver disease, vascular inflammation and insulin resistance are exacerbated by TRAIL deletion in mice. Sci Rep 2017;7:1–12. doi:10.1038/s41598-017-01721-4.

[148] Shao L, Vawter MP. Shared gene expression alterations in schizophrenia and bipolar disorder. Biol Psychiatry 2008;64:89–97. doi:10.1016/j.biopsych.2007.11.010.

[149] Ighodaro OM, Akinloye OA. First line defence antioxidants-superoxide dismutase (SOD), catalase (CAT) and glutathione peroxidase (GPX): Their fundamental role in the entire antioxidant defence grid. Alexandria J Med 2018;54:287–93. doi:10.1016/j.ajme.2017.09.001.

[150] Frey BN, Andreazza AC, Kunz M, Gomes FA, Quevedo J, Salvador M, et al. Increased oxidative stress and DNA damage in bipolar disorder: a twin-case report. Prog Neuropsychopharmacol Biol Psychiatry 2007;31:283–5. doi:10.1016/j.pnpbp.2006.06.011.

[151] Raffa M, Barhoumi S, Atig F, Fendri C, Kerkeni A, Mechri A. Reduced antioxidant defense systems in schizophrenia and bipolar I disorder. Prog Neuro-

Psychopharmacology Biol Psychiatry 2012;39:371–5. doi:10.1016/j.pnpbp.2012.07.013.

[152] Ranjekar PK, Hinge A, Hegde M V., Ghate M, Kale A, Sitasawad S, et al. Decreased antioxidant enzymes and membrane essential polyunsaturated fatty acids in schizophrenic and bipolar mood disorder patients. Psychiatry Res 2003;121:109–22. doi:10.1016/S0165-1781(03)00220-8.

[153] Shin SK, Cho HW, Song SE, Song DK. Catalase and nonalcoholic fatty liver disease. Pflugers Arch Eur J Physiol 2018;470:1721–37. doi:10.1007/s00424-018-2195-z.

[154] Bai J, Rodriguez AM, Melendez JA, Cederbaum AI. Overexpression of catalase in cytosolic or mitochondrial compartment protects HepG2 cells against oxidative injury. J Biol Chem 1999;274:26217–24. doi:10.1074/jbc.274.37.26217.

[155] Sreekumar R, Rosado B, Rasmussen D, Charlton M. Hepatic gene expression in histologically progressive nonalcoholic steatohepatitis. Hepatology 2003;38:244–51. doi:10.1053/jhep.2003.50290.

[156] Videla LA, Rodrigo R, Orellana M, Fernandez V, Tapia G, Quiñones L, et al. Oxidative stress-related parameters in the liver of non-alcoholic fatty liver disease patients. Clin Sci 2004;106:261–8. doi:10.1042/CS20030285.

[157] Chang P, Stearns T. δ-Tubulin and ε-tubulin: Two new human centrosomal tubulins reveal new aspects of centrosome structure and function. Nat Cell Biol 2000;2:30–5. doi:10.1038/71350.

[158] Chang P, Giddings TH, Winey M, Stearns T. E-tubulin is required for centriole duplication and microtubule organization. Nat Cell Biol 2003;5:71–6. doi:10.1038/ncb900.

[159] Dupuis-Williams P, Fleury-Aubusson A, De Loubresse NG, Geoffroy H, Vayssié L, Galvani A, et al. Functional role of ε-tubulin in the assembly of the centriolar microtubule scaffold. J Cell Biol 2002;158:1183–93. doi:10.1083/jcb.200205028.

[160] Iwamoto K, Bundo M, Kato T. Altered expression of mitochondria-related genes in postmortem brains of patients with bipolar disorder or schizophrenia, as revealed by large-scale DNA microarray analysis. Hum Mol Genet 2005;14:241–53. doi:10.1093/hmg/ddi022.

[161] Scaini G, Quevedo J, Velligan D, Roberts DL, Raventos H, Walss-Bass C. Second generation antipsychotic-induced mitochondrial alterations: Implications for increased risk of metabolic syndrome in patients with schizophrenia. Eur Neuropsychopharmacol 2018;28:369–80. doi:10.1016/j.euroneuro.2018.01.004.

[162] Luethi D, Liechti ME, Krähenbühl S. Mechanisms of hepatocellular toxicity associated with new psychoactive synthetic cathinones. Toxicology 2017;387:57–66. doi:10.1016/j.tox.2017.06.004.

[163] Stacey D, Schubert KO, Clark SR, Amare AT, Milanesi E, Maj C, et al. A gene co-expression module implicating the mitochondrial electron transport chain is associated with long-term response to lithium treatment in bipolar affective disorder. Transl Psychiatry 2018;8:183. doi:10.1038/s41398-018-0237-0.

[164] Soliman HM, Wagih HM, Algaidi SA, Hafiz AH. Histological evaluation of the role of atypical antipsychotic drugs in inducing non-alcoholic fatty liver disease in adult male albino rats (Light and Electron Microscopic Study). Folia Biol 2013;59:173–80.

[165] Kurian SM, Le-Niculescu H, Patel SD, Bertram D, Davis J, Dike C, et al. Identification of blood biomarkers for psychosis using convergent functional genomics. Mol Psychiatry 2011;16:37–58. doi:10.1038/mp.2009.117.

[166] Itsumi M, Inoue S, Elia AJ, Murakami K, Sasaki M, Lind EF, et al. Idh1 protects murine hepatocytes from endotoxin-induced oxidative stress by regulating the intracellular NADP +/NADPH ratio. Cell Death Differ 2015;22:1837–48. doi:10.1038/cdd.2015.38.

[167] Abdollahi H, Azodi MZ, Hatami B. Protein interaction mapping interpretation of none alcoholic fatty liver disease model of rats after fat diet feeding. Gastroenterol Hepatol from Bed to Bench 2017;10:S146–53. doi:10.22037/ghfbb.v0i0.1291.

[168] Glickman RM, Rogers M, Glickman JN. Apolipoprotein B synthesis by human liver and intestine in vitro. Proc Natl Acad Sci U S A 1986;83:5296–300. doi:10.1073/pnas.83.14.5296.

[169] Canfrań-Duque A, Casado ME, Pastor Ó, Sánchez-Wandelmer J, De La Penã G, Lerma M, et al. Atypical antipsychotics alter cholesterol and fatty acid metabolism in vitro. J Lipid Res 2013;54:310–24. doi:10.1194/jlr.M026948.

[170] Charlton M, Sreekumar R, Rasmussen D, Lindor K, Nair KS. Apolipoprotein synthesis in nonalcoholic steatohepatitis. Hepatology 2002;35:898–904. doi:10.1053/jhep.2002.32527.

[171] Vinciguerra M, Foti M. PTEN at the crossroad of metabolic diseases and cancer in the liver. Ann Hepatol 2008;7:192–9. doi:10.1016/s1665-2681(19)31848-4.

[172] Qiu W, Federico L, Naples M, Avramoglu RK, Meshkani R, Zhang J, et al. Phosphatase and tensin homolog (PTEN) regulates hepatic lipogenesis, microsomal triglyceride transfer protein, and the secretion of apolipoprotein B-containing lipoproteins. Hepatology 2008;48:1799–809. doi:10.1002/hep.22565.

[173] Horie Y, Suzuki A, Kataoka E, Sasaki T, Hamada K, Sasaki J, et al. Hepatocyte-specific Pten deficiency results in steatohepatitis and hepatocellular carcinomas. J Clin Invest 2004;113:1774–83. doi:10.1172/JCI20513.

[174] Konradi C, Eaton M, MacDonald ML, Walsh J, Benes FM, Heckers S. Molecular evidence for mitochondrial dysfunction in bipolar disorder. Arch Gen Psychiatry 2004;61:300–8. doi:10.1001/archpsyc.61.3.300.

[175] Altar CA, Jurata LW, Charles V, Lemire A, Liu P, Bukhman Y, et al. Deficient hippocampal neuron expression of proteasome, ubiquitin, and mitochondrial genes in multiple schizophrenia cohorts. Biol Psychiatry 2005;58:85–96. doi:10.1016/j.biopsych.2005.03.031.

[176] Bousman CA, Chana G, Glatt SJ, Chandler SD, May T, Lohr J, et al. Positive symptoms of psychosis correlate with expression of ubiquitin proteasome genes in peripheral blood. Am J Med Genet Part B Neuropsychiatr Genet 2010;153:1336–41. doi:10.1002/ajmg.b.31106.

[177] Hanada S, Harada M, Kumemura H, Bishr Omary M, Koga H, Kawaguchi T, et al. Oxidative stress induces the endoplasmic reticulum stress and facilitates inclusion formation in cultured cells. J Hepatol 2007;47:93–102. doi:10.1016/j.jhep.2007.01.039.

[178] Harada M, Strnad P, Toivola DM, Omary MB. Autophagy modulates keratin-containing inclusion formation and apoptosis in cell culture in a context-dependent fashion. Exp Cell Res 2008;314:1753–64. doi:10.1016/j.yexcr.2008.01.035.

[179] Harada M, Hanada S, Toivola DM, Ghori N, Omary MB. Autophagy activation by rapamycin eliminates mouse Mallory-Denk bodies and blocks their proteasome inhibitor-mediated formation. Hepatology 2008;47:2026–35. doi:10.1002/hep.22294.

[180] Kuehl P, Zhang J, Lin Y, Lamba J, Assem M, Schuetz J, et al. Sequence diversity in CYP3A promoters and characterization of the genetic basis of polymorphic CYP3A5 expression. Nat Genet 2001;27:383–91. doi:10.1038/86882.

[181] Cabaleiro T, López-Rodríguez R, Ochoa D, Román M, Novalbos J, Abad-Santos F. Polymorphisms influencing olanzapine metabolism and adverse effects in healthy subjects. Hum Psychopharmacol Clin Exp 2013;28:205–14. doi:10.1002/hup.2308.

[182] Xiang Q, Zhao X, Zhou Y, Duan JL, Cui YM. Effect of CYP2D6, CYP3A5, and MDR1 genetic polymorphisms on the pharmacokinetics of risperidone and its active moiety. J Clin Pharmacol 2010;50:659–66. doi:10.1177/0091270009347867.

[183] Liston HL, Markowitz JS, DeVane CL. Drug glucuronidation in clinical psychopharmacology. J Clin Psychopharmacol 2001;21:500–15. doi:10.1097/00004714-200110000-00008.

[184] Ethell BT, Anderson GD, Burchell B. The effect of valproic acid on drug and steroid glucuronidation by expressed human UDP-glucuronosyltransferases. Biochem Pharmacol 2003;65:1441–9. doi:10.1016/S0006-2952(03)00076-5.

[185] Yalcin EB, More V, Neira KL, Lu ZJ, Cherrington NJ, Slitt AL, et al. Downregulation of sulfotransferase expression and activity in diseased human livers. Drug Metab Dispos 2013;41:1642–50. doi:10.1124/dmd.113.050930.

[186] Ryckman C, Vandal K, Rouleau P, Talbot M, Tessier PA. Proinflammatory activities of S100: proteins S100A8, S100A9, and S100A8/A9 induce neutrophil chemotaxis and adhesion. J Immunol 2003;170:3233–42. doi:10.4049/JIMMUNOL.170.6.3233.

[187] Çakır U, Can Tuman T, Yıldırım O. Increased neutrophil/lymphoctye ratio in patients with bipolar disorder: a preliminary study. Psychiatr Danub 2015;27:180–4.

[188] Mazza MG, Lucchi S, Rossetti A, Clerici M. Neutrophil-lymphocyte ratio, monocyte-lymphocyte ratio and platelet-lymphocyte ratio in non-affective psychosis: A meta-analysis and systematic review. World J Biol Psychiatry 2020;21:326–38. doi:10.1080/15622975.2019.1583371.

[189] Ochs DL, Reed PW. Inhibition of the neutrophil oxidative burst and degranulation by phenothiazines. Biochem Biophys Res Commun 1981;102:958–62. doi:10.1016/0006-291X(81)91631-4.

[190] Lohr KM, Feix JB, Kurth C. Chlorpromazine inhibits neutrophil chemotaxis beyond the chemotactic receptor-ligand interaction. J Infect Dis 1984;150:643–52.

doi:10.1093/infdis/150.5.643.

[191] Hetarinen-Runtti P, Lakari E, Raivio KO, Kinnula VL. Expression of antioxidant enzymes in human inflammatory cells. Am J Physiol Cell Physiol 2000;278:C118–25. doi:10.1152/ajpcell.2000.278.1.c118.

[192] Braicu C, Buse M, Busuioc C, Drula R, Gulei D, Raduly L, et al. A comprehensive review on MAPK: A promising therapeutic target in cancer. Cancers (Basel) 2019;11. doi:10.3390/cancers11101618.

[193] Kettritz R, Schreiber A, Luft FC, Haller H. Role of mitogen-activated protein kinases in activation of human neutrophils by antineutrophil cytoplasmic antibodies. J Am Soc Nephrol 2001;12:37–46.

[194] Gupta A, Schulze TG, Nagarajan V, Akula N, Corona W, Jiang XY, et al. Interaction networks of lithium and valproate molecular targets reveal a striking enrichment of apoptosis functional clusters and neurotrophin signaling. Pharmacogenomics J 2012;12:328–41. doi:10.1038/tpj.2011.9.

[195] Dwivedi Y, Rizavi HS, Roberts RC, Conley RC, Tamminga CA, Pandey GN. Reduced activation and expression of ERK1/2 MAP kinase in the post-mortem brain of depressed suicide subjects. J Neurochem 2001;77:916–28. doi:10.1046/j.1471-4159.2001.00300.x.

[196] Yuan P, Zhou R, Wang Y, Li X, Li J, Chen G, et al. Altered levels of extracellular signal-regulated kinase signaling proteins in postmortem frontal cortex of individuals with mood disorders and schizophrenia. J Affect Disord 2010;124:164–9. doi:10.1016/j.jad.2009.10.017.

[197] Sahu A, Lambris JD. Structure and biology of complement protein C3, a connecting link between innate and acquired immunity. Immunol Rev 2001;180:35–48. doi:10.1034/j.1600-065X.2001.1800103.x.

[198] Maes M, Delange J, Ranjan R, Meltzer HY, Desnyder R, Cooremans W, et al. Acute phase proteins in schizophrenia, mania and major depression: Modulation by psychotropic drugs. Psychiatry Res 1997;66:1–11. doi:10.1016/S0165-1781(96)02915-0.

[199] Reginia A, Kucharska-Mazur J, Jabłoński M, Budkowska M, Dołęgowska B, Sagan L, et al. Assessment of complement cascade components in patients with bipolar disorder. Front Psychiatry 2018;9:614. doi:10.3389/fpsyt.2018.00614.

[200] Akcan U, Karabulut S, Ismail Küçükali C, Çakir S, Tüzün E. Bipolar disorder patients display reduced serum complement levels and elevated peripheral blood complement expression levels. Acta Neuropsychiatr 2018;30:70–8. doi:10.1017/neu.2017.10.

[201] Markiewski MM, Mastellos D, Tudoran R, DeAngelis RA, Strey CW, Franchini S, et al. C3a and C3b activation products of the third component of complement (C3) are critical for normal liver recovery after toxic injury. J Immunol 2004;173:747–54. doi:10.4049/jimmunol.173.2.747.

[202] Logan MR, Lacy P, Odemuyiwa SO, Steward M, Davoine F, Kita H, et al. A critical role for vesicle-associated membrane protein-7 in exocytosis from human eosinophils and neutrophils. Allergy 2006;61:777–84. doi:10.1111/j.1398-9995.2006.01089.x.

[203] Takahashi Y, Fukusato T. Histopathology of nonalcoholic fatty liver disease/nonalcoholic steatohepatitis. World J Gastroenterol 2014;20:15539–15548. doi:10.3748/wjg.v20.i42.15539.

[204] Aravinthan A, Verma S, Coleman N, Davies S, Allison M, Alexander G. Vacuolation in hepatocyte nuclei is a marker of senescence. J Clin Pathol 2012;65:557–60. doi:10.1136/jclinpath-2011-200641.

[205] Ogrodnik M, Miwa S, Tchkonia T, Tiniakos D, Wilson CL, Lahat A, et al. Cellular senescence drives age-dependent hepatic steatosis. Nat Commun 2017;8:15691. doi:10.1038/ncomms15691.

[206] Wiemann SU, Satyanarayana A, Tsahuridu M, Tillmann HL, Zender L, Klempnauer J, et al. Hepatocyte telomere shortening and senescence are general markers of human liver cirrhosis. FASEB J 2002;16:935–42. doi:10.1096/fj.01-0977com.

[207] Krizhanovsky V, Yon M, Dickins RA, Hearn S, Simon J, Miething C, et al. Senescence of activated stellate cells limits liver fibrosis. Cell 2008;134:657–67. doi:10.1016/j.cell.2008.06.049.

[208] Pessayre D, Fromenty B. NASH: a mitochondrial disease. J Hepatol 2005;42:928–40. doi:10.1016/J.JHEP.2005.03.004.

[209] Wei Y, Scott Rector R, Thyfault JP, Ibdah Jamal A Ibdah JA, Ibdah JA, To C. Nonalcoholic fatty liver disease and mitochondrial dysfunction. World J Gastroenterol 2008;14:193–9. doi:10.3748/wjg.14.193.

[210] Cobbina E, Akhlaghi F. Non-alcoholic fatty liver disease (NAFLD)–pathogenesis, classification, and effect on drug metabolizing enzymes and transporters. Drug Metab Rev 2017;49:197–211. doi:10.1080/03602532.2017.1293683.

[211] Pérez-Carreras M, Del Hoyo P, Martín MA, Rubio JC, Martín A, Castellano G, et al. Defective hepatic mitochondrial respiratory chain in patients with nonalcoholic steatohepatitis. Hepatology 2003;38:999–1007. doi:10.1002/hep.1840380426.

[212] Begriche K, Igoudjil A, Pessayre D, Fromenty B. Mitochondrial dysfunction in NASH: Causes, consequences and possible means to prevent it. Mitochondrion 2006;6:1–28. doi:10.1016/j.mito.2005.10.004.

[213] Heber S, Sick B. Quality assessment of Affymetrix GeneChip data. Omi A J Integr Biol 2006;10:358–68. doi:10.1089/omi.2006.10.358.

[214] Fan J, Khanin R, Sakamoto H, Zhong Y, Michael C, Pena D, et al. Quantification of nucleic acid quality in postmortem tissues from a cancer research autopsy program. Oncotarget 2016;7:66906–21. doi:10.18632/oncotarget.11836.

[215] White K, Yang P, Li L, Farshori A, Medina AE, Zielke HR. Effect of postmortem interval and years in storage on RNA quality of tissue at a repository of the NIH NeuroBioBank. Biopreserv Biobank 2018;16:148–57. doi:10.1089/bio.2017.0099.

[216] Malhotra AK, Murphy GM, Kennedy JL. Pharmacogenetics of psychotropic drug response. Am J Psychiatry 2004;161:780–96. doi:10.1176/appi.ajp.161.5.780.

6 Appendix

Table A1. **Differentially expressed genes and enriched pathways assessed in liver tissue of patients with bipolar disorder compared to controls.** Annotated genes are listed with their gene symbol, the appropriate HGNC names and identifiers, as well as the corresponding probe ID of the Affymetrix microarray GeneChip Human Genome U133 Plus 2.0. Genes are listed in ascending order with regard to their expression level presented as fold change (FC) and log_2 fold change (log_2FC). Blue fold changes indicating underexpression and red fold changes indicate overexpression. Adjusted significance levels are presented as false discovery rate (FDR).The respective allocated pathway (P) is denoted with 'R' for genes related to the respiratory electron transport chain, 'L' for the lipid metabolism, 'B' for the biological oxidations, "A" for the amino acid metabolism and "I" for the neutrophil degranulation. [Adapted from [90]]

Gene symbol	HGNC gene name	HGNC ID	Affymetrix probe ID	FC	log_2FC	FDR	P
FMO3	flavin containing dimethylaniline monooxygenase 3	3771	40665_at	0,22	-2,18	4,56E-04	B
SLC38A4	solute carrier family 38 member 4	14679	220786_s_at	0,24	-2,04	2,01E-03	
TNFSF10	TNF superfamily member 10	11925	214329_x_at	0,25	-2,00	3,90E-06	
CAT	catalase	1516	211922_s_at	0,26	-1,95	5,68E-05	I
TUBE1	tubulin epsilon 1	20775	226181_at	0,27	-1,90	2,00E-06	
ALDH1A1	aldehyde dehydrogenase 1 family member A1	402	212224_at	0,27	-1,87	1,56E-03	B
HPGD	15-hydroxyprostaglandin dehydrogenase	5154	211548_s_at	0,27	-1,87	1,75E-03	L
UGT2B4	UDP glucuronosyltransferase family 2 member B4	12553	206505_at	0,29	-1,78	2,08E-03	B
GYS2	glycogen synthase 2	4707	214621_at	0,30	-1,76	6,07E-04	
SLC41A2	solute carrier family 41 member 2	31045	235299_at	0,30	-1,75	2,00E-06	
NADK2	NAD kinase 2, mitochondrial	26404	229299_at	0,30	-1,74	7,51E-05	
CYR61	cysteine rich angiogenic inducer 61	2654	201289_at	0,30	-1,72	2,12E-02	
DPYD	dihydropyrimidine dehydrogenase	3012	204646_at	0,31	-1,70	6,66E-04	
TADA1	transcriptional adaptor 1	30631	225455_at	0,31	-1,69	2,00E-06	
TNFSF10	TNF superfamily member 10	11925	202687_s_at	0,31	-1,69	4,63E-05	
NADK2	NAD kinase 2, mitochondrial	26404	226946_at	0,31	-1,69	1,70E-04	
AGL	amylo-alpha-1, 6-glucosidase, 4-alpha-glucanotransferase	321	203566_s_at	0,31	-1,69	8,90E-04	I
IDH1	isocitrate dehydrogenase (NADP(+)) 1, cytosolic	5382	1555037_a_at	0,31	-1,68	7,76E-04	L/I
PCK2	phosphoenolpyruvate carboxykinase 2, mitochondrial	8725	202847_at	0,32	-1,66	1,14E-03	
HPGD	15-hydroxyprostaglandin dehydrogenase	5154	203914_x_at	0,32	-1,66	2,60E-03	
GPAM	glycerol-3-phosphate acyltransferase, mitochondrial	24865	225424_at	0,32	-1,63	4,43E-02	L
HNMT	histamine N-methyltransferase	5028	204112_s_at	0,33	-1,61	4,31E-04	A
ACBD5	acyl-CoA binding domain containing 5	23338	225663_at	0,33	-1,60	1,01E-03	L
LRRC40	leucine rich repeat containing 40	26004	218577_at	0,33	-1,59	1,46E-04	
ALDH5A1	aldehyde dehydrogenase 5 family member A1	408	203608_at	0,33	-1,59	3,97E-03	
PON1	paraoxonase 1	9204	206345_s_at	0,33	-1,58	8,05E-04	L
RNF128	ring finger protein 128, E3 ubiquitin protein ligase	21153	219263_at	0,33	-1,58	3,63E-03	
SDC2	syndecan 2	10659	212154_at	0,34	-1,57	4,91E-04	
GLS2	glutaminase 2	29570	1564706_s_at	0,34	-1,57	5,29E-04	A
IGFBP3	insulin like growth factor binding protein 3	5472	212143_s_at	0,34	-1,57	1,31E-02	
ART4	ADP-ribosyltransferase 4 (Dombrock blood group)	726	242496_at	0,34	-1,56	5,40E-06	

Gene symbol	HGNC gene name	HGNC ID	Affymetrix probe ID	FC	log_2FC	FDR	P
CRYZ	crystallin zeta	2419	202950_at	0,34	-1,56	1,48E-04	
SLCO1B3	solute carrier organic anion transporter family member 1B3	10961	206354_at	0,34	-1,56	3,61E-03	L
CXCL12	C-X-C motif chemokine ligand 12	10672	209687_at	0,34	-1,54	1,54E-02	
FAM162A	family with sequence similarity 162 member A	17865	223193_x_at	0,35	-1,52	7,85E-04	
RTN4	reticulon 4	14085	211509_s_at	0,35	-1,51	6,93E-03	
TMEM27	collectrin, amino acid transport regulator	29437	223784_at	0,35	-1,50	2,95E-05	
POSTN	periostin	16953	210809_s_at	0,35	-1,50	8,39E-04	
CA2	carbonic anhydrase 2	1373	209301_at	0,35	-1,50	1,60E-03	
DHTKD1	dehydrogenase E1 and transketolase domain containing 1	23537	227094_at	0,35	-1,50	7,08E-03	A
SERPINC1	serpin family C member 1	775	210049_at	0,35	-1,50	9,41E-03	
HHEX	hematopoietically expressed homeobox	4901	215933_s_at	0,36	-1,49	2,17E-04	
GHR	growth hormone receptor	4263	205498_at	0,36	-1,49	2,16E-02	
GATM	glycine amidinotransferase	4175	216733_s_at	0,36	-1,48	2,71E-03	A
RTN4	reticulon 4	14085	210968_s_at	0,36	-1,47	7,05E-03	
KNG1	kininogen 1	6383	206054_at	0,36	-1,46	6,31E-03	
SULT1E1	sulfotransferase family 1E member 1	11377	222940_at	0,37	-1,45	6,17E-05	B
MME	membrane metalloendopeptidase	7154	203434_s_at	0,37	-1,42	5,57E-05	I
HIBADH	3-hydroxyisobutyrate dehydrogenase	4907	224812_at	0,37	-1,42	7,50E-04	A
ANK3	ankyrin 3	494	206385_s_at	0,37	-1,42	3,20E-03	
HPR	haptoglobin-related protein	5156	208471_at	0,37	-1,42	7,02E-03	
SMARCA1	SWI/SNF related, matrix associated, actin dependent regulator of chromatin, subfamily a, member 1	11097	203874_s_at	0,38	-1,41	3,22E-05	
UFL1	UFM1 specific ligase 1	23039	212633_at	0,38	-1,40	4,09E-04	
SLC22A7	solute carrier family 22 member 7	10971	231398_at	0,38	-1,39	2,50E-02	
ELOVL2	ELOVL fatty acid elongase 2	14416	213712_at	0,38	-1,38	2,28E-04	L
UGT2B15	UDP glucuronosyltransferase family 2 member B15	12546	207392_x_at	0,38	-1,38	4,36E-03	B
KLHDC10	kelch domain containing 10	22194	210111_s_at	0,38	-1,38	6,75E-03	
PRKAB2	protein kinase AMP-activated non-catalytic subunit beta 2	9379	225278_at	0,39	-1,37	1,27E-02	L
PGRMC1	progesterone receptor membrane component 1	16090	201120_s_at	0,39	-1,36	1,23E-03	I
UGT2B28	UDP glucuronosyltransferase family 2 member B28	13479	211682_x_at	0,39	-1,36	4,00E-03	
GLUD1	glutamate dehydrogenase 1	4335	215794_x_at	0,39	-1,35	5,12E-04	A
SLCO1B1	solute carrier organic anion transporter family member 1B1	10959	210366_at	0,39	-1,35	2,26E-03	L
ABCG5	ATP binding cassette subfamily G member 5	13886	220383_at	0,40	-1,34	1,21E-03	L
KNG1	kininogen 1	6383	217512_at	0,40	-1,34	1,84E-03	
AADAC	arylacetamide deacetylase	17	205969_at	0,40	-1,34	3,23E-03	B
CYP51A1	cytochrome P450 family 51 subfamily A member 1	2649	202314_at	0,40	-1,34	8,04E-03	
CMBL	carboxymethylenebutenolidase homolog	25090	227522_at	0,40	-1,34	1,66E-02	B
AKAP9	A-kinase anchoring protein 9	379	210962_s_at	0,40	-1,33	8,49E-04	
HMGB1	high mobility group box 1	4983	224731_at	0,40	-1,32	7,39E-04	I
GOLIM4	golgi integral membrane protein 4	15448	238002_at	0,40	-1,32	1,16E-03	
CXCL2	C-X-C motif chemokine ligand 2	4603	209774_x_at	0,40	-1,31	3,39E-02	
SNX4	sorting nexin 4	11175	212652_s_at	0,41	-1,30	1,73E-04	

Gene symbol	HGNC gene name	HGNC ID	Affymetrix probe ID	FC	log_2FC	FDR	P
SLC35A3	solute carrier family 35 member A3	11023	226894_at	0,41	-1,30	4,48E-04	
ACOT13	acyl-CoA thioesterase 13	20999	204565_at	0,41	-1,30	1,01E-03	L
C6	complement C6	1339	210168_at	0,41	-1,30	3,23E-03	
AMACR	alpha-methylacyl-CoA racemase	451	209425_at	0,41	-1,30	3,57E-03	L
DECR1	2,4-dienoyl-CoA reductase 1	2753	202447_at	0,41	-1,30	3,63E-03	L
CYP3A5	cytochrome P450 family 3 subfamily A member 5	2638	205765_at	0,41	-1,30	2,17E-02	B
NUDT7	nudix hydrolase 7	8054	228855_at	0,41	-1,29	2,17E-04	L
C1RL	complement C1r subcomponent like	21265	218983_at	0,41	-1,29	1,48E-03	
ACSM2A	acyl-CoA synthetase medium chain family member 2A	32017	214069_at	0,41	-1,29	2,66E-03	
NR2F2	nuclear receptor subfamily 2 group F member 2	7976	209120_at	0,41	-1,29	3,73E-03	
HFE2	hemojuvelin BMP co-receptor	4887	228621_at	0,41	-1,28	5,45E-04	
CRLS1	cardiolipin synthase 1	16148	223978_s_at	0,41	-1,28	6,07E-04	L
PANK3	pantothenate kinase 3	19365	221751_at	0,41	-1,28	6,90E-03	
LGR4	leucine rich repeat containing G protein-coupled receptor 4	13299	218326_s_at	0,41	-1,27	1,18E-04	
APOM	apolipoprotein M	13916	214910_s_at	0,41	-1,27	2,23E-03	
ETFA	electron transfer flavoprotein subunit alpha	3481	201931_at	0,41	-1,27	3,08E-03	R
UBR3	ubiquitin protein ligase E3 component n-recognin 3	30467	230029_x_at	0,42	-1,26	9,60E-04	
LRP6	LDL receptor related protein 6	6698	225745_at	0,42	-1,26	1,90E-03	
FN1	fibronectin 1	3778	216442_x_at	0,42	-1,26	9,25E-03	
TSPAN12	tetraspanin 12	21641	219274_at	0,42	-1,25	2,47E-05	
ANO6	anoctamin 6	25240	224906_at	0,42	-1,25	1,64E-04	I
KAT2B	lysine acetyltransferase 2B	8638	203845_at	0,42	-1,25	5,65E-04	
ACSS3	acyl-CoA synthetase short chain family member 3	24723	229222_at	0,42	-1,25	8,16E-04	L
PSMA2	proteasome subunit alpha 2	9531	201317_s_at	0,42	-1,25	3,48E-03	A/I
FN1	fibronectin 1	3778	210495_x_at	0,42	-1,25	9,32E-03	
PPP3CA	protein phosphatase 3 catalytic subunit alpha	9314	202429_s_at	0,42	-1,24	2,86E-04	
TBC1D9	TBC1 domain family member 9	21710	212956_at	0,42	-1,24	4,56E-04	
CPEB2	cytoplasmic polyadenylation element binding protein 2	21745	226939_at	0,42	-1,24	3,92E-03	
FN1	fibronectin 1	3778	212464_s_at	0,42	-1,24	1,32E-02	
SOD1	superoxide dismutase 1	11179	200642_at	0,42	-1,24	1,41E-02	
FBXL5	F-box and leucine rich repeat protein 5	13602	209004_s_at	0,43	-1,23	3,20E-03	
HRG	histidine rich glycoprotein	5181	206226_at	0,43	-1,23	6,66E-03	
HMGCS2	3-hydroxy-3-methylglutaryl-CoA synthase 2	5008	204607_at	0,43	-1,23	1,34E-02	L
HLTF	helicase like transcription factor	11099	202983_at	0,43	-1,22	1,46E-04	
NAT8	N-acetyltransferase 8 (putative)	18069	210289_at	0,43	-1,22	5,29E-04	
ARHGAP29	Rho GTPase activating protein 29	30207	203910_at	0,43	-1,22	3,40E-03	
PRDX5	peroxiredoxin 5	9355	1560587_s_at	0,43	-1,21	2,83E-03	
LYPLA1	lysophospholipase I	6737	212449_s_at	0,43	-1,21	3,14E-03	
CFHR2	complement factor H related 2	4890	206910_x_at	0,43	-1,21	1,58E-02	
AHSG	alpha 2-HS glycoprotein	349	204551_s_at	0,43	-1,21	1,90E-02	I
PAWR	pro-apoptotic WT1 regulator	8614	226223_at	0,44	-1,20	2,86E-04	

Gene symbol	HGNC gene name	HGNC ID	Affymetrix probe ID	FC	log_2FC	FDR	P
TDO2	tryptophan 2,3-dioxygenase	11708	205943_at	0,44	-1,20	1,48E-02	A
LRPPRC	leucine rich pentatricopeptide repeat containing	15714	211971_s_at	0,44	-1,19	9,59E-04	R
IMPA1	inositol monophosphatase 1	6050	203011_at	0,44	-1,19	1,27E-03	
CYP51A1	cytochrome P450 family 51 subfamily A member 1	2649	216607_s_at	0,44	-1,19	1,40E-03	
ESD	esterase D	3465	215096_s_at	0,44	-1,19	3,92E-03	B
RALGPS2	Ral GEF with PH domain and SH3 binding motif 2	30279	227533_at	0,44	-1,18	3,03E-04	
ABCG2	ATP binding cassette subfamily G member 2 (Junior blood group)	74	209735_at	0,44	-1,18	7,50E-04	
SCOC	short coiled-coil protein	20335	224786_at	0,44	-1,18	1,01E-03	
TMEM106B	transmembrane protein 106B	22407	226529_at	0,44	-1,18	1,40E-03	
MAOB	monoamine oxidase B	6834	204041_at	0,44	-1,18	1,42E-03	B
APOB	apolipoprotein B	603	223579_s_at	0,44	-1,18	5,47E-03	L
MTHFD1	methylenetetrahydrofolate dehydrogenase, cyclohydrolase and formyltetrahydrofolate synthetase 1	7432	202309_at	0,44	-1,17	3,08E-03	
GBE1	1,4-alpha-glucan branching enzyme 1	4180	203282_at	0,44	-1,17	1,29E-02	
COPS5	COP9 signalosome subunit 5	2240	201652_at	0,45	-1,16	2,98E-04	
FMO5	flavin containing monooxygenase 5	3773	205776_at	0,45	-1,16	1,30E-03	
EPHX2	epoxide hydrolase 2	3402	209368_at	0,45	-1,16	1,90E-03	L
C3	complement C3	1318	217767_at	0,45	-1,16	1,25E-02	I
APOA2	apolipoprotein A2	601	219465_at	0,45	-1,16	2,40E-02	L
PYGL	glycogen phosphorylase L	9725	202990_at	0,45	-1,15	1,70E-04	I
RGN	regucalcin	9989	210751_s_at	0,45	-1,15	3,22E-04	
METAP2	methionyl aminopeptidase 2	16672	209861_s_at	0,45	-1,15	5,33E-04	
HAO1	hydroxyacid oxidase 1	4809	220224_at	0,45	-1,15	1,90E-03	A
APOM	apolipoprotein M	13916	205682_x_at	0,45	-1,15	3,24E-03	
CMTM6	CKLF like MARVEL transmembrane domain containing 6	19177	223047_at	0,45	-1,15	1,02E-02	I
HACL1	2-hydroxyacyl-CoA lyase 1	17856	223211_at	0,45	-1,14	5,68E-05	L
SMG1	SMG1, nonsense mediated mRNA decay associated PI3K related kinase	30045	224842_at	0,45	-1,14	1,04E-03	
OSBPL9	oxysterol binding protein like 9	16386	218047_at	0,45	-1,14	2,20E-03	L
EID1	EP300 interacting inhibitor of differentiation 1	1191	208669_s_at	0,45	-1,14	3,61E-03	
GNMT	glycine N-methyltransferase	4415	210328_at	0,45	-1,14	3,07E-02	A
TMEM19	transmembrane protein 19	25605	226860_at	0,46	-1,13	1,15E-03	
UPB1	beta-ureidopropionase 1	16297	224043_s_at	0,46	-1,13	2,28E-03	
BAAT	bile acid-CoA:amino acid N-acyltransferase	932	206913_at	0,46	-1,13	6,27E-03	L
GCSH	glycine cleavage system protein H	4208	213129_s_at	0,46	-1,13	8,48E-03	A
RBL2	RB transcriptional corepressor like 2	9894	212331_at	0,46	-1,12	1,46E-04	
PDE8A	phosphodiesterase 8A	8793	212522_at	0,46	-1,12	6,07E-04	
ENOSF1	enolase superfamily member 1	30365	204143_s_at	0,46	-1,12	1,68E-03	
PSMG2	proteasome assembly chaperone 2	24929	218467_at	0,46	-1,12	2,09E-03	
CPB2	carboxypeptidase B2	2300	206651_s_at	0,46	-1,12	1,25E-02	
FDPS	farnesyl diphosphate synthase	3631	201275_at	0,46	-1,12	1,54E-02	L
FMC1	formation of mitochondrial complex V assembly factor 1 homolog	26946	226780_s_at	0,46	-1,11	8,52E-04	

Gene symbol	HGNC gene name	HGNC ID	Affymetrix probe ID	FC	log_2FC	FDR	P
SMIM15	small integral membrane protein 15	33861	224740_at	0,46	-1,11	4,28E-03	
ABCB4	ATP binding cassette subfamily B member 4	45	207819_s_at	0,46	-1,11	5,88E-03	L
OCIAD1	OCIA domain containing 1	16074	223011_s_at	0,46	-1,11	7,10E-03	
RBP4	retinol binding protein 4	9922	219140_s_at	0,46	-1,11	4,00E-02	
RABGAP1L	RAB GTPase activating protein 1 like	24663	203020_at	0,47	-1,10	5,68E-05	
BAG4	BCL2 associated athanogene 4	940	228189_at	0,47	-1,10	2,77E-03	
CREG1	cellular repressor of E1A stimulated genes 1	2351	201200_at	0,47	-1,10	4,15E-03	I
TM4SF4	transmembrane 4 L six family member 4	11856	209937_at	0,47	-1,10	7,45E-03	
HSD17B11	hydroxysteroid 17-beta dehydrogenase 11	22960	217989_at	0,47	-1,10	9,26E-03	L
TMEM64	transmembrane protein 64	25441	225974_at	0,47	-1,09	1,83E-03	
ABCC2	ATP binding cassette subfamily C member 2	53	206155_at	0,47	-1,09	2,03E-03	
SMLR1	small leucine rich protein 1	44670	230716_at	0,47	-1,09	3,43E-03	
FAM96A	cytosolic iron-sulfur assembly component 2A	26235	224779_s_at	0,47	-1,09	7,16E-03	
MSRB2	methionine sulfoxide reductase B2	17061	218773_s_at	0,47	-1,09	1,17E-02	
CFHR5	complement factor H related 5	24668	208088_s_at	0,47	-1,09	1,21E-02	
SRD5A2	steroid 5 alpha-reductase 2	11285	235945_at	0,47	-1,08	6,80E-04	L
ENPEP	glutamyl aminopeptidase	3355	204844_at	0,47	-1,08	7,95E-04	
VPS13C	vacuolar protein sorting 13 homolog C	23594	218396_at	0,47	-1,08	1,09E-03	
PCMTD1	protein-L-isoaspartate (D-aspartate) O-methyltransferase domain containing 1	30483	226119_at	0,47	-1,08	1,60E-03	
TMEM14C	transmembrane protein 14C	20952	223106_at	0,47	-1,08	1,83E-03	
TSPYL1	TSPY like 1	12382	221493_at	0,47	-1,08	3,39E-03	
HGD	homogentisate 1,2-dioxygenase	4892	205221_at	0,47	-1,08	1,21E-02	A
ADI1	acireductone dioxygenase 1	30576	217761_at	0,47	-1,08	1,21E-02	A
GNE	glucosamine (UDP-N-acetyl)-2-epimerase/N-acetylmannosamine kinase	23657	205042_at	0,47	-1,08	2,49E-02	
SKP2	S-phase kinase associated protein 2	10901	203625_x_at	0,48	-1,07	4,80E-04	
AGTR1	angiotensin II receptor type 1	336	208016_s_at	0,48	-1,07	7,50E-04	
ARSE	arylsulfatase E	719	205894_at	0,48	-1,07	1,80E-03	L
RMDN1	regulator of microtubule dynamics 1	24285	218549_s_at	0,48	-1,07	2,13E-03	
CHN2	chimerin 2	1944	213385_at	0,48	-1,07	2,88E-03	
RHEB	Ras homolog, mTORC1 binding	10011	213404_s_at	0,48	-1,07	3,49E-03	
SSBP1	single stranded DNA binding protein 1	11317	202591_s_at	0,48	-1,07	1,27E-02	
CFB	complement factor B	1037	202357_s_at	0,48	-1,07	3,66E-02	
AMACR	alpha-methylacyl-CoA racemase	451	209426_s_at	0,48	-1,06	9,00E-04	
FAM35A	shieldin complex subunit 2	28773	220547_s_at	0,48	-1,06	4,41E-03	
TMEM97	transmembrane protein 97	28106	212282_at	0,48	-1,06	1,64E-02	
SUB1	SUB1 homolog, transcriptional regulator	19985	224587_at	0,48	-1,05	4,56E-04	
REEP5	receptor accessory protein 5	30077	208873_s_at	0,48	-1,05	2,01E-03	
WASHC4	WASH complex subunit 4	29174	212795_at	0,48	-1,05	2,61E-03	
HHIP	hedgehog interacting protein	14866	230135_at	0,48	-1,05	3,29E-03	
SLC35D1	solute carrier family 35 member D1	20800	209712_at	0,48	-1,05	2,60E-02	B
SLC3A1	solute carrier family 3 member 1	11025	205799_s_at	0,48	-1,05	2,63E-02	

Gene symbol	HGNC gene name	HGNC ID	Affymetrix probe ID	FC	log_2FC	FDR	P
SLC35B3	solute carrier family 35 member B3	21601	222691_at	0,49	-1,04	3,30E-04	B
SPG11	SPG11, spatacsin vesicle trafficking associated	11226	203513_at	0,49	-1,04	1,60E-03	
TMEM30A	transmembrane protein 30A	16667	217743_s_at	0,49	-1,04	2,04E-03	I
LSM5	LSM5 homolog, U6 small nuclear RNA and mRNA degradation associated	17162	211747_s_at	0,49	-1,04	2,65E-03	
PIK3R4	phosphoinositide-3-kinase regulatory subunit 4	8982	212740_at	0,49	-1,04	2,72E-03	L
CYP2D6	cytochrome P450 family 2 subfamily D member 6	2625	207498_s_at	0,49	-1,04	1,15E-02	
NDUFB4	NADH:ubiquinone oxidoreductase subunit B4	7699	218226_s_at	0,49	-1,04	1,19E-02	R
ALDH2	aldehyde dehydrogenase 2 family member	404	201425_at	0,49	-1,04	1,35E-02	B
CP	ceruloplasmin	2295	204846_at	0,49	-1,04	3,75E-02	
NT5DC1	5'-nucleotidase domain containing 1	21556	223177_at	0,49	-1,03	5,68E-05	
BDH1	3-hydroxybutyrate dehydrogenase 1	1027	211715_s_at	0,49	-1,03	2,83E-03	L
PSMD6	proteasome 26S subunit, non-ATPase 6	9564	202753_at	0,49	-1,03	1,01E-02	A/I
ARL6IP1	ADP ribosylation factor like GTPase 6 interacting protein 1	697	211935_at	0,49	-1,03	1,48E-02	
PLS3	plastin 3	9091	201215_at	0,49	-1,03	2,91E-02	
RTN4	reticulon 4	14085	214629_x_at	0,49	-1,03	3,06E-02	
GLOD4	glyoxalase domain containing 4	14111	209092_s_at	0,49	-1,02	1,42E-03	
PLEKHA5	pleckstrin homology domain containing A5	30036	220952_s_at	0,49	-1,02	3,04E-03	L
ALG5	ALG5, dolichyl-phosphate beta-glucosyltransferase	20266	218203_at	0,49	-1,02	4,37E-03	
SEC63	SEC63 homolog, protein translocation regulator	21082	201916_s_at	0,49	-1,02	6,95E-03	
SF3B1	splicing factor 3b subunit 1	10768	211185_s_at	0,49	-1,02	1,24E-02	
UGT1A5	UDP glucuronosyltransferase family 1 member A5	12537	208596_s_at	0,49	-1,02	3,54E-02	
CDH1	cadherin 1	1748	201131_s_at	0,49	-1,02	4,87E-02	
ZMYM4	zinc finger MYM-type containing 4	13055	202051_s_at	0,50	-1,01	7,10E-06	
CPNE3	copine 3	2316	202118_s_at	0,50	-1,01	5,18E-04	L/I
MARCH6	membrane associated ring-CH-type finger 6	30550	212498_at	0,50	-1,01	1,57E-03	
CHP1	calcineurin like EF-hand protein 1	17433	214665_s_at	0,50	-1,01	8,41E-03	
ANAPC16	anaphase promoting complex subunit 16	26976	229145_at	0,50	-1,01	1,39E-02	
ATP5G3	ATP synthase membrane subunit c locus 3	843	207507_s_at	0,50	-1,01	1,66E-02	R
N4BP2L2	NEDD4 binding protein 2 like 2	26916	202258_s_at	0,50	-1,00	9,60E-04	
ATXN10	ataxin 10	10549	208833_s_at	0,50	-1,00	1,09E-03	
PCBD1	pterin-4 alpha-carbinolamine dehydratase 1	8646	203557_s_at	0,50	-1,00	4,98E-03	A
TMEM14B	transmembrane protein 14B	21384	221452_s_at	0,50	-1,00	5,53E-03	
SLTM	SAFB like transcription modulator	20709	217828_at	0,50	-1,00	7,33E-03	
ABCB4	ATP binding cassette subfamily B member 4	45	209994_s_at	0,50	-1,00	1,71E-02	
ABCC6	ATP binding cassette subfamily C member 6	57	214033_at	0,50	-0,99	3,78E-04	
SLC25A5	solute carrier family 25 member 5	10991	200657_at	0,50	-0,99	7,55E-03	
ATP5F1	ATP synthase peripheral stalk-membrane subunit b	840	211755_s_at	0,50	-0,99	8,41E-03	R
CD302	CD302 molecule	30843	203799_at	0,50	-0,99	1,22E-02	
SDHB	succinate dehydrogenase complex iron sulfur subunit B	10681	202675_at	0,50	-0,99	1,76E-02	R
TMX4	thioredoxin related transmembrane protein 4	25237	201581_at	0,51	-0,98	3,29E-03	
ATP5O	ATP synthase peripheral stalk subunit OSCP	850	200818_at	0,51	-0,98	9,93E-03	R

Gene symbol	HGNC gene name	HGNC ID	Affymetrix probe ID	FC	log_2FC	FDR	P
KLKB1	kallikrein B1	6371	206541_at	0,51	-0,98	1,58E-02	
ACSS2	acyl-CoA synthetase short chain family member 2	15814	234312_s_at	0,51	-0,98	3,25E-02	B
SLC2A13	solute carrier family 2 member 13	15956	227176_at	0,51	-0,97	1,97E-04	
ZNF638	zinc finger protein 638	17894	211257_x_at	0,51	-0,97	2,20E-03	
ITGA1	integrin subunit alpha 1	6134	226731_at	0,51	-0,97	3,53E-03	
HP1BP3	heterochromatin protein 1 binding protein 3	24973	224591_at	0,51	-0,97	5,46E-03	
RAB18	RAB18, member RAS oncogene family	14244	224787_s_at	0,51	-0,97	5,51E-03	I
SIGIRR	single Ig and TIR domain containing	30575	52940_at	0,51	-0,97	1,14E-02	
WRB	tryptophan rich basic protein	12790	202749_at	0,51	-0,96	2,83E-04	
VPS4B	vacuolar protein sorting 4 homolog B	10895	218171_at	0,51	-0,96	7,85E-04	
EMC4	ER membrane protein complex subunit 4	28032	223043_at	0,51	-0,96	3,68E-03	
GDA	guanine deaminase	4212	224209_s_at	0,51	-0,96	7,62E-03	
MFAP3L	microfibril associated protein 3 like	29083	205442_at	0,51	-0,96	1,36E-02	
PANK1	pantothenate kinase 1	8598	226649_at	0,51	-0,96	4,36E-02	
CLCN3	chloride voltage-gated channel 3	2021	201734_at	0,52	-0,95	4,23E-04	
THOC7	THO complex 7	29874	218334_at	0,52	-0,95	1,09E-03	
COL1A2	collagen type I alpha 2 chain	2198	202403_s_at	0,52	-0,95	5,06E-03	
TCEA1	transcription elongation factor A1	11612	216241_s_at	0,52	-0,95	5,35E-03	
SORD	sorbitol dehydrogenase	11184	201562_s_at	0,52	-0,95	5,93E-03	
PTPRK	protein tyrosine phosphatase, receptor type K	9674	203038_at	0,52	-0,95	3,41E-02	
CAAP1	caspase activity and apoptosis inhibitor 1	25834	219276_x_at	0,52	-0,94	2,15E-04	
USP9X	ubiquitin specific peptidase 9 X-linked	12632	201099_at	0,52	-0,94	1,76E-03	
UBE2E1	ubiquitin conjugating enzyme E2 E1	12477	212519_at	0,52	-0,94	1,92E-03	
CYP2J2	cytochrome P450 family 2 subfamily J member 2	2634	205073_at	0,52	-0,94	2,03E-03	B/L
PEX13	peroxisomal biogenesis factor 13	8855	235093_at	0,52	-0,94	2,58E-03	
SS18L1	SS18L1, nBAF chromatin remodeling complex subunit	15592	213140_s_at	0,52	-0,94	8,02E-03	
PCSK6	proprotein convertase subtilisin/kexin type 6	8569	207414_s_at	0,52	-0,94	1,20E-02	L
NT5E	5'-nucleotidase ecto	8021	203939_at	0,52	-0,93	3,97E-04	
CGGBP1	CGG triplet repeat binding protein 1	1888	224599_at	0,52	-0,93	1,04E-03	
NR1I3	nuclear receptor subfamily 1 group I member 3	7969	207007_at	0,52	-0,93	1,37E-03	
MBTPS2	membrane bound transcription factor peptidase, site 2	15455	226760_at	0,52	-0,93	4,73E-03	L
SEC31A	SEC31 homolog A, COPII coat complex component	17052	200945_s_at	0,52	-0,93	2,42E-02	
TMEM176B	transmembrane protein 176B	29596	220532_s_at	0,52	-0,93	4,53E-02	
IFIT1	interferon induced protein with tetratricopeptide repeats 1	5407	203153_at	0,53	-0,92	1,08E-03	
RALGPS2	Ral GEF with PH domain and SH3 binding motif 2	30279	227224_at	0,53	-0,92	1,12E-03	
ATP5J2	ATP synthase membrane subunit f	848	202961_s_at	0,53	-0,92	9,52E-03	R
LIPA	lipase A, lysosomal acid type	6617	201847_at	0,53	-0,92	1,60E-02	L
FAM120A	family with sequence similarity 120A	13247	200774_at	0,53	-0,92	3,60E-02	
DCUN1D1	defective in cullin neddylation 1 domain containing 1	18184	218583_s_at	0,53	-0,91	2,06E-04	
MYH10	myosin heavy chain 10	7568	212372_at	0,53	-0,91	1,27E-03	
SERBP1	SERPINE1 mRNA binding protein 1	17860	217724_at	0,53	-0,91	2,08E-03	

Gene symbol	HGNC gene name	HGNC ID	Affymetrix probe ID	FC	log_2FC	FDR	P
MEST	mesoderm specific transcript	7028	202016_at	0,53	-0,91	3,15E-03	
DEK	DEK proto-oncogene	2768	200934_at	0,53	-0,91	3,65E-03	
GGCX	gamma-glutamyl carboxylase	4247	205351_at	0,53	-0,91	3,84E-03	
NDUFB3	NADH:ubiquinone oxidoreductase subunit B3	7698	203371_s_at	0,53	-0,91	4,64E-03	R
CRLS1	cardiolipin synthase 1	16148	225324_at	0,53	-0,91	5,60E-03	
ALDH9A1	aldehyde dehydrogenase 9 family member A1	412	201612_at	0,53	-0,91	6,38E-03	A
RNF144B	ring finger protein 144B	21578	228153_at	0,53	-0,91	6,61E-03	
NMD3	NMD3 ribosome export adaptor	24250	231870_s_at	0,53	-0,91	1,18E-02	
CD164	CD164 molecule	1632	208405_s_at	0,53	-0,91	1,49E-02	
MAOA	monoamine oxidase A	6833	212741_at	0,53	-0,91	1,74E-02	B
SPP2	secreted phosphoprotein 2	11256	214478_at	0,53	-0,91	1,83E-02	
GHITM	growth hormone inducible transmembrane protein	17281	209248_at	0,53	-0,91	1,93E-02	
MALSU1	mitochondrial assembly of ribosomal large subunit 1	21721	226385_s_at	0,53	-0,91	3,38E-02	
AIFM1	apoptosis inducing factor mitochondria associated 1	8768	205512_s_at	0,54	-0,90	6,52E-04	
ZNF644	zinc finger protein 644	29222	222580_at	0,54	-0,90	2,87E-03	
LIFR	LIF receptor alpha	6597	225575_at	0,54	-0,90	7,89E-03	
CDKN1B	cyclin dependent kinase inhibitor 1B	1785	209112_at	0,54	-0,90	8,48E-03	
ATP5G3	ATP synthase membrane subunit c locus 3	843	207508_at	0,54	-0,90	1,29E-02	
MBNL1	muscleblind like splicing regulator 1	6923	201153_s_at	0,54	-0,90	1,36E-02	
TXNL1	thioredoxin like 1	12436	201588_at	0,54	-0,90	1,94E-02	
RNF5	ring finger protein 5	10068	209111_at	0,54	-0,89	4,21E-04	
RBBP7	RB binding protein 7, chromatin remodeling factor	9890	201092_at	0,54	-0,89	9,60E-04	
ACO1	aconitase 1	117	207071_s_at	0,54	-0,89	1,41E-03	
CTSO	cathepsin O	2542	203758_at	0,54	-0,89	2,49E-03	
KDELR2	KDEL endoplasmic reticulum protein retention receptor 2	6305	200698_at	0,54	-0,89	1,54E-02	
TJP1	tight junction protein 1	11827	202011_at	0,54	-0,89	2,01E-02	
NCOA4	nuclear receptor coactivator 4	7671	210774_s_at	0,54	-0,89	2,23E-02	
ANPEP	alanyl aminopeptidase, membrane	500	202888_s_at	0,54	-0,89	4,50E-02	I
MME	membrane metalloendopeptidase	7154	203435_s_at	0,54	-0,88	2,47E-04	
FUCA1	alpha-L-fucosidase 1	4006	202838_at	0,54	-0,88	9,59E-04	I
CAMTA1	calmodulin binding transcription activator 1	18806	225693_s_at	0,54	-0,88	1,30E-03	
SLC39A6	solute carrier family 39 member 6	18607	202088_at	0,54	-0,88	1,37E-03	
NUDT5	nudix hydrolase 5	8052	223100_s_at	0,54	-0,88	3,25E-03	
NDUFAF1	NADH:ubiquinone oxidoreductase complex assembly factor 1	18828	204125_at	0,54	-0,88	3,36E-03	R
YME1L1	YME1 like 1 ATPase	12843	201352_at	0,54	-0,88	4,31E-03	
PDGFC	platelet derived growth factor C	8801	218718_at	0,54	-0,88	5,22E-03	
HOOK1	hook microtubule tethering protein 1	19884	225792_at	0,54	-0,88	5,36E-03	
NFIA	nuclear factor I A	7784	224976_at	0,54	-0,88	7,34E-03	
EIF2AK1	eukaryotic translation initiation factor 2 alpha kinase 1	24921	217736_s_at	0,54	-0,88	8,67E-03	
TUBB	tubulin beta class I	20778	211714_x_at	0,54	-0,88	1,23E-02	I
DNAJC15	DnaJ heat shock protein family (Hsp40) member C15	20325	218435_at	0,54	-0,88	1,79E-02	

Gene symbol	HGNC gene name	HGNC ID	Affymetrix probe ID	FC	log_2FC	FDR	P
PGM1	phosphoglucomutase 1	8905	201968_s_at	0,54	-0,88	1,86E-02	I
TGOLN2	trans-golgi network protein 2	15450	212043_at	0,54	-0,88	3,98E-02	
DIAPH2	diaphanous related formin 2	2877	205726_at	0,55	-0,87	9,46E-04	
EPB41L5	erythrocyte membrane protein band 4.1 like 5	19819	229292_at	0,55	-0,87	1,82E-03	
PDCD10	programmed cell death 10	8761	210907_s_at	0,55	-0,87	2,04E-03	
MTIF2	mitochondrial translational initiation factor 2	7441	203095_at	0,55	-0,87	2,70E-03	
HDHD2	haloacid dehalogenase like hydrolase domain containing 2	25364	223155_at	0,55	-0,87	2,88E-03	
MOCS2	molybdenum cofactor synthesis 2	7193	218212_s_at	0,55	-0,87	3,22E-03	
ZMPSTE24	zinc metallopeptidase STE24	12877	202939_at	0,55	-0,87	8,43E-03	
ATL2	atlastin GTPase 2	24047	222700_at	0,55	-0,87	9,93E-03	
KARS	lysyl-tRNA synthetase	6215	200840_at	0,55	-0,87	2,03E-02	A
TIMM23	translocase of inner mitochondrial membrane 23	17312	225535_s_at	0,55	-0,87	3,22E-02	
ALCAM	activated leukocyte cell adhesion molecule	400	201952_at	0,55	-0,86	9,58E-04	
MAOA	monoamine oxidase A	6833	204388_s_at	0,55	-0,86	3,96E-03	
PCGF5	polycomb group ring finger 5	28264	226326_at	0,55	-0,86	8,42E-03	
ANAPC16	anaphase promoting complex subunit 16	26976	224664_at	0,55	-0,86	9,16E-03	
MAP2K1	mitogen-activated protein kinase kinase 1	6840	202670_at	0,55	-0,86	1,13E-02	
ZC3H15	zinc finger CCCH-type containing 15	29528	201595_s_at	0,55	-0,86	1,62E-02	
SUN1	Sad1 and UNC84 domain containing 1	18587	212074_at	0,55	-0,86	1,63E-02	
MCCC1	methylcrotonoyl-CoA carboxylase 1	6936	218440_at	0,55	-0,85	4,47E-04	A
CREBL2	cAMP responsive element binding protein like 2	2350	201989_s_at	0,55	-0,85	4,61E-04	
MRPL15	mitochondrial ribosomal protein L15	14054	218027_at	0,55	-0,85	4,31E-03	
VPS29	VPS29, retromer complex component	14340	223026_s_at	0,55	-0,85	1,21E-02	
SLC4A4	solute carrier family 4 member 4	11030	203908_at	0,55	-0,85	1,33E-02	
TM9SF3	transmembrane 9 superfamily member 3	21529	222399_s_at	0,55	-0,85	1,64E-02	
YPEL5	yippee like 5	18329	222408_s_at	0,55	-0,85	1,94E-02	I
RORA	RAR related orphan receptor A	10258	226682_at	0,55	-0,85	3,46E-02	L
PIGP	phosphatidylinositol glycan anchor biosynthesis class P	3046	221689_s_at	0,56	-0,84	6,07E-04	
CYFIP1	cytoplasmic FMR1 interacting protein 1	13759	208923_at	0,56	-0,84	1,31E-03	I
NUP54	nucleoporin 54	17359	218256_s_at	0,56	-0,84	1,60E-03	
GOT2	glutamic-oxaloacetic transaminase 2	4433	200708_at	0,56	-0,84	6,19E-03	A
GALNT1	polypeptide N-acetylgalactosaminyltransferase 1	4123	201724_s_at	0,56	-0,84	6,33E-03	
RANBP9	RAN binding protein 9	13727	202582_s_at	0,56	-0,84	7,24E-03	
UBA1	ubiquitin like modifier activating enzyme 1	12469	200964_at	0,56	-0,84	8,00E-03	
NR0B2	nuclear receptor subfamily 0 group B member 2	7961	206410_at	0,56	-0,84	8,03E-03	
CLCN5	chloride voltage-gated channel 5	2023	226274_at	0,56	-0,84	1,02E-02	
SGPL1	sphingosine-1-phosphate lyase 1	10817	212322_at	0,56	-0,83	1,51E-03	L
FOPNL	FGFR1OP N-terminal like	26435	225087_at	0,56	-0,83	3,50E-03	
TTC3	tetratricopeptide repeat domain 3	12393	210645_s_at	0,56	-0,83	3,97E-03	
WNK3	WNK lysine deficient protein kinase 3	14543	236236_at	0,56	-0,83	4,42E-03	
PCM1	pericentriolar material 1	8727	202174_s_at	0,56	-0,83	5,99E-03	

Gene symbol	HGNC gene name	HGNC ID	Affymetrix probe ID	FC	log_2FC	FDR	P
PPP1CC	protein phosphatase 1 catalytic subunit gamma	9283	200726_at	0,56	-0,83	6,25E-03	L
GLMP	glycosylated lysosomal membrane protein	29436	225401_at	0,56	-0,83	6,26E-03	
COL4A3BP	collagen type IV alpha 3 binding protein	2205	226277_at	0,56	-0,83	7,14E-03	L
SNTB1	syntrophin beta 1	11168	226438_at	0,56	-0,83	1,45E-02	
C4orf3	chromosome 4 open reading frame 3	19225	224602_at	0,56	-0,83	1,61E-02	
TECR	trans-2,3-enoyl-CoA reductase	4551	208336_s_at	0,56	-0,83	1,64E-02	
CUX2	cut like homeobox 2	19347	213920_at	0,56	-0,83	2,07E-02	
DSTN	destrin, actin depolymerizing factor	15750	201021_s_at	0,56	-0,83	2,76E-02	
CCDC6	coiled-coil domain containing 6	18782	225010_at	0,57	-0,82	2,99E-03	
PSMB2	proteasome subunit beta 2	9539	200039_s_at	0,57	-0,82	7,16E-03	A
SLC22A7	solute carrier family 22 member 7	10971	220554_at	0,57	-0,82	7,89E-03	
PLSCR4	phospholipid scramblase 4	16497	218901_at	0,57	-0,82	1,29E-02	
PLPP1	phospholipid phosphatase 1	9228	210946_at	0,57	-0,82	1,41E-02	L
EMC7	ER membrane protein complex subunit 7	24301	217898_at	0,57	-0,82	1,43E-02	
MXRA5	matrix remodeling associated 5	7539	209596_at	0,57	-0,82	1,55E-02	
CLIC4	chloride intracellular channel 4	13518	201560_at	0,57	-0,82	1,58E-02	
HNRNPD	heterogeneous nuclear ribonucleoprotein D	5036	200073_s_at	0,57	-0,82	2,10E-02	
CDHR5	cadherin related family member 5	7521	220075_s_at	0,57	-0,82	3,30E-02	
RBP5	retinol binding protein 5	15847	223820_at	0,57	-0,81	6,87E-03	
STT3B	STT3B, catalytic subunit of the oligosaccharyltransferase complex	30611	224700_at	0,57	-0,81	9,25E-03	
LIN7C	lin-7 homolog C, crumbs cell polarity complex component	17789	221568_s_at	0,57	-0,81	1,14E-02	
DPM3	dolichyl-phosphate mannosyltransferase subunit 3	3007	219373_at	0,57	-0,81	1,35E-02	
NDUFS5	NADH:ubiquinone oxidoreductase subunit S5	7712	201757_at	0,57	-0,81	2,91E-02	R
YWHAE	tyrosine 3-monooxygenase/tryptophan 5-monooxygenase activation protein epsilon	12851	210996_s_at	0,57	-0,81	3,13E-02	
TMEM14B	transmembrane protein 14B	21384	223105_s_at	0,57	-0,81	3,59E-02	
ARL5A	ADP ribosylation factor like GTPase 5A	696	226617_at	0,57	-0,80	5,54E-04	
TPMT	thiopurine S-methyltransferase	12014	203672_x_at	0,57	-0,80	9,67E-04	B
PFN2	profilin 2	8882	204992_s_at	0,57	-0,80	2,91E-03	
FMO4	flavin containing monooxygenase 4	3772	206263_at	0,57	-0,80	3,32E-03	
PPP1R16A	protein phosphatase 1 regulatory subunit 16A	14941	225203_at	0,57	-0,80	1,29E-02	
GCLM	glutamate-cysteine ligase modifier subunit	4312	203925_at	0,57	-0,80	2,36E-02	B/A
EIF1B	eukaryotic translation initiation factor 1B	30792	201738_at	0,57	-0,80	2,41E-02	
TPM1	tropomyosin 1	12010	210986_s_at	0,57	-0,80	4,16E-02	
PLD1	phospholipase D1	9067	226636_at	0,58	-0,79	4,26E-04	L/I
GGCX	gamma-glutamyl carboxylase	4247	235413_at	0,58	-0,79	9,93E-04	
RNF170	ring finger protein 170	25358	226104_at	0,58	-0,79	1,31E-03	
COPS2	COP9 signalosome subunit 2	30747	202467_s_at	0,58	-0,79	1,02E-02	
RICTOR	RPTOR independent companion of MTOR complex 2	28611	226312_at	0,58	-0,79	1,21E-02	
SECISBP2L	SECIS binding protein 2 like	28997	212450_at	0,58	-0,79	1,41E-02	
TUBB	tubulin beta class I	20778	209026_x_at	0,58	-0,79	1,44E-02	
PAFAH1B1	platelet activating factor acetylhydrolase 1b regulatory subunit 1	8574	200816_s_at	0,58	-0,79	1,64E-02	

Gene symbol	HGNC gene name	HGNC ID	Affymetrix probe ID	FC	log_2FC	FDR	P
U2SURP	U2 snRNP associated SURP domain containing	30855	212058_at	0,58	-0,79	1,66E-02	
NDUFA3	NADH:ubiquinone oxidoreductase subunit A3	7686	218563_at	0,58	-0,79	2,18E-02	R
NDUFA1	NADH:ubiquinone oxidoreductase subunit A1	7683	202298_at	0,58	-0,79	2,52E-02	R
TRA2B	transformer 2 beta homolog	10781	200893_at	0,58	-0,79	3,34E-02	
MAF	MAF bZIP transcription factor	6776	209348_s_at	0,58	-0,79	3,34E-02	
H1FX	H1 histone family member X	4722	204805_s_at	0,58	-0,79	3,81E-02	
RNLS	renalase, FAD dependent amine oxidase	25641	223824_at	0,58	-0,78	7,47E-04	
ALS2	ALS2, alsin Rho guanine nucleotide exchange factor	443	226291_at	0,58	-0,78	9,58E-04	
PLA2G12B	phospholipase A2 group XIIB	18555	231009_at	0,58	-0,78	1,25E-03	
TRIM24	tripartite motif containing 24	11812	204391_x_at	0,58	-0,78	1,51E-03	
KPNA1	karyopherin subunit alpha 1	6394	202059_s_at	0,58	-0,78	3,01E-03	
HMGB1	high mobility group box 1	4983	200679_x_at	0,58	-0,78	5,44E-03	
USF3	upstream transcription factor family member 3	30494	227433_at	0,58	-0,78	6,27E-03	
MRPL32	mitochondrial ribosomal protein L32	14035	225260_s_at	0,58	-0,78	6,80E-03	
PPTC7	PTC7 protein phosphatase homolog	30695	225213_at	0,58	-0,78	1,52E-02	
SLC35E2B	solute carrier family 35 member E2B	33941	217122_s_at	0,58	-0,78	1,58E-02	
VAMP8	vesicle associated membrane protein 8	12647	202546_at	0,58	-0,78	1,72E-02	I
DST	dystonin	1090	215016_x_at	0,58	-0,78	1,80E-02	
PSMA4	proteasome subunit alpha 4	9533	203396_at	0,58	-0,78	2,70E-02	A
CHST13	carbohydrate sulfotransferase 13	21755	239647_at	0,58	-0,78	2,74E-02	
LIPG	lipase G, endothelial type	6623	219181_at	0,58	-0,78	4,11E-02	L
ACSM5	acyl-CoA synthetase medium chain family member 5	26060	89977_at	0,58	-0,78	4,36E-02	B
COLEC11	collectin subfamily member 11	17213	219873_at	0,58	-0,78	4,47E-02	
SYPL1	synaptophysin like 1	11507	201259_s_at	0,59	-0,77	7,92E-03	
ECI1	enoyl-CoA delta isomerase 1	2703	209759_s_at	0,59	-0,77	8,65E-03	L
NDUFA10	NADH:ubiquinone oxidoreductase subunit A10	7684	217860_at	0,59	-0,77	1,14E-02	R
DENR	density regulated re-initiation and release factor	2769	221509_at	0,59	-0,77	1,22E-02	
MAGED1	MAGE family member D1	6813	209014_at	0,59	-0,77	1,67E-02	
MINPP1	multiple inositol-polyphosphate phosphatase 1	7102	209585_s_at	0,59	-0,77	1,85E-02	
SUMO3	small ubiquitin-like modifier 3	11124	200740_s_at	0,59	-0,77	2,29E-02	
LCLAT1	lysocardiolipin acyltransferase 1	26756	226996_at	0,59	-0,76	2,10E-03	L
THNSL1	threonine synthase like 1	26160	222931_s_at	0,59	-0,76	2,69E-03	
ACP1	acid phosphatase 1	122	201630_s_at	0,59	-0,76	3,41E-03	
NCOR1	nuclear receptor corepressor 1	7672	200854_at	0,59	-0,76	3,82E-03	L
NCKAP1	NCK associated protein 1	7666	207738_s_at	0,59	-0,76	1,37E-02	
NOTCH2	notch 2	7882	202443_x_at	0,59	-0,76	1,71E-02	
UQCRC1	ubiquinol-cytochrome c reductase core protein 1	12585	201903_at	0,59	-0,76	2,15E-02	R
CAMK2N1	calcium/calmodulin dependent protein kinase II inhibitor 1	24190	218309_at	0,59	-0,76	2,43E-02	
COL18A1	collagen type XVIII alpha 1 chain	2195	209081_s_at	0,59	-0,76	3,59E-02	
RNF11	ring finger protein 11	10056	208924_at	0,59	-0,76	4,59E-02	
CYP3A7-CYP3A51P	CYP3A7-CYP3A51P readthrough	51504	211843_x_at	0,59	-0,76	4,88E-02	

Gene symbol	HGNC gene name	HGNC ID	Affymetrix probe ID	FC	log_2FC	FDR	P
VPS35	VPS35, retromer complex component	13487	222388_s_at	0,59	-0,75	3,48E-04	
OARD1	O-acyl-ADP-ribose deacylase 1	21257	213322_at	0,59	-0,75	4,74E-04	
SMC6	structural maintenance of chromosomes 6	20466	218781_at	0,59	-0,75	8,39E-04	
DIMT1	DIM1 dimethyladenosine transferase 1 homolog	30217	204405_x_at	0,59	-0,75	2,01E-03	
DEPTOR	DEP domain containing MTOR interacting protein	22953	218858_at	0,59	-0,75	2,03E-03	
RBKS	ribokinase	30325	57540_at	0,59	-0,75	2,30E-03	
MSRA	methionine sulfoxide reductase A	7377	219281_at	0,59	-0,75	3,01E-03	
SPG21	SPG21, maspardin	20373	217827_s_at	0,59	-0,75	4,57E-03	
C7orf55-LUC7L2	C7orf55-LUC7L2 readthrough	44671	226781_at	0,59	-0,75	9,53E-03	
USP34	ubiquitin specific peptidase 34	20066	212066_s_at	0,59	-0,75	1,32E-02	
CTSB	cathepsin B	2527	200838_at	0,59	-0,75	1,67E-02	I
MORF4L1	mortality factor 4 like 1	16989	221381_s_at	0,59	-0,75	1,95E-02	
ADAM10	ADAM metallopeptidase domain 10	188	202603_at	0,59	-0,75	2,44E-02	I
SON	SON DNA binding protein	11183	214988_s_at	0,59	-0,75	3,50E-02	
PSMD14	proteasome 26S subunit, non-ATPase 14	16889	212296_at	0,59	-0,75	3,77E-02	A/I
SLC38A3	solute carrier family 38 member 3	18044	205972_at	0,59	-0,75	4,02E-02	
OCIAD1	OCIA domain containing 1	16074	223010_s_at	0,60	-0,74	2,11E-03	
TCAIM	T cell activation inhibitor, mitochondrial	25241	1555906_s_at	0,60	-0,74	3,07E-03	
NT5C1B-RDH14	NT5C1B-RDH14 readthrough	38831	222203_s_at	0,60	-0,74	4,00E-03	
CEP57	centrosomal protein 57	30794	203494_s_at	0,60	-0,74	7,17E-03	
TMEM256	transmembrane protein 256	28618	227063_at	0,60	-0,74	7,45E-03	
MARCH6	membrane associated ring-CH-type finger 6	30550	201736_s_at	0,60	-0,74	9,35E-03	
SMDT1	single-pass membrane protein with aspartate rich tail 1	25055	225795_at	0,60	-0,74	1,42E-02	
SNAP23	synaptosome associated protein 23	11131	209130_at	0,60	-0,74	1,79E-02	I
SRP14	signal recognition particle 14	11299	200007_at	0,60	-0,74	2,25E-02	I
PPP2CA	protein phosphatase 2 catalytic subunit alpha	9299	208652_at	0,60	-0,74	2,79E-02	
UBQLN2	ubiquilin 2	12509	215884_s_at	0,60	-0,74	3,36E-02	
PRKAR2A	protein kinase cAMP-dependent type II regulatory subunit alpha	9391	225011_at	0,60	-0,74	4,44E-02	
ADGRL2	adhesion G protein-coupled receptor L2	18582	206953_s_at	0,60	-0,73	2,09E-03	
PTEN	phosphatase and tensin homolog	9588	228006_at	0,60	-0,73	3,29E-03	L
RAB7A	RAB7A, member RAS oncogene family	9788	211961_s_at	0,60	-0,73	7,21E-03	I
IL13RA1	interleukin 13 receptor subunit alpha 1	5974	201887_at	0,60	-0,73	7,73E-03	
CASC4	cancer susceptibility 4	24892	224619_at	0,60	-0,73	8,95E-03	
PUM2	pumilio RNA binding family member 2	14958	201493_s_at	0,60	-0,73	9,93E-03	
CPED1	cadherin like and PC-esterase domain containing 1	26159	228728_at	0,60	-0,73	1,17E-02	
KARS	lysyl-tRNA synthetase	6215	200079_s_at	0,60	-0,73	1,18E-02	
VDAC3	voltage dependent anion channel 3	12674	208845_at	0,60	-0,73	1,93E-02	
IER3IP1	immediate early response 3 interacting protein 1	18550	223071_at	0,60	-0,73	2,24E-02	
ZC3H13	zinc finger CCCH-type containing 13	20368	212402_at	0,60	-0,73	2,54E-02	
PSME4	proteasome activator subunit 4	20635	212219_at	0,60	-0,73	2,57E-02	A
UQCR10	ubiquinol-cytochrome c reductase, complex III subunit X	30863	218190_s_at	0,60	-0,73	2,70E-02	R

Gene symbol	HGNC gene name	HGNC ID	Affymetrix probe ID	FC	log_2FC	FDR	P
ISCU	iron-sulfur cluster assembly enzyme	29882	209075_s_at	0,60	-0,73	3,39E-02	
LRRC8D	leucine rich repeat containing 8 VRAC subunit D	16992	218684_at	0,61	-0,72	7,29E-03	
ZNF664	zinc finger protein 664	25406	224593_at	0,61	-0,72	1,44E-02	
PKLR	pyruvate kinase L/R	9020	210451_at	0,61	-0,72	1,46E-02	
UBXN4	UBX domain protein 4	14860	212006_at	0,61	-0,72	2,16E-02	
FYN	FYN proto-oncogene, Src family tyrosine kinase	4037	210105_s_at	0,61	-0,72	2,25E-02	L
TWF1	twinfilin actin binding protein 1	9620	201745_at	0,61	-0,72	3,49E-02	
NOL7	nucleolar protein 7	21040	210097_s_at	0,61	-0,72	3,71E-02	
ANXA9	annexin A9	547	211712_s_at	0,61	-0,71	1,93E-03	
SNRNP25	small nuclear ribonucleoprotein U11/U12 subunit 25	14161	218493_at	0,61	-0,71	3,35E-03	
MTFR1	mitochondrial fission regulator 1	29510	203208_s_at	0,61	-0,71	3,41E-03	
TTC3	tetratricopeptide repeat domain 3	12393	208073_x_at	0,61	-0,71	3,63E-03	
TARDBP	TAR DNA binding protein	11571	200020_at	0,61	-0,71	9,66E-03	
EPS15	epidermal growth factor receptor pathway substrate 15	3419	217887_s_at	0,61	-0,71	1,02E-02	
NDUFS4	NADH:ubiquinone oxidoreductase subunit S4	7711	209303_at	0,61	-0,71	1,15E-02	R
SAR1A	secretion associated Ras related GTPase 1A	10534	201542_at	0,61	-0,71	1,32E-02	
MASP2	mannan binding lectin serine peptidase 2	6902	210798_x_at	0,61	-0,71	1,93E-02	
CERS2	ceramide synthase 2	14076	222212_s_at	0,61	-0,71	2,47E-02	L
FST	follistatin	3971	207345_at	0,61	-0,71	2,57E-02	
UBR2	ubiquitin protein ligase E3 component n-recognin 2	21289	212760_at	0,62	-0,70	7,95E-04	
SCAF11	SR-related CTD associated factor 11	10784	225336_at	0,62	-0,70	2,93E-03	
UBL3	ubiquitin like 3	12504	201535_at	0,62	-0,70	4,45E-03	
TMEM220	transmembrane protein 220	33757	229693_at	0,62	-0,70	6,93E-03	
SEC11A	SEC11 homolog A, signal peptidase complex subunit	17718	216274_s_at	0,62	-0,70	1,87E-02	
YME1L1	YME1 like 1 ATPase	12843	201351_s_at	0,62	-0,70	1,93E-02	
TAT	tyrosine aminotransferase	11573	206916_x_at	0,62	-0,70	2,20E-02	A
DIP2C	disco interacting protein 2 homolog C	29150	212503_s_at	0,62	-0,70	3,78E-02	
UQCRB	ubiquinol-cytochrome c reductase binding protein	12582	205849_s_at	0,62	-0,70	3,88E-02	R
PPP1R3B	protein phosphatase 1 regulatory subunit 3B	14942	1552670_a_at	0,62	-0,70	4,42E-02	
POLR3GL	RNA polymerase III subunit G like	28466	223269_at	0,62	-0,69	7,76E-04	
NDUFA9	NADH:ubiquinone oxidoreductase subunit A9	7693	208969_at	0,62	-0,69	3,61E-03	R
LACTB	lactamase beta	16468	226354_at	0,62	-0,69	3,90E-03	
NUDT9	nudix hydrolase 9	8056	218375_at	0,62	-0,69	5,44E-03	
EFHD1	EF-hand domain family member D1	29556	209343_at	0,62	-0,69	6,08E-03	
SYNPO2	synaptopodin 2	17732	225720_at	0,62	-0,69	1,29E-02	
TMEM41B	transmembrane protein 41B	28948	212623_at	0,62	-0,69	1,58E-02	
TKFC	triokinase and FMN cyclase	24552	218688_at	0,62	-0,69	3,52E-02	
RNF138	ring finger protein 138	17765	218738_s_at	0,62	-0,69	4,59E-02	
SEC14L2	SEC14 like lipid binding 2	10699	204541_at	0,62	-0,69	4,75E-02	
HOGA1	4-hydroxy-2-oxoglutarate aldolase 1	25155	239093_at	0,62	-0,69	4,79E-02	
CDK14	cyclin dependent kinase 14	8883	204604_at	0,62	-0,68	1,38E-03	

Gene symbol	HGNC gene name	HGNC ID	Affymetrix probe ID	FC	log_2FC	FDR	P
ATP6V1A	ATPase H+ transporting V1 subunit A	851	201972_at	0,62	-0,68	4,36E-03	
RAB10	RAB10, member RAS oncogene family	9759	222981_s_at	0,62	-0,68	9,10E-03	I
MYO5B	myosin VB	7603	225301_s_at	0,62	-0,68	9,83E-03	
METTL5	methyltransferase like 5	25006	221570_s_at	0,62	-0,68	1,41E-02	
HNRNPA3	heterogeneous nuclear ribonucleoprotein A3	24941	211932_at	0,62	-0,68	1,61E-02	
MOCOS	molybdenum cofactor sulfurase	18234	219959_at	0,62	-0,68	1,77E-02	
YTHDC1	YTH domain containing 1	30626	212455_at	0,62	-0,68	2,82E-02	
SCARB2	scavenger receptor class B member 2	1665	201646_at	0,62	-0,68	2,89E-02	
COX7A2	cytochrome c oxidase subunit 7A2	2288	201597_at	0,62	-0,68	3,28E-02	
SULT1A3	sulfotransferase family 1A member 3	11455	203615_x_at	0,62	-0,68	4,85E-02	
PTDSS1	phosphatidylserine synthase 1	9587	201433_s_at	0,63	-0,67	7,91E-03	L
RETSAT	retinol saturase	25991	218124_at	0,63	-0,67	1,14E-02	
PNRC2	proline rich nuclear receptor coactivator 2	23158	217779_s_at	0,63	-0,67	1,29E-02	
SYNCRIP	synaptotagmin binding cytoplasmic RNA interacting protein	16918	217833_at	0,63	-0,67	1,66E-02	
SHOC2	SHOC2, leucine rich repeat scaffold protein	15454	202777_at	0,63	-0,67	3,19E-02	
PPM1B	protein phosphatase, Mg2+/Mn2+ dependent 1B	9276	209296_at	0,63	-0,67	3,52E-02	
UBP1	upstream binding protein 1	12507	218082_s_at	0,63	-0,67	4,32E-02	
SKP1	S-phase kinase associated protein 1	10899	200711_s_at	0,63	-0,67	4,38E-02	
CYP27A1	cytochrome P450 family 27 subfamily A member 1	2605	203979_at	0,63	-0,67	4,78E-02	B/L
HMGCS2	3-hydroxy-3-methylglutaryl-CoA synthase 2	5008	240110_at	0,63	-0,67	4,93E-02	
WASHC2C	WASH complex subunit 2C	23414	212370_x_at	0,63	-0,66	1,30E-03	
OXSM	3-oxoacyl-ACP synthase, mitochondrial	26063	219133_at	0,63	-0,66	1,52E-03	
CUL4B	cullin 4B	2555	202214_s_at	0,63	-0,66	1,67E-03	
ATIC	5-aminoimidazole-4-carboxamide ribonucleotide formyltransferase/IMP cyclohydrolase	794	208758_at	0,63	-0,66	3,22E-03	
GLB1	galactosidase beta 1	4298	201576_s_at	0,63	-0,66	4,96E-03	L/I
ARHGAP15	Rho GTPase activating protein 15	21030	218870_at	0,63	-0,66	8,15E-03	
CLIP1	CAP-Gly domain containing linker protein 1	10461	201975_at	0,63	-0,66	8,33E-03	
CMTM8	CKLF like MARVEL transmembrane domain containing 8	19179	235099_at	0,63	-0,66	1,42E-02	
VPS26A	VPS26, retromer complex component A	12711	201807_at	0,63	-0,66	1,43E-02	
EWSR1	EWS RNA binding protein 1	3508	209214_s_at	0,63	-0,66	1,80E-02	
MAP3K20	mitogen-activated protein kinase kinase kinase 20	17797	225665_at	0,63	-0,66	2,57E-02	
MAPK1	mitogen-activated protein kinase 1	6871	224621_at	0,63	-0,66	3,40E-02	I
KIAA0232	KIAA0232	28992	212441_at	0,63	-0,66	3,50E-02	
PPP1CB	protein phosphatase 1 catalytic subunit beta	9282	201409_s_at	0,64	-0,65	4,99E-03	L
KCNJ8	potassium voltage-gated channel subfamily J member 8	6269	205304_s_at	0,64	-0,65	1,04E-02	
DCTD	dCMP deaminase	2710	210137_s_at	0,64	-0,65	1,25E-02	
VDAC3	voltage dependent anion channel 3	12674	208846_s_at	0,64	-0,65	1,93E-02	
GNS	glucosamine (N-acetyl)-6-sulfatase	4422	212334_at	0,64	-0,65	2,13E-02	I
SNRPD3	small nuclear ribonucleoprotein D3 polypeptide	11160	202567_at	0,64	-0,65	3,31E-02	
ZFR	zinc finger RNA binding protein	17277	201857_at	0,64	-0,65	3,70E-02	
TM2D3	TM2 domain containing 3	24128	221702_s_at	0,64	-0,65	3,83E-02	

Gene symbol	HGNC gene name	HGNC ID	Affymetrix probe ID	FC	log_2FC	FDR	P
MPC1	mitochondrial pyruvate carrier 1	21606	218024_at	0,64	-0,65	4,92E-02	R
GPR89B	G protein-coupled receptor 89B	13840	220642_x_at	0,64	-0,64	2,16E-03	
NDUFS2	NADH:ubiquinone oxidoreductase core subunit S2	7708	201966_at	0,64	-0,64	5,66E-03	R
ZNF22	zinc finger protein 22	13012	218005_at	0,64	-0,64	8,45E-03	
ZBTB33	zinc finger and BTB domain containing 33	16682	226255_at	0,64	-0,64	9,41E-03	
ANAPC13	anaphase promoting complex subunit 13	24540	209001_s_at	0,64	-0,64	1,02E-02	
JAGN1	jagunal homolog 1	26926	223104_at	0,64	-0,64	1,25E-02	
RAP1A	RAP1A, member of RAS oncogene family	9855	202362_at	0,64	-0,64	1,42E-02	I
OAZ2	ornithine decarboxylase antizyme 2	8096	201364_s_at	0,64	-0,64	1,54E-02	A
GTF3C6	general transcription factor IIIC subunit 6	20872	225083_at	0,64	-0,64	1,97E-02	
CSNK2B	casein kinase 2 beta	2460	201390_s_at	0,64	-0,64	2,19E-02	L/I
GALM	galactose mutarotase	24063	235256_s_at	0,64	-0,64	2,65E-02	
TTC19	tetratricopeptide repeat domain 19	26006	217964_at	0,64	-0,64	3,29E-02	
CUTA	cutA divalent cation tolerance homolog	21101	221488_s_at	0,64	-0,64	4,11E-02	
CBR1	carbonyl reductase 1	1548	209213_at	0,64	-0,64	4,66E-02	L
TTC39C	tetratricopeptide repeat domain 39C	26595	1552307_a_at	0,64	-0,64	4,77E-02	
MOGAT1	monoacylglycerol O-acyltransferase 1	18210	1553062_at	0,64	-0,64	4,83E-02	L
TMCO1	transmembrane and coiled-coil domains 1	18188	208715_at	0,65	-0,63	9,96E-04	
UBE2E2	ubiquitin conjugating enzyme E2 E2	12478	225651_at	0,65	-0,63	2,91E-03	
USP16	ubiquitin specific peptidase 16	12614	218386_x_at	0,65	-0,63	1,29E-02	
PSMD4	proteasome 26S subunit, non-ATPase 4	9561	211609_x_at	0,65	-0,63	1,49E-02	A
COX4I1	cytochrome c oxidase subunit 4I1	2265	200086_s_at	0,65	-0,63	1,61E-02	R
METTL14	methyltransferase like 14	29330	227601_at	0,65	-0,63	2,22E-02	
DAP3	death associated protein 3	2673	208822_s_at	0,65	-0,63	2,24E-02	
VAMP3	vesicle associated membrane protein 3	12644	201336_at	0,65	-0,63	2,41E-02	
AZIN1	antizyme inhibitor 1	16432	212461_at	0,65	-0,63	2,70E-02	A
OSBPL11	oxysterol binding protein like 11	16397	218304_s_at	0,65	-0,63	3,64E-02	
CD99	CD99 molecule (Xg blood group)	7082	201029_s_at	0,65	-0,63	4,23E-02	
SKP2	S-phase kinase associated protein 2	10901	211042_x_at	0,65	-0,62	3,18E-03	
CISD1	CDGSH iron sulfur domain 1	30880	218597_s_at	0,65	-0,62	1,31E-02	
CCL16	C-C motif chemokine ligand 16	10614	207354_at	0,65	-0,62	1,37E-02	
TROVE2	TROVE domain family member 2	11313	210438_x_at	0,65	-0,62	1,54E-02	
SMIM10L1	small integral membrane protein 10 like 1	49847	221847_at	0,65	-0,62	1,87E-02	
CHD9	chromodomain helicase DNA binding protein 9	25701	212616_at	0,65	-0,62	2,04E-02	L
AZIN1	antizyme inhibitor 1	16432	201772_at	0,65	-0,62	2,97E-02	
TBL1XR1	transducin beta like 1 X-linked receptor 1	29529	223013_at	0,65	-0,62	3,47E-02	L
ASH1L	ASH1 like histone lysine methyltransferase	19088	222667_s_at	0,65	-0,62	3,50E-02	
SEPT11	septin 11	25589	201307_at	0,66	-0,61	5,32E-03	
SPRYD4	SPRY domain containing 4	27468	225616_at	0,66	-0,61	5,53E-03	
DCTD	dCMP deaminase	2710	201572_x_at	0,66	-0,61	1,13E-02	
ELAVL1	ELAV like RNA binding protein 1	3312	201726_at	0,66	-0,61	1,39E-02	

Gene symbol	HGNC gene name	HGNC ID	Affymetrix probe ID	FC	log_2FC	FDR	P
PPM1K	protein phosphatase, Mg2+/Mn2+ dependent 1K	25415	226773_at	0,66	-0,61	1,78E-02	A
RNF181	ring finger protein 181	28037	223064_at	0,66	-0,61	1,88E-02	
TPD52	tumor protein D52	12005	201690_s_at	0,66	-0,61	1,93E-02	
SYNPO2	synaptopodin 2	17732	225721_at	0,66	-0,61	3,28E-02	
PRDX6	peroxiredoxin 6	16753	200845_s_at	0,66	-0,61	3,68E-02	I
CRK	CRK proto-oncogene, adaptor protein	2362	202225_at	0,66	-0,61	3,98E-02	
WEE1	WEE1 G2 checkpoint kinase	12761	212533_at	0,66	-0,61	4,22E-02	
CCDC92	coiled-coil domain containing 92	29563	218175_at	0,66	-0,61	4,64E-02	
GPR89A	G protein-coupled receptor 89A	31984	225463_x_at	0,66	-0,60	1,53E-03	
DNAJA2	DnaJ heat shock protein family (Hsp40) member A2	14884	209157_at	0,66	-0,60	1,90E-02	
GNG12	G protein subunit gamma 12	19663	212294_at	0,66	-0,60	2,49E-02	
HMGN1	high mobility group nucleosome binding domain 1	4984	200944_s_at	0,66	-0,60	2,90E-02	
RIOK3	RIO kinase 3	11451	202130_at	0,66	-0,60	3,74E-02	
PRPS1	phosphoribosyl pyrophosphate synthetase 1	9462	209440_at	0,66	-0,59	3,77E-03	
PPP1CB	protein phosphatase 1 catalytic subunit beta	9282	201408_at	0,66	-0,59	3,92E-03	
ADCY9	adenylate cyclase 9	240	204497_at	0,66	-0,59	1,19E-02	
BET1	Bet1 golgi vesicular membrane trafficking protein	14562	202710_at	0,66	-0,59	1,52E-02	
PSMD4	proteasome 26S subunit, non-ATPase 4	9561	200882_s_at	0,66	-0,59	2,10E-02	
DDOST	dolichyl-diphosphooligosaccharide--protein glycosyltransferase non-catalytic subunit	2728	208675_s_at	0,66	-0,59	3,07E-02	I
SLC6A2	solute carrier family 6 member 2	11048	216611_s_at	1,52	0,60	5,94E-03	
MYO1C	myosin IC	7597	214656_x_at	1,52	0,60	6,96E-03	
APOL2	apolipoprotein L2	619	221013_s_at	1,52	0,60	1,02E-02	
CCDC152	coiled-coil domain containing 152	34438	237475_x_at	1,52	0,60	3,26E-02	
DUX4	double homeobox 4	50800	216473_x_at	1,53	0,61	7,21E-03	
OCIAD1	OCIA domain containing 1	16074	239748_x_at	1,53	0,61	3,20E-02	
HAUS2	HAUS augmin like complex subunit 2	25530	220071_x_at	1,55	0,63	1,67E-02	
MAPK8IP2	mitogen-activated protein kinase 8 interacting protein 2	6883	205050_s_at	1,56	0,64	6,62E-03	
SSC4D	scavenger receptor cysteine rich family member with 4 domains	14461	236529_at	1,57	0,65	7,15E-03	
PDE4C	phosphodiesterase 4C	8782	206792_x_at	1,58	0,66	2,31E-02	
TNFRSF1B	TNF receptor superfamily member 1B	11917	203508_at	1,58	0,66	2,45E-02	
PLA2G4F	phospholipase A2 group IVF	27396	235958_at	1,61	0,69	1,37E-03	L
DLG4	discs large MAGUK scaffold protein 4	2903	210684_s_at	1,62	0,70	6,84E-03	
IRS2	insulin receptor substrate 2	6126	209184_s_at	1,64	0,71	4,66E-02	
TNFRSF12A	TNF receptor superfamily member 12A	18152	218368_s_at	1,66	0,73	1,80E-02	
PIM3	Pim-3 proto-oncogene, serine/threonine kinase	19310	224739_at	1,68	0,75	2,56E-02	
ATP8B1	ATPase phospholipid transporting 8B1	3706	214594_x_at	1,71	0,77	3,70E-02	
CSRNP1	cysteine and serine rich nuclear protein 1	14300	225557_at	1,89	0,92	4,72E-02	
TNFSF14	TNF superfamily member 14	11930	207907_at	1,91	0,93	4,79E-03	
DNAJB1	DnaJ heat shock protein family (Hsp40) member B1	5270	200666_s_at	2,16	1,11	3,68E-02	
IL1RN	interleukin 1 receptor antagonist	6000	212657_s_at	2,50	1,32	9,48E-03	
S100A9	S100 calcium binding protein A9	10499	203535_at	2,73	1,45	5,37E-03	I

Gene symbol	HGNC gene name	HGNC ID	Affymetrix probe ID	FC	log_2FC	FDR	P
S100A8	S100 calcium binding protein A8	10498	202917_s_at	2,85	1,51	2,67E-02	I
SAA2	serum amyloid A2	10514	208607_s_at	3,12	1,64	4,84E-02	
S100A12	S100 calcium binding protein A12	10489	205863_at	3,16	1,66	1,35E-03	I